

# Electro Magnetic Compatibility of Cabling and Wiring in Buildings and Installations

(Proefschrift)

Ter verkrijging van de graad van doctor  
aan de Technische Universiteit Delft,  
op gezag van de Rector Magnificus prof. dr. ir. J.T. Fokkema,  
voorzitter van het College voor Promoties,  
in het openbaar te verdedigen op woensdag 4 juni 2008 om 12:30 uur  
door Herre Tjerk STEENSTRA  
elektrotechnisch ingenieur  
geboren te Kampen

Dit proefschrift is goedgekeurd door de promotor:

Prof. dr. J.J. Smit

Samenstelling promotiecommissie:

Rector Magnificus, Voorzitter

Prof. dr. J.J. Smit, Technische Universiteit Delft, promotor

Prof. dr. F. Canavero, Politecnico di Torino

Prof. dr. F. Rachidi-Haeri, Ecole Polytechnique Fédérale de Lausanne

Prof. dr. J.A. Ferreira, Technische Universiteit Delft

Prof. dr. ir. J.H. Blom, Technische Universiteit Eindhoven

Dr. A.P.J. van Deursen, Technische Universiteit Eindhoven

Dr. ir. S. Meijer, Technische Universiteit Delft

Prof. ir. P. van Genderen, reservelid, Technische Universiteit Delft

The research described in this thesis has been financially supported by Senter-Novem in the form of an IOP project.

ISBN: 978-90-8559-382-9

© 2008 H.T. Steenstra

Voor Angélique en Anna



# Contents

<b>Summary</b>	<b>v</b>
<b>Samenvatting</b>	<b>vii</b>
<b>1 Introduction</b>	<b>1</b>
1.1 Definitions . . . . .	2
1.2 Current situation . . . . .	4
1.3 Goal of the research . . . . .	5
1.4 Definition of the research . . . . .	6
1.5 Organisation of the thesis . . . . .	7
<b>2 Measurement methods</b>	<b>9</b>
2.1 Micro level measurements . . . . .	11
2.1.1 Transmission line parameters . . . . .	11
2.1.2 Transfer impedance . . . . .	13
2.1.3 Transfer impedance of screened cables . . . . .	17
2.1.4 Transfer impedance of unscreened cables . . . . .	24
2.2 Macro level measurements . . . . .	28
2.2.1 Coupling between cables in frequency-domain . . . . .	28
2.2.2 Coupling between cables in time-domain . . . . .	30
2.2.3 Current distributions . . . . .	30
2.3 Correction of measurements with current probes . . . . .	31
2.4 Resistive matching network . . . . .	32

<b>3</b>	<b>Signals</b>	<b>35</b>
3.1	Subdivision . . . . .	36
3.1.1	Pulses . . . . .	36
3.1.2	Continuous signals . . . . .	39
3.1.3	Modulated signals . . . . .	40
3.2	Levels . . . . .	41
3.3	Examples . . . . .	42
3.3.1	Signals generated by a Variable Frequency Drive . . . . .	42
3.3.2	Signals generated by a GSM telephone . . . . .	46
3.4	Definitions . . . . .	48
3.4.1	Digital Fourier Transform . . . . .	48
<b>4</b>	<b>Modelling of coupling paths</b>	<b>51</b>
4.1	Introduction . . . . .	51
4.2	Multi Conductor Transmission Line model . . . . .	53
4.2.1	Transmission lines . . . . .	53
4.2.2	Extension to multiple conductors . . . . .	55
4.2.3	The interconnecting networks . . . . .	58
4.2.4	Step-by-step procedure . . . . .	59
4.3	MTL-parameter matrices . . . . .	59
4.4	Application . . . . .	61
4.5	Distributed source . . . . .	62
4.6	Numerical modelling . . . . .	63
<b>5</b>	<b>Coupling in a large-scale installation with underground cables</b>	<b>65</b>
5.1	Introduction . . . . .	65
5.2	Choice of the various current loops . . . . .	68
5.3	Multi conductor Transmission Line approach . . . . .	70
5.4	Measurement of cable TL parameters . . . . .	71
5.4.1	Transfer parameters . . . . .	72
5.5	Modelling soil and other buried cables . . . . .	75
5.5.1	TL2 . . . . .	75
5.5.2	TL3 – N . . . . .	76
5.5.3	Coupling between TL2 and other buried cables . . . . .	76

5.6	Simulation results for the actual installation . . . . .	78
5.7	Discussion . . . . .	82
5.8	Conclusion . . . . .	84
<b>6</b>	<b>Case studies of parts of installations</b>	<b>85</b>
6.1	Two conductors parallel to a metal plate . . . . .	85
6.1.1	Asymmetrical transmission lines . . . . .	86
6.1.2	Symmetrical transmission line . . . . .	89
6.1.3	Coupling between the two lines in frequency-domain . . . . .	91
6.1.4	Coupling between two lines in time-domain . . . . .	92
6.1.5	Influence of line matching . . . . .	98
6.2	Transfer impedance of V0-YMvKas cable . . . . .	101
6.2.1	Approximation and Measurement . . . . .	101
6.2.2	Influence of current distribution . . . . .	104
6.2.3	Conclusion . . . . .	105
6.3	Transfer impedance of symmetrical cables . . . . .	107
6.3.1	Measurement setup . . . . .	108
6.3.2	Calculation . . . . .	111
6.3.3	Comparison of measurement and calculation . . . . .	114
6.3.4	Changing load conditions . . . . .	115
6.3.5	Conclusion . . . . .	115
6.4	Common mode current distribution . . . . .	118
<b>7</b>	<b>Buildings and Installations</b>	<b>121</b>
7.1	Buildings . . . . .	122
7.1.1	Foundation . . . . .	123
7.1.2	Skeleton . . . . .	124
7.1.3	Floors . . . . .	124
7.1.4	Walls . . . . .	125
7.1.5	Roofs . . . . .	126
7.1.6	EM properties of concrete . . . . .	126
7.1.7	Remarks . . . . .	126
7.2	Installations . . . . .	127
7.3	Conclusion . . . . .	128

<b>8 Optimization procedure</b>	<b>129</b>
8.1 Optimum with respect to EMC . . . . .	129
8.2 Additional conditions for optimization . . . . .	130
8.3 Description of the procedure . . . . .	131
8.3.1 Optimization steps . . . . .	132
8.4 Example . . . . .	135
<b>9 Conclusions and recommendations</b>	<b>141</b>
9.1 Conclusions . . . . .	141
9.2 Recommendations for future work . . . . .	144
<b>Abbreviations</b>	<b>145</b>
<b>A Calculation of MTL</b>	<b>147</b>
<b>B Impedance of metal return plate</b>	<b>151</b>
<b>C Legislation</b>	<b>155</b>
<b>Acknowledgments</b>	<b>165</b>
<b>Curriculum Vitae</b>	<b>167</b>



# Summary

## *Electro Magnetic Compatibility of Cabling and Wiring in Buildings and Installations*

EMC is defined as “The ability of an equipment or system to function satisfactorily in its electro magnetic environment without introducing intolerable electro magnetic disturbances to anything in that environment”. EMC means that equipment shall be designed and manufactured, in such a way that:

- (a) the electro magnetic disturbance generated does not exceed the level above which radio and telecommunications equipment or other equipment cannot operate as intended;
- (b) it has a level of immunity to the electro magnetic disturbance to be expected in its intended use which allows it to operate without unacceptable degradation of its intended use.

The cables and wires connected to equipment play an important role in the coupling of disturbance signals between pieces of equipment. This thesis is dealing with the properties of cabling and wiring in the framework of EMC. Cables and wires have to be installed in such a way that a minimum of disturbance is coupled to others and a minimum of disturbance generated by others is picked up.

For this optimisation the following steps are performed:

Methods have been developed to measure the coupling between cables and to determine the transfer impedance of cables. Two situations are distinguished: one of screened cables and the other of unscreened cables. Furthermore, a method is described to correct the imperfections in the frequency transfer of a current transformer.

After that, the signals that cause disturbance to equipment are described and measurements are performed to characterise the disturbance signals generated by a variable frequency drive.

A calculation procedure has been developed for the couplings between parallel cables. The multi conductor transmission line model has been used as a basis for the development of this procedure.

Several case studies are performed in which the calculation method and the measurement methods are used.

The first case study is the calculation and measurement of the coupling between two parallel conductors both having the same metal plate as return conductor. The calculation is performed using the multi conductor transmission line method as well as using an EM simulation program, based on the finite integration technique. The results of the three methods are compared.

The most extensive case study is dealing with cables in the soil. In this case one cable, connected to a variable frequency drive and a motor, caused common mode currents in the soil and in other cables which were buried parallel to the cable under consideration. These currents are measured and the multi conductor transmission line model is used to calculate these currents, thereby taking into account the transfer impedance of the cables, the mutual inductance between the cables, the conductivity of the soil, etc.

Another case study describes the transfer of common mode current to differential mode voltage in a symmetrical cable. This transfer is the result of an imperfection in the symmetry in the form of unequal diameters of the two conductors. This transfer is calculated as well as measured.

Finally the transfer impedance of an installation cable and the current distributions in conductors in the presence of electro magnetic pulses are measured.

In order to apply the calculation methods in buildings and installations, the location of conducting structures in the vicinity of the cable have to be known as well as their interconnection. Next to that the electric and magnetic parameters of the media between the conductors have to be known. For buildings, research is performed to make clear the location and interconnection of the conductive structures, including the electric and magnetic properties of concrete. For installations the situation has to be investigated for every single installation.

Finally, a procedure is developed to support the decision process in the treatment of EMC issues in a large and complex installation. In such a case, with hundreds or thousands of cables it is practically impossible to calculate the coupling between every combination of two cables. As a result, one needs to know the order of importance of the couplings, so that the most important couplings can be treated first and unimportant couplings can be ignored. A method is developed to rank the couplings in an installation, which makes it possible to decide which couplings have to be decreased.

# Samenvatting

## *Elektro Magnetische Compatibiliteit van Bekabeling en Bedrading in Gebouwen en Installaties*

EMC wordt gedefinieerd als: “Het vermogen van een apparaat of systeem om naar tevredenheid te functioneren in zijn elektro magnetische omgeving zonder onacceptabele elektro magnetische verstoringen te introduceren naar iets in die omgeving”. EMC houdt in dat apparatuur ontworpen en gefabriceerd dient te worden, zodanig dat:

- (a) de opgewekte elektro magnetische verstoring het niveau niet overschrijdt waarboven radio- en telecommunicatie apparatuur of andere apparatuur niet kan functioneren zoals bedoeld, en,
- (b) dat het een niveau van immuniteit heeft voor te verwachten elektro magnetische verstoring, bij gebruik in de omgeving waar het voor bedoeld is, zodanig dat het kan functioneren zonder onacceptabele degradatie van het bedoeld gebruik.

De kabels en draden die aangesloten zijn op de apparatuur spelen een belangrijke rol in de koppeling van stoorsignalen tussen diverse apparatuur. Dit proefschrift handelt over de EMC eigenschappen van bekabeling en bedrading in het kader van EMC. Kabels en draden moeten zodanig geïnstalleerd worden dat een minimale hoeveelheid storing gekoppeld wordt naar anderen en een minimum aan storing, die opgewekt is door anderen, opgepikt wordt.

Voor deze optimalisatie zijn de volgende stappen uitgevoerd:

Methoden zijn ontwikkeld om de koppeling tussen kabels te meten en om de koppelimpedantie van kabels vast te stellen. Hierbij worden twee situaties onderscheiden: één van afgeschermd kabels en de ander van niet-afgeschermd kabels. Daarnaast wordt een methode beschreven om de niet-idealiteiten in de frequentie overdracht van een stroomtransformator te corrigeren.

Daarna zijn de signalen beschreven die verstoring van apparatuur veroorzaken en zijn metingen uitgevoerd om de stoorsignalen die opgewekt worden door een frequentie omzetter te karakteriseren.

Een berekeningsprocedure is ontwikkeld om de koppeling tussen parallelle kabels te berekenen. De ‘multi conductor transmission line’ methode wordt gebruikt als basis voor de ontwikkeling van deze procedure.

Verschillende studies zijn uitgevoerd waarin de berekeningsmethode en de meetmethodes zijn gebruikt.

De eerste is de berekening en meting van de koppeling tussen twee parallelle geleiders die beide dezelfde metalen plaat als retourgeleider hebben. De berekening is uitgevoerd met de ‘multi conductor transmission line’ methode en met een elektro magnetisch simulatie pakket gebaseerd op de ‘finite integration technique’. De resultaten van de drie methoden zijn vervolgens met elkaar vergeleken.

De meest uitgebreide studie gaat over kabels in de grond. In dit geval veroorzaakt een kabel die in de grond ligt en die verbonden is met een frequentie omzetter en een motor, common mode stromen in de grond en in andere kabels die naast deze kabel ingegraven liggen. Deze stromen zijn gemeten en het ‘multi conductor transmission line’ model is gebruikt om deze stromen te berekenen, daarbij rekening houdend met de koppelimpedantie van de kabels, de wederzijdse inductie tussen de kabels, de geleiding van de grond, etc.

Een andere studie beschrijft de omzetting van common mode stroom naar differential mode spanning in een symmetrische kabel. Deze omzetting is het resultaat van een imperfectie in de symmetrie in de vorm van ongelijkheid in de diameters van de kabel. Deze koppelimpedantie is zowel gemeten als berekend.

Tenslotte is de koppelimpedantie van een installatiekabel gemeten en de stroomverdeling in geleiders als gevolg van een aanwezige elektro magnetische puls.

Om de berekeningsmethode toe te passen in gebouwen en installaties moet de aanwezigheid van geleidende structuren in de nabijheid van de kabel bekend zijn en ook of deze onderling verbonden zijn. Daarnaast moeten de elektrische en magnetische eigenschappen van de materialen tussen de geleiders bekend zijn. Met betrekking tot gebouwen is er onderzoek verricht om de locatie en onderlinge verbondenheid van geleidende structuren zichtbaar te maken, inclusief de elektrische en magnetische eigenschappen van het tussenliggende beton. Met betrekking tot installaties moet de situatie onderzocht worden voor elke afzonderlijke installatie.

Tenslotte is er een procedure ontwikkeld die het beslissingsproces ondersteund in de behandeling van EMC zaken in een grote en complexe installatie. In zo’n geval, met honderden of zelfs duizenden kabels is het praktisch onmogelijk om de koppeling uit te rekenen tussen elke combinatie van twee kabels. Daarom is het nodig het belang van de koppeling tussen de kabels te weten, zodat de belangrijkste als eerste behandeld kunnen worden en onbelangrijke overgeslagen kunnen worden.

Een methode is ontwikkeld om de koppelingen in een installatie te rangschikken, waarmee het mogelijk is te beslissen welke koppelingen verminderd moeten worden.

H.T. Steenstra



# Chapter 1

## Introduction

If one travels by airplane, it is requested to switch off mobile phones during take-off and landing. In a hospital, at the intensive-care department, the use of mobile phones is prohibited as well. Listening to an AM broadcast station with your radio standing close to a personal computer is nearly impossible because of the amount of noise or rattle from your radio. Sound recording engineers who use long microphone cables ( $\geq 10\text{m.}$ ) use special cables and connect their microphones in another way than domestic microphones with short cables to prevent noise picked up from e.g. fluorescent tubes. The following examples show that these measures are not taken unnecessarily: Some years ago, in the Netherlands, a wheelchair unintentionally drove off a subway platform, badly injuring the owner of the wheelchair. After investigation by EMC experts it appeared that the wheelchair could easily be upset by signals at 1.89 GHz, a commonly used GSM frequency [1]. More severe examples are the loss of the HMS Sheffield in 1982, where the missile detection system was temporarily switched off because of interference with the radio communication system. At the same moment a missile was launched to hit the ship [2].

All these examples are dealing with one thing: Some electronic equipment (mobile phone, computer, fluorescent tubes, radio-frequency transmitter) cause disturbance to other equipment (airplane instruments, heart monitoring equipment, microphone(cable)s, wheelchair control circuit, missile detection system).

The disturbance signals can travel from one device to another via two different ways: conduction and radiation. In case of conduction there are one or more conductors between the two devices carrying the disturbance signal. There is talk of radiation if the disturbance signal travels in the form of an electro magnetic wave from one device to the other. The device generating the disturbance will be

called *disturbance source* while the device suffering from the disturbance will be called *receptor* in this thesis. The path between disturbance source and receptor, whether it is conductive or radiative, will be called *coupling path*. These three aspects are present in every case dealing with Electro Magnetic Compatibility (EMC). They are also found in most of the books dealing with EMC. A graphical representation of these three aspects is given in figure 1.1.

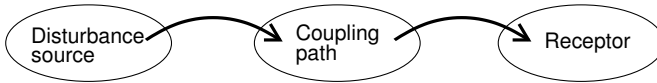


Figure 1.1: The three aspects of EMC

## 1.1 Definitions

In this section definitions are given which are necessary for a correct understanding of this thesis. The subject this thesis is dealing with is Electro Magnetic Compatibility, which will from now on be abbreviated as EMC. A definition of EMC can be found in the International Electro technical Vocabulary of the IEC [3] and is repeated here (the numbers between brackets refer to the definition numbers in the IEC document):

### **Electro Magnetic Compatibility (EMC)**

*The ability of an equipment or system to function satisfactorily in its electro magnetic environment without introducing intolerable electro magnetic disturbances to anything in that environment.*  
(161-01-07)

In the EMC directive of 2004 the following essential requirements are given for equipment to be EM compatible: ‘Equipment shall be so designed and manufactured, having regard to the state of the art, as to ensure that:

- (a) the electro magnetic disturbance generated does not exceed the level above which radio and telecommunications equipment or other equipment cannot operate as intended;
- (b) it has a level of immunity to the electro magnetic disturbance to be expected in its intended use which allows it to operate without unacceptable degradation of its intended use.’



Further information on legislative aspects is found in Appendix C.

The term ‘electro magnetic environment’, as used in this definition, is also defined:

**Electro magnetic environment**

*The totality of electro magnetic phenomena existing at a given location. (161-01-01)*

In the scope of EMC often the term Electro Magnetic Interference (EMI) is used. In the same IEC document a definition of EMI is given, as well as a definition of Electro Magnetic disturbance.

**Electro Magnetic Interference (EMI)**

*Degradation of the performance of an equipment, transmission channel or system caused by an electro magnetic disturbance.*

*Note: The English words “interference” and “disturbance” are often used indiscriminately. (161-01-06)*

**Electro magnetic disturbance**

*Any electro magnetic phenomenon which may degrade the performance of a device, equipment or system, or adversely affect living or inert matter. (161-01-05)*

Now that the most important definitions are given describing the background of the thesis, the keywords of the thesis itself will be defined. The thesis is dealing with optimization of cabling and wiring in buildings and installations. The most important terms will be defined here.

**Cable**

*A combination of two or more conductors, electrically insulated from each other, kept together by insulating (synthetic) material.*

**Cabling**

*All cables in a building or installation that are used to connect equipment in that building or installation to each other or to anything external to that building or installation.*

**Wire**

*A single conductor*

**Wiring**

*All wires in a building or installation that are used to connect equipment in that building or installation to each other or to anything external to that building or installation.*

**Building**

*A structure with a roof and walls, such as a house or factory [4].*

**Installation**

*An optional combination of several apparatus, to perform a specific task where the end-user is the person who decides which apparatus are used to construct the so-called “installation” and where the apparatus were not intended to be placed on the market as a single functional unit. (derived from [5] and explained in [6])*

Installations can be separated into ‘fixed’ and ‘mobile’ installations [7]:

**Fixed installation**

*A particular combination of several types of apparatus and, where applicable, other devices, which are assembled, installed and intended to be used permanently at a predefined location.*

**Mobile installation**

*A combination of apparatus and, where applicable, other devices, intended to be moved and operated in a range of locations.*

## 1.2 Current situation

A lot of research is performed to EMC aspects of specific equipment, especially to the emission and reception properties.

Standards have been developed giving advice on how to make an installation EM Compatible [8]. A lot of experience is available relating to this subject. However, much of this experience is qualitative. The author does not know of a quantitative

approach of an integral installation.

A lot of research has been performed on parts of installations, for example on cable conduits [9, 10, 11].

Other research is performed on cables as such, for example the transfer of differential mode signals to common mode currents which can cause radiation [12, 13] and the radiation resistance which applies in such a situation [14].

The shielding effectiveness of a concrete reinforcement grid is simulated successfully with NEC (Numerical Electro magnetic Code, a computer code to numerically solve electro magnetic problems) as well as measured [15]. Next to that the effect of adding steel fibres in concrete to enhance the shielding properties are investigated [16].

Some research is performed to the coupling between cables [17, 18] and the radiation from cables. This research can be used as input for our research.

All mentioned research paths have in common that they are dealing with only one (small) aspect of installations or buildings. That is in contrast to our research where techniques of these researches are used to calculate and measure coupling in more complex situations like a building or an installation.

### 1.3 Goal of the research

The research is part of the IOP EMVT programme. IOP means *Innovatief Onderzoeks Programma* (Innovative Research Program). EMVT means *Electro Magnetische Vermogens Techniek* (Electro Magnetic Power Technique). It is a group of research programmes financed by the Dutch Ministry of Economic Affairs. The EMVT programmes are seen as an enabling technology for “integrated electro magnetic systems with a high power density, high frequency and a high rendement”. The emphasis within the EMVT is on applications in the energy sector, whereby “the immunity against electro magnetic influence and disturbance plays an important role” [19]. In this case, to enable the reliable operation of sensitive equipment in the vicinity of equipment generating a high level of EMI e.g. by fast switching of large voltages and currents, the coupling of EMI to this sensitive equipment must be minimized. Due to the fact that much of this coupling takes place via the cabling and wiring, research has been carried out, within the context of EMVT, to the EMC properties of cabling and wiring.

The goal of this research, described in this thesis, is *to find a methodology to optimize the cabling and wiring in buildings and installations with respect to EMC.*

Designers of buildings and installations need to be able to calculate beforehand the EMC performance of a certain cable laid at a certain location. They should be able to judge which kind of cable at which location performs better than another

kind of cable and/or location. It should be possible to judge not only qualitatively, what is already possible, but also quantitatively (“If I route the cable via the other wall the disturbance from a nearby broadcast transmitter at a given frequency will be 20 dB lower.”).

To obtain this result the following sub-goals are defined:

- (a) A *calculation method* that can be used to predict the coupling from one cable to another, given the kind of cable and the layout of the environment (especially the conductive parts in the environment).
- (b) A *measurement method* to measure the necessary parameters of cables and structures of buildings and installations needed to perform the before mentioned calculations.

In the next section a description is given how these goals are dealt with in this thesis.

## 1.4 Definition of the research

The subject of the research is related to the coupling path aspect of EMC. Cables, wires and conductive structures in buildings and installations are considered. All these aspects have influence on the coupling of disturbance from one apparatus to another. The following aspects are taken into account:

1. Cables and wires
2. Concrete reinforcement
3. Metal bars, plates, piping, etc.

1) Cables and wires can act as a conductive path to guide disturbance signals from one apparatus to another apparatus directly.

2) Concrete reinforcement can act as a screen that interacts with (radiated) electro magnetic waves. It can reflect waves away from a possible receptor but also in the direction of a receptor. This behaviour is directly related to radiative coupling. The same can be said of metal bars and plates.

Concrete reinforcement can also act as a part of a conductive path. If, for instance, a cable is carrying a CM current, the reinforcement can behave as a ground plane to form a transmission line. If this ground plane is shared by different transmission lines, crosstalk can occur.

3) Pipes and other stretched conductive structures can act as transmission lines to conduct disturbance signals from one part of a building or installation to another part, sometimes in combination with other conductive structures (e.g. pipe over ground plane).

Measurement and modeling methods are developed in order to apply these for calculating beforehand the coupling properties of cabling and wiring in buildings and installations to provide tools to optimize the design.

### Subjects in this thesis

The following aspects will be treated in this thesis:

- A Coupling can take place between cables (crosstalk). This aspect is investigated, especially the transfer impedance of different cables.
- B If a common mode current is flowing in a cable, a resulting differential mode voltage can be observed. This is a well known phenomenon for *coaxial* cables. It is investigated if and how this phenomenon occurs in *non-coaxial* cables, like low-voltage power cables.
- C In a building conductive structures can be present. Research is performed to the locations and interconnections of these structures, especially at locations where they are invisible, i.e. inside concrete.
- D Cables can show antenna behaviour. The frequency dependency of cables is investigated (especially the length in combination with the way it is connected).
- E Some examples of EMI signals are given and one example, i.e. the signals generated by a variable frequency drive, is investigated further.
- F Finally, a method is presented that can be used to gain insight in the risks of the involved couplings between sources and receptors. As a result, the couplings can be ranked from high to low risk. Thus, the couplings with high risk can be treated with a high priority.

## 1.5 Organisation of the thesis

In chapter 2, measurement methods are described for both measurements at micro level (transfer impedance of cables) and at macro level (coupling between devices within an installation).

In the next chapter, chapter 3, some typical EMI signals are described as well as some measurements and investigations into one of these signals.

For the modeling of couplings between cables, a multi conductor transmission line model is used, which is described in chapter 4.

In chapters 5 and 6, the measurement methods of chapter 2 and the calculation method using the model described in chapter 4 are used in some practical situations. Chapter 5 describes the calculated and measured macro level coupling in a large-scale installation while chapter 6 describes couplings in parts of installations and micro level cases.

The research to the location and interconnection of metals in a building is described in chapter 7. In the same chapter, results of a literature research to the permittivity of concrete is presented as well as some remarks about installations.

Given a certain installation, in general, it is hard to decide which coupling paths should be treated in order to improve the EMC design. A tool to provide structure in this process is described in chapter 8.

The conclusions are found in chapter 9 (p.141) as well as the recommendations for future research.

On pages 145–146 a list of abbreviations used in this thesis is found.

The implementation of the MTL calculation is given in appendix A.

The impedance of a metal plate in the situation of a round conductor with a metal plate as return is calculated in appendix B.

Some brief background information on the legislative aspect of EMC is presented in appendix C.

# Chapter 2

## Measurement methods

This chapter describes two levels of measurements, called macro and micro level:

**macro level** In the context of this thesis, macro level means system level. An example of a system is an installation or an apparatus. The size of the system does not matter. An important property of a system is that at the same time several physical phenomena can play a significant role.

**micro level** In contrast to macro level, micro level is dealing with one aspect of a system, where only one physical phenomenon plays a significant role. During micro level measurements the influence of the remaining of the system is excluded as much as possible.

Macro level measurements are measurements on a complete system. They are intended as a check of calculations or simulations and are used in a real installation as a means to determine coupling between cables and to determine levels and kinds of disturbance signals.

The following measurements on macro level will be described in this chapter:

1. Coupling between (long) cables in frequency domain. The results of these measurements can be used to compare different couplings quantitatively. Measurement results of coupling in frequency domain give a better understanding than those in time domain. Next to that, many disturbance signals are described in frequency domain, e.g. RF (radio frequency) signals. Often, disturbance levels in standards are given in frequency domain. The calculation of coupling in frequency domain is easier than in time domain.
2. Coupling between (long) cables in time domain. This must be seen as a final check. Time domain disturbance is especially important in digital sys-

tems. This result can be calculated from the frequency domain coupling. Sometimes the disturbance signal is only available as a pulse, which is better described in time-domain. It is important to know how much of the pulse is found in other cables. It is sometimes, in case of a very weak coupling, easier to make a high power pulse than to make a CW (continuous wave) signal at a high power, especially if the CW signal has to sweep or if it is at a high frequency.

3. Current distributions. If the transfer impedance of a cable is known, the distribution of disturbance current can be used as input to calculate the disturbance voltage in the cable. These measurements are especially important for indirect lightning and coupling of EM waves (e.g. a radio broadcast transmitter or a mobile phone).

On the other hand, micro level measurements are measurements on a, usually small, part of an installation, for instance a cable or a connector. This level has a clearer relation to the physical backgrounds of phenomena. Micro level measurements are designed in such a way that, if possible, the effect of only one physical phenomenon is measured, while excluding other effects. This kind of measurements is performed in a laboratory most of the times. In contrast to this, macro measurements are performed on a complete installation which is usually build up on-site. The phenomena measured at macro level are usually caused by a combination of several physical phenomena which can not always be separated. Micro level measurements used in this research are:

1. Transmission line parameters. E.g. of the transmission lines formed by a cable and a conductive part of an installation, for example a steel bar or a cable conduit. These parameters are needed to calculate the coupling between cables but are sometimes hard to calculate. Next to that, calculated parameters need to be checked.
2. Transfer impedance measurements. These measurements are done on both screened and unscreened cables. The latter is also called longitudinal conversion loss.

In section 2.1 the measurements on micro level will be described and in section 2.2 those on macro level. Finally, in section 2.3 a method is described to take into account the transfer function of a current probe.



## 2.1 Micro level measurements

### 2.1.1 Transmission line parameters

Transmission lines are described in numerous textbooks, e.g. [20, 21, 22, 23, 24]. In general, two different sets of parameters are used to describe transmission lines:

- I The characteristic impedance  $Z_0$  together with the complex propagation constant  $\gamma = \alpha + j\beta$ , where the attenuation constant  $\alpha$  describes the attenuation in Neper per meter and  $\beta$  is the phase constant in  $rad/m$ .
- II The per-unit-length parameters  $R', L', C'$  and  $G'$ , which describe the series resistance and inductance and the parallel capacitance and conductance per unit length, respectively.

Both sets of parameters are interchangeable. The relation between them is given by:

$$Z_0 = \sqrt{\frac{R' + j\omega L'}{G' + j\omega C'}} \quad (2.1)$$

$$\gamma = \sqrt{(R' + j\omega L')(G' + j\omega C')} \quad (2.2)$$

Where  $\omega = 2\pi f$ , the angular frequency of the EM-wave.

One approach is not better than the other, however, because of the straightforward calculation of the per-unit-length TL parameters  $R', L', G'$  and  $C'$ , approach II will be used in this text.

An infinitesimal part of a transmission line, parallel to the  $z$ -axis, is shown in Fig. 2.1. The  $R', L', G'$  and  $C'$  are the per-unit-length transmission line parameters.  $R'$  is the series resistance of the conductors of the TL in  $\Omega/m$ . It is a function of conductivity and cross-sectional area of the conductors. It is also a function of frequency via the skin-effect.  $L'$  is the series inductance in  $H/m$  which is a function of the geometry of the TL.  $C'$  is the capacitance between the two conductors in  $F/m$  and  $G'$  is the shunt conductance between the two conductors in  $S/m$ . It is related to the losses of the insulating material.

### Measuring the TL parameters

A TL can be regarded as a 2-port network of which the  $S$ -parameters can be measured by a vector network analyser (VNA).

$S$ -parameters is an abbreviation of *scattering parameters*. Properties and applications of scattering parameters are, amongst many others, described in [25, 26, 27].

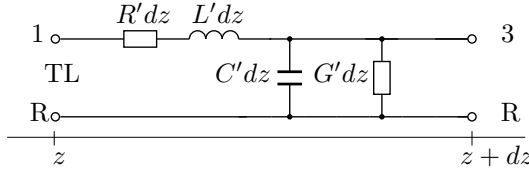


Figure 2.1: Infinitesimal part of a transmission line.

$S$ -parameters describe the relation between incident and outgoing power waves of electrical networks. Although the waves are called power waves, they are in fact voltage waves which are normalized to the impedance of the port under consideration.  $S$ -parameters have two indices,  $x$  and  $y$ :  $S_{xy}$ . The first index,  $x$ , refers to the port of the outgoing wave and the second index,  $y$ , refers to the port of the incident wave. So,  $S_{12}$  is the ratio of the wave going out of port 1 to the wave incident at port 2. So, it is the transfer function from port 2 to port 1. Likewise,  $S_{11}$  is the ratio of the reflected wave at port 1 to the incident wave at port 1, and is thus equal to the reflection coefficient at port 1.

Of a 2 port network the following  $S$ -parameters can be measured:  $S_{11}$ ,  $S_{21}$ ,  $S_{12}$  and  $S_{22}$ . The transmission lines under consideration in this text are assumed to be reciprocal, which means that the two ports can be interchanged without affecting the measured result. As a result  $S_{11}$  is equal to  $S_{22}$  and  $S_{21}$  is equal to  $S_{12}$ . The  $S$ -parameters of a TL with length  $l$  can be expressed as:

$$S_{11} = S_{22} = \frac{(\bar{Z}_0^2 - 1) \sinh(\gamma l)}{2\bar{Z}_0 \cosh(\gamma l) + (\bar{Z}_0^2 + 1) \sinh(\gamma l)} \quad (2.3)$$

where  $\bar{Z}_0$  is the characteristic impedance of the TL, normalized to the characteristic impedance of the VNA, which is  $50 \Omega$  in this case. Thus  $\bar{Z}_0 = Z_0/50$ .

$$S_{21} = S_{12} = \frac{2\bar{Z}_0}{2\bar{Z}_0 \cosh(\gamma l) + (\bar{Z}_0^2 + 1) \sinh(\gamma l)} \quad (2.4)$$

Using equations 2.1 and 2.2 the  $S$ -parameters can be expressed as functions of the per-unit-length transmission line parameters.

The next step is to measure the  $S$ -parameters and to use a curve-fitting program to fit them to curves according to (2.3) and (2.4) where the per-unit-length line parameters are used as fitting parameters.

### Example

As an example the TL parameters of a 1.0 m. long TL consisting of two solid copper conductors separated by a distance of 8.0 cm. are derived via curve fitting the  $S$ -

parameters. The two conductors are both parallel to a metal plate at a distance of 2.0 cm. (the same configuration as the one to be described in section 6.1.2). The S-parameters are measured using a vector network analyser.

To keep the curve-fitting process simple, the resistance of the wires is taken as a real constant value over the whole frequency range (0 - 300 MHz). The skin-effect is not taken into account in this example. The shunt conductance is taken as zero which is a reasonable assumption due to the air insulation.

In figure 2.2 the result is shown. The  $R'$ ,  $L'$  and  $C'$  are used by the curve fitting program as parameters that are changed until the calculated  $S_{21}$  fits with the measured  $S_{21}$ .

In table 2.1 the resultant TL parameters are shown. From these parameters the characteristic impedance can be derived and is equal to 436  $\Omega$ .

Table 2.1: TL parameters derived via curve-fitting of  $S_{21}$ .  $G'$  is mentioned for completeness, however it is not involved in the curve-fitting process, see text.

$R'$	$L'$	$G'$	$C'$
10.9 $m\Omega/m$	1.45 $\mu H/m$	0 $S/m$	7.62 $pF/m$

Calculation of these TL parameters will be done in section 6.1.2).

### 2.1.2 Transfer impedance

In order to explain the concept of transfer impedance, the terms differential mode (DM) and common mode (CM) will be defined first.

Imagine a circuit consisting of a source and a load connected by a forward conductor and by a return conductor, see circuit 1 in figure 2.3(a). Let us assume that there is another circuit of which the same return conductor is part (circuit 2 in the figure). In this circuit a current is generated which is flowing in the return conductor of circuit 1 as well as in the forward conductor of circuit 1, see the current indicated in the figure. This is a CM current for circuit 1 because it is not flowing in the opposite direction in the other conductor of the circuit *under consideration* (circuit 1). Whether a current is a CM or a DM current depends on the point of view, or the circuit under consideration. The current indicated in the figure is a CM current for circuit 1 and a DM current for circuit 2.

The DM current for circuit 1 is the current generated by the generator  $V_1$  which delivers power to the load  $Z_L$ . This current flows from the generator via the conductor to the load and back via the return conductor. This is the differential mode current because the current flows in one direction in one conductor and in the opposite direction in the other conductor of the circuit *under consideration*

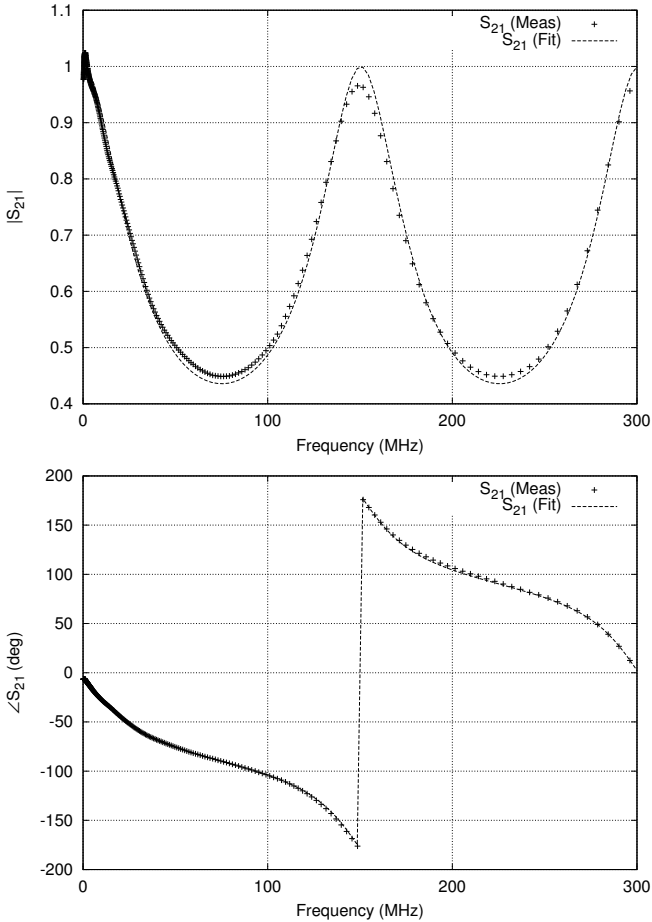
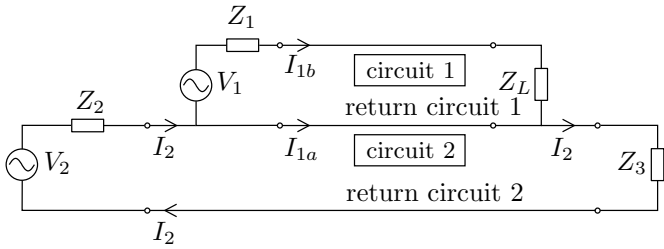
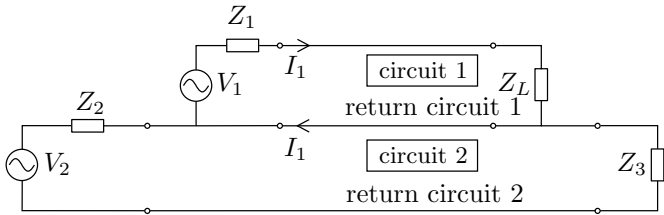


Figure 2.2: Result of the curve fitting process. In the top plot the magnitudes of the measured and fitted  $S_{21}$  parameter are shown. In the bottom plot the angles of the same  $S_{21}$  parameter are shown.



(a) CM current flowing in circuit 1



(b) DM current flowing in circuit 1

Figure 2.3: CM and DM.

(circuit 1).

Now that the CM and DM current are defined, the CM voltage will be defined. If a DM current is flowing in circuit 2 and this current flows back via circuit 1, the CM voltage of circuit 1 is the average of the voltages of the conductors of circuit 1 with respect to the return conductor of circuit 2. This same voltage is the DM voltage of circuit 2.

**Common mode current**

*A current flowing in a circuit that is flowing back in one or more conductors of another circuit.*

**Differential mode current**

*A current flowing in a circuit that is flowing back entirely in that circuit.*

**Common mode voltage**

*The average of the voltages of the conductors carrying the CM current w.r.t. the return conductor of the CM current.*

**Differential mode voltage**

*The voltage of the conductor carrying the DM current w.r.t. the return conductor of the DM current.*

**Transfer impedance**

Look again at figure 2.3. Circuit 1 is a sensitive measuring circuit and circuit 2 is a circuit transporting large signals. The current in circuit 2,  $I_2$ , is much larger than the current in circuit 1. Let us assume that the current of circuit 2 is flowing back entirely via the return conductor of circuit 1 which is common to both circuits. If this conductor has a certain impedance  $Z$ , this current will generate a voltage  $V = I_2 Z$  in circuit 1. This voltage appears as a DM voltage in circuit 1 and is regarded as disturbance. In this case the impedance of the common conductor,  $Z$ , is called the transfer impedance, because it transfers (a part of) the signal of circuit 2 to a disturbance signal in circuit 1.

The transfer impedance is the ratio of a DM voltage of a circuit to the CM current flowing in that same circuit. Referring to figure 2.3, the transfer impedance of the cable connecting generator and load of circuit 1 is the voltage measured between the conductors of the cable, while  $V_1 = 0$  V, divided by the CM current flowing in these conductors generated by  $V_2$ . The transfer impedance is usually expressed

as a per-unit-length parameter, in which case this ratio has to be divided by the length  $l$  of the cable:

$$Z'_t = \frac{U_{DM}}{I_{CM}l} \quad (\Omega/m) \quad (2.5)$$

### Transfer impedance

*Ratio of the DM voltage in a circuit divided by the CM current causing this voltage.*

### 2.1.3 Transfer impedance of screened cables

When measuring a transfer impedance one needs to generate a CM current while at the same time measuring the DM voltage. In general two circuits can be defined, a CM circuit and a DM circuit. A schematic drawing of a setup is shown in figure 2.4.

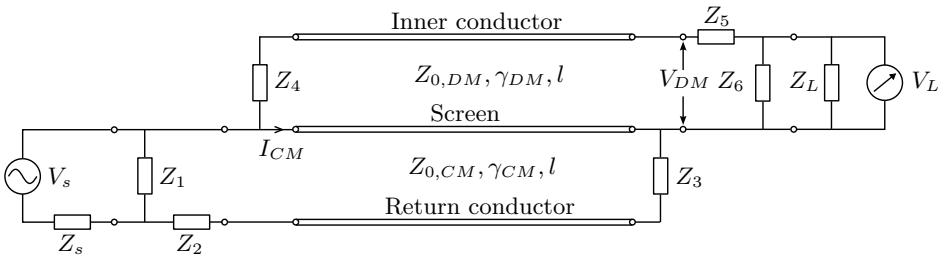


Figure 2.4: Measurement setup for transfer impedance measurement of a coaxial cable

The cable under test (CUT), consisting of the inner conductor and the screen, is a coaxial cable. The CM current in this case is flowing in the screen of the cable, while the DM voltage is the voltage between the screen and the inner conductor of the cable.

#### CM circuit

The CM circuit consists of the source  $V_s$  with internal impedance  $Z_s$ , which is  $50 \Omega$  throughout this text, the CM transmission line, formed by the screen of the CUT and the return conductor, and the load impedance  $Z_3$ . The network consisting of  $Z_1$  and  $Z_2$  is an impedance matching network. The return conductor of the transmission line is a conductor outside the cable. The transmission line is characterized by its characteristic impedance  $Z_{0,CM}$  and complex propagation constant

$\gamma_{CM}$ . Finally,  $l$  is the length of the TL. To force a constant current distribution in the transmission line, the reflections at both ends should be minimized. This can be obtained when both ends of the line have a load equal to the characteristic impedance of the line. So,  $Z_3$  must be equal to  $Z_{0,CM}$ . Likewise, the combination of  $Z_1$ ,  $Z_2$  and  $Z_s$  must equal  $Z_{0,CM}$ .

Description of the resistive matching network can be found in section 2.4.

## DM circuit

The DM circuit is formed by the remainder of the circuit. The transmission line consists of the CUT. Its characteristic impedance and propagation constant are  $Z_{0,DM}$  and  $\gamma_{DM}$ , respectively. The length,  $l$ , is equal to the length of the outer circuit. The load,  $Z_4$ , must equal  $Z_{0,DM}$ . The circuit consisting of  $Z_5$  and  $Z_6$  is an impedance matching circuit, as described before.  $V_L$  is the measured voltage and  $Z_L$  the internal impedance of the voltmeter.

## Measured quantity

The measurement can be done with two separate instruments, but it is more convenient and more precise to use a vector network analyser. In that case the phase of the transfer impedance is measured as well, which gives additional insight in the nature of the transfer impedance.

In case a VNA is used, one must be aware of the fact that the outer conductors of the ports are connected to each other inside the VNA. This is indicated by the  $\perp$ -signs in figure 2.5. As a result, for low frequencies, the current generated by port 1 of the VNA flows in the return conductor ( $I_{CM,1}$ ) and then via  $Z_3$  directly to the ground conductor of port 2 ( $I_{false}$ ). Thus, the CM current is not flowing in the screen, as was intended. The path followed by  $I_{false}$  is a low-resistance path for *low frequencies*. For high frequencies the impedance of this path is much higher because of the inductance due to the big loop formed by the two cables connected to the VNA. For low frequencies a transformer can be applied between the source and the CUT to avoid erroneous measurements, as will be seen in the example below.

If two separate instruments are used and the phase need to be known, the two instruments have to be connected to each other. To prevent false currents, the connection can be made with an optical link.

If a VNA is used the measurement can be performed in two ways: via the S-parameters or directly by measuring the DM voltage and the CM current.



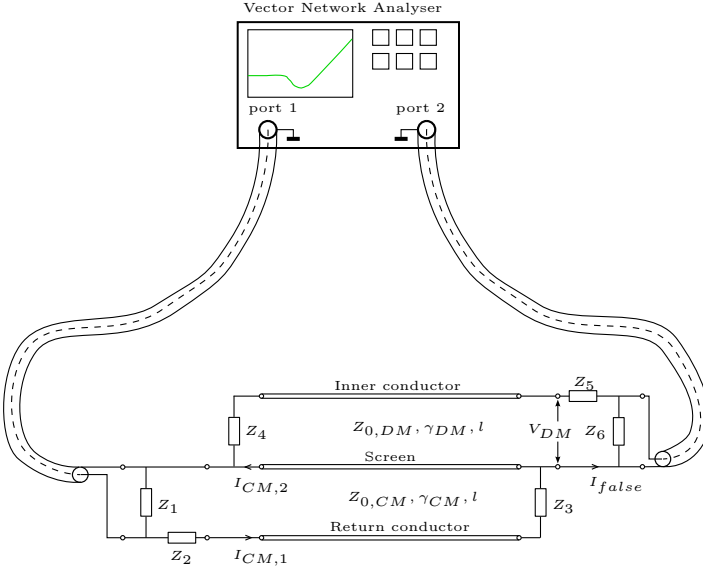


Figure 2.5: Measurement setup for transfer impedance measurement of a coaxial cable

*Via the S-parameters*

Port 1 of a VNA is connected to the CM part of the circuit ( $V_s$  and  $Z_s$ ) and port 2 to the DM part ( $V_L$  and  $Z_L$ ).  $S_{11}$  and  $S_{22}$  are the reflection coefficients at both ports, which should be as small as possible over the frequency range of interest. The other two parameters are equal in case of a reciprocal circuit. All circuits discussed here are reciprocal. If the reflection at the two ports is small enough, the  $S_{21}$  parameter is equal to the voltage ratio  $V_L/V_s$ . The reflection is small enough when the current distribution is flat enough. A measure of the flatness of the current distribution is the standing wave ratio (SWR), which is the ratio of the maximum to the minimum voltage or current along the line:

$$SWR = \frac{I_{max}}{I_{min}} = \frac{1 + |\Gamma|}{1 - |\Gamma|} \tag{2.6}$$

$\Gamma$  is the reflection coefficient and equal to  $S_{xx}$ . So, if the variation of the current along the line must be smaller than 5%, the SWR must be smaller than 1.11 and the reflection coefficient must be smaller than 0.05 or -26dB.

The ratio  $V_L/V_s$ , and thus the  $S_{21}$  parameter, is proportional to the transfer impedance.

The CM current is equal to:

$$I_{CM} = \frac{Z_1}{Z_1 + Z_2 + Z_3} \frac{V_s}{2Z_s} \quad (2.7)$$

where  $Z_s$  is the impedance of port 1. The DM voltage is given by:

$$V_{DM} = \frac{Z_6 Z_L + Z_5 Z_6 + Z_4 Z_6 + Z_5 Z_L + Z_4 Z_L}{Z_6 Z_L} V_L \quad (2.8)$$

where  $Z_L$  is the impedance of port 2. For both equations, the transmission lines are assumed to be matched at both sides as well as the ports of the network analyser. The transfer impedance is the ratio of (2.8) and (2.7):

$$Z'_t = \frac{(Z_6 Z_L + Z_5 Z_6 + Z_4 Z_6 + Z_5 Z_L + Z_4 Z_L)(Z_1 + Z_2 + Z_3)2Z_s}{Z_6 Z_L Z_1 l} S_{21} \quad (\Omega/m) \quad (2.9)$$

Another option to determine the transfer impedance is to calculate the  $Z_{21}$  parameter from the  $S_{21}$  parameter. The  $Z_{21}$  parameter is the voltage measured at port 2 divided by the current delivered at port 1, considering no output current at port 2. The  $Z_{21}$  is given by [28]:

$$Z_{21} = 2 \frac{\sqrt{Z_{0,1} - Z_{0,2}}}{S_{21}} - (Z_{0,1} + Z_{0,2}) \quad (\Omega) \quad (2.10)$$

where  $Z_{0,1}$  and  $Z_{0,2}$  are the characteristic impedances of port 1 and 2, respectively. The transfer impedance can be calculated from  $Z_{12}$  by:

$$Z'_t = \frac{(Z_1 + Z_2 + Z_3)(Z_5 + Z_6)}{Z_1 Z_6 l} Z_{12} \quad (\Omega/m) \quad (2.11)$$

### *Voltage and current measured separately*

If the VNA has three or more ports, the DM voltage and CM current can be measured separately. One port is used as the source of the CM current. The second port is used to measure the DM voltage directly and the third is used to measure the CM current. The CM current is given by:

$$I_{CM} = \frac{V_3}{H} \quad (2.12)$$

$V_3$  is the voltage measured at the third port of the VNA.  $H$  is the transfer function of the current monitor in  $V/A$  (also called 'transfer impedance').

$$V_{DM} = \frac{Z_4 Z_6 + Z_4 Z_L + Z_5 Z_6 + Z_5 Z_L + Z_6 Z_L}{Z_6 Z_L} V_L \quad (2.13)$$

$Z_{4,5,6}$  are given in figure 2.4 and  $Z_L$  is the internal impedance of the second port of the VNA. The transfer impedance is given by:

$$Z'_t = \frac{H(Z_4Z_6 + Z_4Z_L + Z_5Z_6 + Z_5Z_L + Z_6Z_L) V_L}{Z_6Z_L l} \frac{V_L}{V_3} \quad (\Omega/m) \quad (2.14)$$

An example of the method is given below.

### Example

The transfer impedance of a V0-YMvKas-cable has been measured. V0-YMvKas is a code describing the cable according to the Dutch standard NEN-3207 [29]. The meaning of the code is as follows:

**V** The outermost insulation layer of the cable is made of PVC.

**0** The armor of the cable consists of a metal braid around the cable.

**Y** The insulation material of the individual conductors is made of cross-linked polyethylene (PE-X).

**MvK** The inner isolation layer, between the individual conductors and the armor, is made of PVC.

**as** The cable has a grounding litz<sup>1</sup>.

The measurement is performed using a VNA with two output ports and two input ports (Anritsu MS4630B). This is a VNA without  $S$ -parameter measurement capabilities, so the second method is used. A schematic drawing of the setup is given in figure 2.6.

Port 1 of the VNA is the source port delivering the CM current. It is connected to the CUT via a transformer, which is coloured grey. The reason is that the a measurement is performed without transformer and one is performed with transformer. The difference will be discussed later.

Port 2 of the VNA is connected to a current transformer (Pearson Model 110). The current transformer is placed such that it picks up the current in the screen, which is exactly the CM current causing the DM voltage.

Port 3 is connected to one end of the CUT without the matching network used ( $Z_5 = 0 \Omega$  and  $Z_6 = open$ ) while the other end is short circuited to the screen ( $Z_4 = 0 \Omega$ ).

---

<sup>1</sup>The word ‘litz’ in this thesis indicates an uninsulated wire consisting of uninsulated strands. In other texts ‘litz’ can refer to a wire consisting of insulated strands, e.g. in [30].

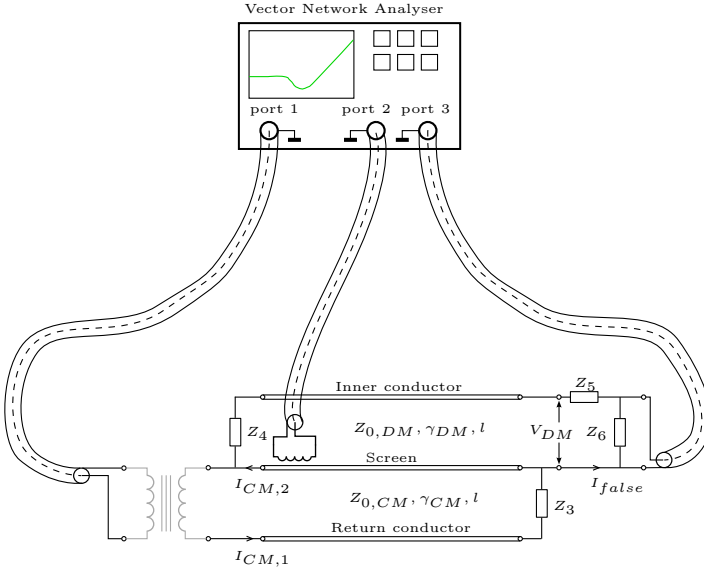


Figure 2.6: Measurement setup for transfer impedance measurement of a V0-YMvKas cable.

The frequency range is from 10 Hz to 10 MHz. The length of the CUT is 60 cm. and the wavelength at 10 MHz is approximately 30 m. due to the fact that the CM circuit was almost entirely air-filled. Because the CUT is so small compared to the wavelength, the current distribution in the CUT will always be flat. Therefore  $Z_3 = 0 \Omega$ .

Three measurements are performed the results of which are shown in figure 2.7:

**without transformer** In this measurement the VNA is connected to the CUT directly. The transformer in figure 2.6 is replaced by two conductors. The resulting transfer impedance is flat until 1 kHz after which it is decreasing until 10 kHz and between 10 kHz and 10 MHz it increases proportional to the square root of the frequency which indicates the influence of the skin-effect. The expected curve for the transfer impedance is different: First a flat part where the DC resistance of the screen is dominant and from a certain frequency an increase due to the skin-effect.

**with transformer** To prevent the CM current from flowing back to the analyser via the cables attached to ports 2 and 3 ( $I_{false}$  in figure 2.6), the transformer is used. The result for frequencies below 100 kHz is now closer to the expected result. For frequencies above 100 kHz the CM current is so low

that an accurate measurement is no longer possible. This is caused by the transformer which did not perform at higher frequencies than 100 kHz.

**manual measurement** To check the assumption that for frequencies lower than 10 kHz the measurement with transformer gives more accurate results and above 10 kHz the measurement without transformer gives better results, the transfer impedance is measured with a separate signal generator and oscilloscope. The grounds of the oscilloscope and of the signal generator are not directly connected, so the current  $I_{false}$  is very small due to a path with high impedance. The measurement points are at every decade in the frequency domain as well as at the lowest frequency (50 Hz) and some additional points in the region between 1 kHz and 100 kHz where the two plots start deviating.

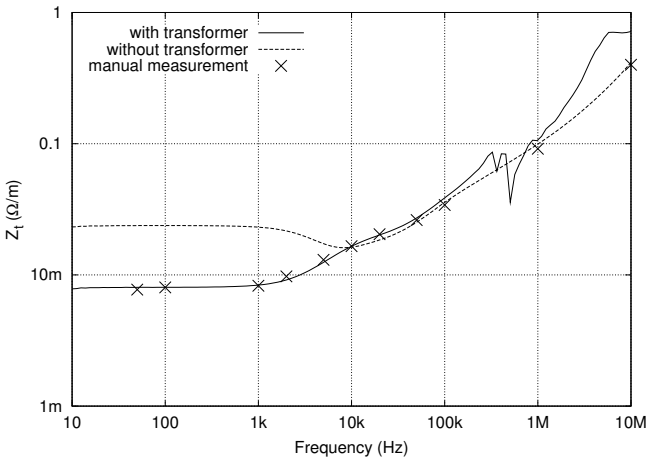


Figure 2.7: Measured transfer impedance of V0-YMvKas cable.

From the measurements it can be concluded that at low frequencies one should be aware of the fact that the CM current can flow in another place than expected.

## Conclusion

If the transfer impedance of a screened cable is measured at very low frequencies, with a (vector) network analyser, special attention must be given to the CM current flows in order to minimize measurement errors. These errors are prevented by using a galvanic separation, e.g. a transformer.

### 2.1.4 Transfer impedance of unscreened cables

In case of unscreened cables, the CM current is assumed not to flow in one conductor alone, but in the two conductors together. This makes the measurement of the DM voltages more complex. See again figure 2.3. The CM current is generated in circuit 2. Most of this current is flowing in the return conductor of circuit 1 and only a small fraction in the forward conductor of circuit 1. In the measurements the connection between circuit 1 and circuit 2 will be made in such a way that the CM current is nearly equally divided between the two conductors of circuit 1. This can be done in two different ways: One way where a so-called MacFarlane probe is used and one where a ‘balanced measurements’ option of a vector network analyser is used.

#### Measurement setup with MacFarlane probe

The CUT is a symmetrical cable which means that its two conductors are both carrying half the signal voltage (w.r.t. a common ground) in opposite phase. A measuring instrument with an asymmetrical port can not be connected directly to the CUT, because in that case one of the conductors of the CUT is connected to ground via the measuring instrument and, as a result, the CUT is no longer symmetrical. To overcome this problem, a MacFarlane probe is used, which has a symmetrical port (also called ‘balanced’ port) to connect to the CUT [12]. The other three ports of the MacFarlane probe are asymmetrical ports at which the CM and DM voltage of the CUT can be measured without disturbing the symmetry of the CUT.

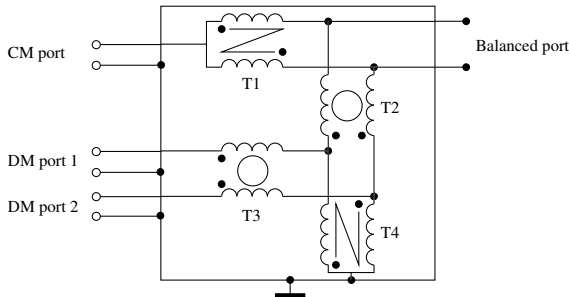


Figure 2.8: Schematic of the MacFarlane probe.

The MacFarlane probe, shown in figure 2.8, can be regarded as a filter designed to split CM from DM signals. If a CM signal enters the probe at the balanced port, this signal is passed by transformer T1. At the same time transformers T2 and

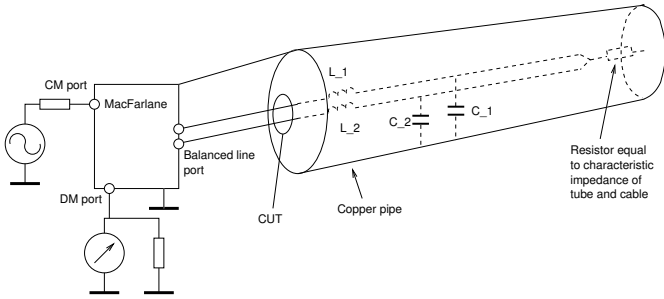


Figure 2.9: The setup of the transfer impedance measurement

T3 block the CM signal. The small remainder of the CM signal that is left after T2 is connected to ground via T4.

A DM signal entering the balanced port is blocked by T1 so it does not reach the CM port. The DM signal is passed by the transformers T2 and T3 so that it can reach the DM ports. Transformer T4 does not play a role in this case because it can be regarded as an open connection for the DM signals. At each of the DM ports half the DM voltage (the voltage between the two conductors of the CUT which is connected to the balanced port) can be measured in opposite phase. In a practical situation, at the two ports equal cables are connected. At one cable the measuring instrument is connected and at the other cable a matching impedance equal to the internal impedance of the measuring instrument resulting in an equal load for the two ports and thus for the two conductors of the CUT. The signal measured with the instrument has to be multiplied by 2 to get the voltage between the conductors of the CUT, which is the DM voltage of the CUT.

The complete measurement setup is shown in figure 2.9. The CM current is supplied at the CM port of the MacFarlane probe and it is measured using a current probe surrounding the CUT, as seen in figure 2.10. The transfer function of the current probe is taken into account using the approach described in section 2.3.

To ensure a uniform current distribution in the CUT a setup is chosen in which the CUT is one of the conductors of a TL which is matched at both sides. The chosen TL is a coaxial TL and the CUT is the inner conductor, where the outer conductor is a copper pipe. The setup is comparable to one used for transfer impedance measurement of coaxial cables [31]. In figure 2.9 a sketch of the setup is given. The CM current flows through the CUT and the resistor at the end of the pipe and flows back via the pipe to the housing of the MacFarlane probe.

The characteristic impedance of the coaxial TL is determined by the inner diameter of the outer conductor and the outer diameter of the inner conductor and the

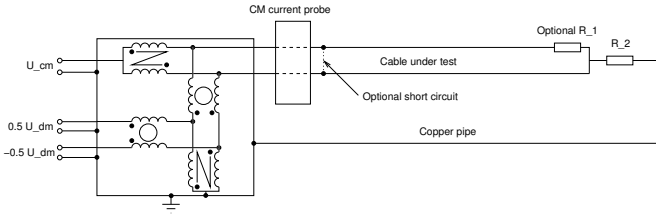


Figure 2.10: Measurement setup with MacFarlane probe.

electro magnetic properties ( $\epsilon$ ,  $\mu$  and  $\sigma$ ) of the material in between. At the end of the coaxial TL a resistor is placed which is approximately equal to its characteristic impedance to prevent reflections and thus standing waves in the pipe and as a result providing a uniform current distribution over the length of the CUT. At the other end, the CUT is connected to the CM source via the ‘MacFarlane probe’. Between the CM source and the MacFarlane probe an impedance matching network can be placed, if necessary.

### Measurement setup with ‘balanced measurements option’

The MacFarlane probe has some limitations: It is not very accurate and it can not be used at higher frequencies than 40 or 50 MHz [32]. To overcome these limitations, another method is developed. For this method a more complex vector network analyser is needed. The network analyser should have at least three ports and the option to combine two ports to a balanced port. At the balanced port, the complex difference of the signals of the two ports is calculated.

When measuring at higher frequencies, it is no longer possible to measure the CM current with a current probe in the used measurement setup. To measure with a current probe the distance between the two conductors of the TL has to be large enough to enable the insertion of the current probe. The higher the frequency, the more reflections occur because of the discontinuity in the TL. For this reason, when measuring with the balanced measurement option of the VNA, the current probe is omitted and the current is derived from the CM voltage applied in the same way as described in section “Measured quantity” (page 18).

A schematic representation of the measurement setup is given in figure 2.11. TL1 and TL2 are the two conductors of the CUT. The CM current  $I_{CM}$ , which is equal to  $I_1 + I_2$ , flows back via the return conductor. The two conductors form two TLs which should be matched at both sides. On the left side a matching network, consisting of  $R_1$  and  $R_2$ , is inserted, which is necessary only if the CM characteristic impedance of TL1 and TL2 is not equal to  $Z_s$ . If the right side is



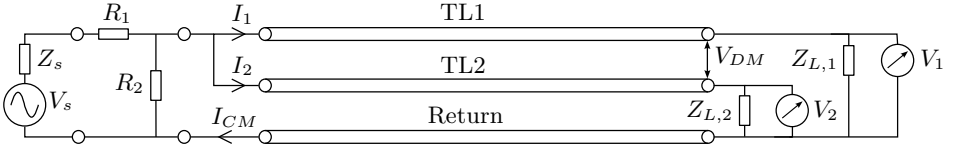


Figure 2.11: Schematic drawing of the measurement setup with balanced measurement option.

not matched, two equal matching networks should be applied, one for each TL.

Three ports of the VNA are used. One port,  $V_s$  with internal impedance  $Z_s$ , is used as CM current source. Two other ports,  $V_1$  and  $V_2$  with internal impedances  $Z_{L,1}$  and  $Z_{L,2}$ , respectively, are combined to one balanced port which is used to measure the DM voltage,  $V_{DM}$ .

### Deriving transfer impedance from $S$ -parameters

The transfer impedance is the DM voltage divided by the CM current. The DM voltage is equal to  $V_1 - V_2$ , which is the voltage measured at the balanced port of the VNA. The voltage at a port of the VNA can be calculated from the power waves,  $a_i$  and  $b_i$ , which are used to calculate the  $S$ -parameters [33]:

$$V_i = \frac{p_i}{\sqrt{|\operatorname{Re}(Z_i)|}} (Z_i^* a_i + Z_i b_i) \quad (2.15)$$

and

$$I_i = \frac{p_i}{\sqrt{|\operatorname{Re}(Z_i)|}} (a_i - b_i) \quad (2.16)$$

$p_i$  is 1 if  $\operatorname{Re}(Z_i) > 0$  and -1 if  $\operatorname{Re}(Z_i) < 0$ .  $Z_i$  is the impedance of the VNA port, which is  $50 \Omega$  for the source port and  $100 \Omega$  for the balanced port,  $a_i$  and  $b_i$  are the power waves traveling into the CUT and out of the CUT respectively. If we consider a matched system,  $a_2 = 0$  and  $b_1 = 0$  and if we consider the internal impedance of the VNA real and positive, these expressions can be simplified into:

$$V_i = \frac{(Z_i b_2)}{\sqrt{Z_i}} \quad (2.17)$$

and

$$I_i = \frac{(a_1)}{\sqrt{Z_i}} \quad (2.18)$$

The DM voltage is then equal to  $V_{DM} = V_i = b_i \sqrt{Z_i}$ . The CM current through the CUT is smaller than the port current, because of the matching network,

by a factor  $R_2/(R_2 + Z_{CM,CUT})$ . Thus the CM current is  $I_{CM} = (R_2/(R_2 + Z_{CM,CUT}))a_i/\sqrt{Z_i}$ . The transfer impedance can then be calculated using the following expression:

$$Z'_t = \frac{V_{DM}}{I_{CM}l} = \frac{R_2 + Z_{CM,CUT}}{R_2l} \sqrt{Z_s Z_L} \frac{b_2}{a_1} = \frac{R_2 + Z_{CM,CUT}}{R_2l} \sqrt{Z_s Z_L} S_{21} \quad (\Omega/m) \quad (2.19)$$

For each cable or pair of wires first a zero measurement is performed. The zero measurement is a measurement with the CUT short circuited at the terminals where the CUT is connected to the balanced port. The result of this measurement is subtracted from the normal measurement with that particular CUT.

An example of a result of the measurement of  $Z'_t$  of a combination of two wires of different diameters, commonly used in installations, is given in section 6.3.

## 2.2 Macro level measurements

The measurements at macro level are based on the same principles as the measurements at micro level.

The main differences between micro- and macro level measurements are:

- In principle a whole system is measured in stead of only one (small) aspect of a system.
- Often, it is not possible to measure one aspect at a time. The measured results are often caused by several mechanisms at the same time. Therefore, understanding the results of these measurements is more complex. It is not always possible to separate different coupling mechanisms and paths.
- These measurements are performed on a complete installation, usually at the location where the installation will be used. There is less control over the situation and one must be aware of the fact that interference from other sources may occur.
- There is a direct relation with actual disturbance situations. These measurements are therefore important.
- Macro measurements are often applied as a (final) check of disturbance coupling calculations.

### 2.2.1 Coupling between cables in frequency-domain

In many cases, coupling of disturbance signals takes place via cables. The disturbance signal manifests itself as a voltage between the terminals of a cable of,

for example, a sensitive input. This disturbance signal is often picked up from another cable carrying a large signal.

Let us have a look at an example:

The source of disturbance consists of a voltage source connected to a load by a cable. The voltage source is generating voltages in a certain frequency band.

The receptor of the disturbance signal consists of a sensor generating small electrical signals which are propagating along a cable to an amplifier.

To predict the amount of disturbance at the input of the amplifier, the following things should be known:

- The amplitude of the voltages generated by the disturbance source as a function of frequency,  $V_i(f)$ .
- The transfer function of this voltage to the voltage at the input of the amplifier,  $H(f)$ . This has to be determined for the working situation, i.e. when everything is connected the way it is when the installation is in use.

To obtain the voltage  $V_o(f)$  at the input terminal of the amplifier, the disturbance source voltage has to be multiplied by the transfer function:

$$V_o(f) = H(f)V_i(f) \quad (2.20)$$

Now, the amplitude of the disturbance voltage as a function of frequency is known at the input terminal of the amplifier. Whether this voltage is harmful depends on the application and is beyond the scope of this research. The subject of this chapter is the measurement of  $H(f)$ .

To measure  $H(f)$ , a network analyser (NA) is used or a combination of a signal generator and a spectrum analyser. The NA may be a vector- or a scalar network analyser. Oscilloscopes are less convenient because of they are less sensitive and are not bandwidth limited.

The source has to be connected in stead of the disturbance source. The meter has to be connected at the place where the disturbance is expected, e.g. the input terminals of the amplifier of the before mentioned example. If a NA is used one must keep in mind that the return conductors of the in- and output are connected to each other. If that is unacceptable, a combination of voltage source and spectrum analyser should be used. This combination is harder to use and is more prone to errors.

Most NA's have  $50 \Omega$  inputs, although some have inputs of  $1 \text{ M}\Omega$ , which causes less influence of the circuit. However, for higher frequencies, this will cause more reflections. If necessary, a matching network should be applied.

## 2.2.2 Coupling between cables in time-domain

The goal and procedure of these measurements are equal to those of the previous section. The difference between time- and frequency domain measurements are:

- Time domain measurements are better suited to get insight in disturbance of digital signals. Digital signals are more likely to be disturbed by impulses than by continuous signals.
- Time domain measurements can be performed with instruments (oscilloscopes) which are more widely available than frequency domain instruments (network- and spectrum analysers).
- It is easier to generate a pulse of high amplitude than to make a continuously variable sine wave at high amplitude.
- Sometimes time domain measurements have preference because there can be a direct relation to actual disturbance signals.

## 2.2.3 Current distributions

If the length of a conductor is in the order of a wavelength or larger, the current in the conductor is not necessarily equal at every location along that conductor. This phenomenon happens in antennas where at the terminal a current is flowing but at the ends the current is decreased to 0 A. From the terminal to the end there is a gradual decrease of current. This is called a current distribution.

A current distribution can be caused by a present electro magnetic field generated by a broadcast transmitter, lightning or a (mostly CM) current in another cable.

If a CM current is present in a cable a DM voltage appears at the terminals of the cable. To calculate the DM voltage at the terminals caused by the CM current the transfer impedance of the cable is needed as well as the CM current distribution. The measurement of transfer impedance of cables is treated earlier in this chapter and the method to calculate the DM voltage is given in another chapter (Modeling of coupling paths).

The measurement of the CM current is performed with a current transformer and a voltmeter. The voltmeter can be either an oscilloscope or a spectrum analyser. The current can be measured at any number of points at any locations along the cable, but it makes sense to use a number of points which is sufficient to predict the current at the intermediate locations.

The current distribution is caused by reflections at both ends of the line that bring the current on the line into oscillation. This oscillation has a sine-wave shape. To reconstruct the current distribution the smallest wavelength expected should be

covered by several points, at least 2, but preferably more. Expected oscillations occur where the length of the cable is equal to integer multiples of a quarter wavelength until the highest frequency in the source signal.

## 2.3 Correction of measurements with current probes

For the measurement of current often a current probe is used. This current probe is in fact a current transformer, where the current carrying conductor is the primary winding and the windings of the probe are the secondary winding.

The transfer function of this current probe has to be taken into account. Because it is a transformer, it is impossible to measure DC currents. Because of this, its transfer function has always a high-pass behaviour. Usually, depending on the quality and the application of the probe, the transfer function is flat in a certain frequency band and falls off again at high frequencies [34].

A current transformer can be modeled by the circuit shown in figure 2.12. The current  $I(\omega)$  is the current to be measured. The voltage source is related to this current by the following relation:

$$U = j\omega MI(\omega) \quad (2.21)$$

where  $M$  is the magnetic coupling between the current carrying conductor and the windings of the current transformer. The voltage of the voltage source is directly proportional to the frequency, causing the high-pass behavior. At low frequencies the impedance of the inductance  $Z = j\omega L$  is much smaller than the internal impedance  $R_L$  of the measuring instrument, a voltmeter. At a certain frequency these two impedances are equal in magnitude and from that frequency on the transfer impedance of the current transformer is flat. At even higher frequencies the impedance of the capacitance  $C$  becomes smaller than  $R_L$  causing the transfer function to fall off again.

The transfer function of the transformer is the ratio of the voltage  $U_L$  to the current  $I(\omega)$  and is called transfer impedance.

Using this model the mathematical expression of the transfer function is derived and expressed as:

$$\frac{U_L(\omega)}{I(\omega)} = \frac{j\omega MR_L}{j\omega L + R_L - \omega^2 LCR_L} \quad (2.22)$$

In time domain the current as function of the measured voltage can be expressed as:

$$i(t) = \frac{1}{M} \int_0^t u(t)dt + \frac{L}{MR_L} u(t) + \frac{LC}{M} \frac{d}{dt} u(t) \quad (2.23)$$

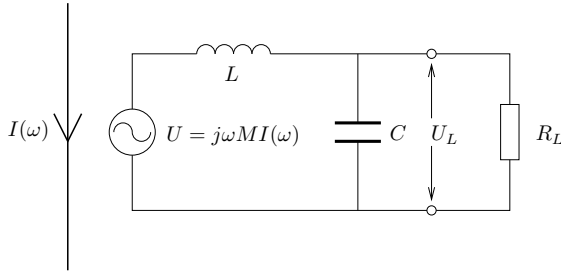


Figure 2.12: Model of a current transformer. Especially the coupling  $M$  and the inductance  $L$  are important parameters.

The two expressions (2.22) and (2.23) are used to correct the measured currents insofar they do not fall in the flat area of the transfer function.

**Conclusion**

If a current probe is used at frequencies where the transfer function of the probe is not flat, the current has to be corrected using a model consisting of a mutual inductance, a self inductance and a capacitance.

**2.4 Resistive matching network**

If a source with an internal impedance  $Z_s$  has to be matched to a load  $Z_L$ , one of the options is to do that with a resistive matching network, shown in figure 2.13.

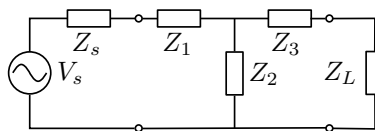


Figure 2.13: Resistive matching network consisting of  $Z_1$ ,  $Z_2$  and  $Z_3$ .

The goal of this network is that the source ‘sees’ an impedance equal to its internal impedance and the load ‘sees’ an impedance equal to the load:

$$Z_s = Z_1 + \frac{Z_2(Z_3 + Z_L)}{Z_2 + Z_3 + Z_L} \tag{2.24}$$

and

$$Z_L = Z_3 + \frac{Z_2(Z_s + Z_1)}{Z_2 + Z_s + Z_1} \quad (2.25)$$

Two cases can be distinguished:

$Z_s < Z_L$  In this case  $Z_1$  can be omitted and the other resistors can be calculated by:

$$Z_2 = \sqrt{\frac{-Z_s^2 Z_L}{Z_s - Z_L}}$$

$$Z_3 = \frac{Z_2 Z_L + Z_s Z_L - Z_2 Z_s}{Z_2 + Z_s}$$

$Z_s > Z_L$  In this case  $Z_3$  can be omitted, so that in fact the matching circuit is flipped horizontally, and the resistors can be calculated by:

$$Z_2 = \sqrt{\frac{-Z_L^2 Z_s}{Z_L - Z_s}}$$

$$Z_1 = \frac{Z_2 Z_s + Z_L Z_s - Z_2 Z_L}{Z_2 + Z_L}$$

The advantage of using a resistive matching network over a lossless network is that it is easy to implement and that it is applicable in a wide bandwidth. The disadvantage that some power is lost in the matching network.





# Chapter 3

## Signals

EMC is dealing with signals generated by a disturbance source and received by a receptor *unintentionally*. EMC problems exist, among others, by the grace of signals. This chapter is dealing with signals and aspects of signals which are of importance to EMC. A signal can be defined as: A physical phenomenon that is used to transport information from one location to another location.

There are a lot of different kinds of signals. Examples are smoke signals used by the Indians to send messages over a distance ranging from several hundred meters to some kilometres. Next to that, sound signals are used by animals to warn each other for threatening dangers. Humans use sound signals in the form of spoken words to communicate to each other. On board of ships there was always a so called Aldis-light that could be used to send light signals to other ships.

A different example is the 50 Hz voltage of the power distribution network. That is not intended as a signal, because it is not intended to carry information, but it is a flow of energy. However, if you are trying to make a music recording with a microphone with unscreened cable, this 50 Hz electro magnetic field will appear as a very annoying disturbance signal in your recording, informing you that there is a 50 Hz EM field present.

From this it can be concluded that what is regarded as an EM field by one can be perceived as (disturbance) signal by others.

In this chapter, and in EMC in general, all signals mentioned are *electrical* signals.

## 3.1 Subdivision

The signals that are of importance to EMC will be subdivided into three different types, according to the wave shapes of the signals:

**Pulses** Non-periodic signals of a duration that is short compared to the time span of interest.

**Continuous signals** These signals are split in periodic and non-periodic signals. Periodic continuous signals have a long duration compared to one period of that signal and do not change in amplitude and frequency during that time. Non-periodic continuous signals, also called DC-signals, have a constant value that does not change periodically.

**Modulated signals** Periodic signals that are modulated in amplitude, frequency or phase or non-periodic signals that change in amplitude.

All three kinds of signals have their own characteristics and can be expected in certain distinct environments.

The coupling of disturbance signals can be divided in two different kinds: conducted and radiated disturbance. In case of conducted disturbance coupling, the physical information carriers are electrons which travel from source to receiver via conductive paths. The radiated disturbance coupling takes place via electromagnetic waves.

The levels of the signals are described by voltages between and currents in the conductors. In case of radiated disturbance coupling the signals are transported by means of electric and magnetic fields.

### 3.1.1 Pulses

An example of a pulse is given in figure 3.1. The shape of the pulse in this example is arbitrarily chosen, it can have many different shapes. An important characteristic of a pulse is that it is a single event, in contrast to continuous periodic signals, although it can show oscillating behaviour. One can see that the voltage before the pulse, which starts at  $0.0 \mu s$ , is equal to the voltage level after the pulse.

Pulses can occur at time instances which are not necessarily correlated to each other. This is the case, for example, when they are caused by switching on a lamp by human interaction. On the other hand, pulses can occur at fixed times. In that case the repetition of the pulses is periodic, but the pulse itself is not.

The most important parameters of a pulse are its rise and decay times and its amplitude. The rise and decay times determine its frequency content. In case of

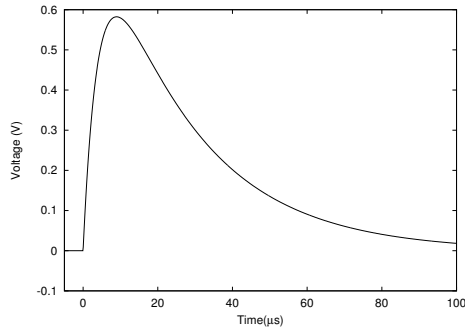


Figure 3.1: An example of a single pulse.

repetitive pulses the repetition frequency also influences the frequency content of the signal. The rise time, according to IEC 61000-4-5 [35] is defined as the time taken by the pulse to rise from 10 % to 90 % of its maximum value. In this example, the rise time is approximately  $5 \mu\text{s}$ , resulting in a spectrum until approximately 65 kHz. The amplitude and length of the pulse determine the amount of energy in the pulse.

## Influence

The influence of a pulse is dependent on the risetime of the pulse. The shorter the risetime, the stronger the coupling to a receptor circuit. In case of inductive coupling, the generated voltage in the receptor circuit will be larger and in case of capacitive coupling the induced current will be larger.

Pulses of high energy, for example lightning pulses, can have much influence on a receiving system. Because of the large amount of energy, they penetrate far into a system if it is not sufficiently protected and it is hard to block them completely. They can influence signals by appearing as spikes superimposed on them. On the other hand they can destroy circuitry if they have enough energy. In case of lightning they can even destroy large structures like trees.

The influence of pulses of low energy depends largely on the nature of the signal to be influenced. In analog signals, for example radio signals, pulses have influence on the audibility of the signal, but if they appear only now and then, the disturbed system remains fully functional. If they appear a number of times per second, the radio channel will become nearly or entirely unusable.

In digital systems, on the other hand, one single pulse can in principle make a huge difference. If a '0' is interpreted as a '1', and it is a critical bit, than completely wrong conclusions can be drawn. However, most digital systems are designed with

error detection and correction, so that a relatively small number of erroneous bits can be detected and corrected. In case of a digital communication channel, for example an Ethernet computer link, the speed of the connection will decrease if bits are distorted by pulses regularly. The system will detect errors and resend the message. That means that the message will be delivered, but with a delay. If, for example, thousand times per second a message has to be resent, the link will be slower.

### Pulses in the IEC 61000 standards

In the IEC 61000 series of EMC standards, a lot of different types of disturbance are dealt with. Examples of pulses from these standards are:

**HEMP** High-altitude Electro Magnetic Pulse. Electro magnetic pulse produced by a nuclear explosion outside the earth's atmosphere (typically above an altitude of 30 km). In [36] an example is given: On the 8<sup>th</sup> of July, 1962, a nuclear bomb with a yield of approximately 1 MT was detonated at 400 km altitude at the Jonston Atoll in the Pacific ocean. As a result, radio communication was not possible for times up to 30 minutes due to ionospheric disruptions. Also, burglar alarms and air-raid sirens were activated and streetlights were extinguished because of blown fuses on Hawaii, which is more than 2000 km away from the explosion.

**HPEM** High-Power Electro Magnetic fields. Intentional EMI, i.e. the signals that are generated intentionally to disturb or even destroy equipment. For example for military, terrorist or criminal purposes. [37, 38]

**Electrostatic discharge** (ESD) "A transfer of electric charge between bodies of different electrostatic potential in proximity or through direct contact" [39]. These discharges appear in the form of pulses with voltages in the order of kilovolts (up to 15 kV in the standards) and with rise times of maximum 1 ns, which results in a frequency spectrum until approximately 300 MHz.

**Electrical fast transients** (EFT) "A transient is a phenomenon or quantity which varies between two consecutive steady states during a time interval which is short compared with the time-scale of interest" [40]. In the standard pulses of 2.5 or 5 kV are used with repetition rates of 5 or 2.5 kHz.

**Surge** "A transient wave of electrical current, voltage, or power propagating along a line or a circuit and characterised by a rapid increase followed by a slower decrease" [35].

### 3.1.2 Continuous signals

Continuous signals are periodic signals that, in contrast to pulses, stay present for a period that is long compared to one period of the signal. Continuous signals can have different origins, for example the 50 Hz power distribution network.

#### Influence

Whether a continuous signal has a disturbing influence on a signal or system depends on two aspects: the amplitude and the frequency(s). The amplitude can be so high that copies of the signal are detectable on every conductor in the system. If the frequency of the disturbance signal does not coincide with the frequency(s) used in the system to be disturbed, the disturbance signal can be blocked by applying filters on (all) ports of the system. If the frequencies coincide, such filters can not be used because the wanted signal is then suppressed as well.

One effect of a continuous disturbance is that it can cause interference with the wanted signal, resulting in a signal that differs in amplitude, phase and/or frequency from what it should be. A second effect is that a continuous disturbance can cause electronic circuits to saturate, even if it is outside the frequency band of interest. If the electronics are saturated, the wanted signal will be distorted or suppressed.

#### Continuous signals in the IEC 61000 standards

The following types of continuous disturbance signals are mentioned in the 61000 series of standards of the IEC:

**Mains signalling** Signals generated and used by energy suppliers for management purposes. Four types can be distinguished: Ripple control systems (110 Hz – 3 kHz), medium-frequency power-line carrier systems (3 kHz – 20 kHz), high-frequency power-line carrier systems (20 kHz – 148.5 kHz) and mains-mark systems. [41].

**Radio frequency EM fields** Fields generated by e.g. fixed and hand-held radio transmitters and, unintentionally, by welders, fluorescent lights, and so on. The field strength in the far field (locations more than  $2\pi/\text{wavelength}$  away from the source of EM fields) is expressed in either  $V/m$ ,  $A/m$  or  $W/m^2$ . Knowing one of these three quantities, the other two can be calculated. In the near field the relation between electric and magnetic field strength is far more complex, so that they are mentioned separately [42].

**Power frequency H-field** The test deals with immunity for magnetic fields generated by a power frequency source (i.e. 16 2/3, 50 or 60 Hz). The waveform to be applied is a sinusoid. The EUT is tested by the ‘immersion method’, by a coil surrounding the EUT. Three orthogonal coils are used in turn [43].

### 3.1.3 Modulated signals

Modulated signals are continuous signals of which the amplitude, phase or frequency is changed over time. These changes contain the information to be transported. The signals generated by radio transmitters are modulated signals.

A frequency modulated signal is a signal of constant amplitude and a varying frequency, where the frequency deviation is proportional to the modulating signal. An amplitude modulated signal is a signal of constant frequency where the amplitude is changing according to the modulating signal.

An example of an amplitude modulated signal is seen in figure 3.2. In this case the modulating signal is a square wave. If the amplitude of the modulated signal returns to zero at the smaller parts of the signal shown in the figure, then there is talk of on-off-keying modulation.

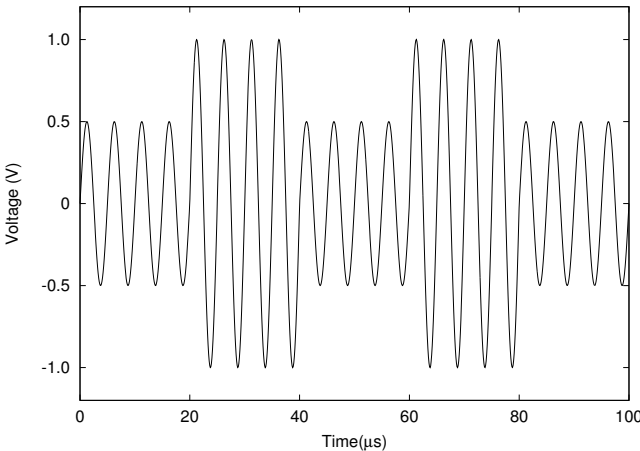


Figure 3.2: Sine wave amplitude modulated with a square wave.

### Influence

The influence of the modulated signal is the same as that of unmodulated signals. Next to that, because of non-linear effects in electronics where the disturbance

appears, the disturbance may be demodulated, which demodulated signal may cause additional effects.

### Modulated signals in the IEC 61000 standards

In the IEC 61000 series of standards equipment under test is exposed to AM signals in some cases:

**Voltage fluctuations and flicker** Voltage fluctuation: Series of changes of RMS voltage evaluated as a single value for each successive half-period between zero-crossings of the voltage source. Flicker: Impression of unsteadiness of visual sensation induced by a light stimulus whose luminance or spectral distribution fluctuates with time. [44]

## 3.2 Levels

In EMC standards a lot of levels pass in revue. Some levels and limits that are of importance in EMC standards are explained here. Explanations are derived from the International Electrotechnical Vocabulary [3].

**Compatibility level** The specified maximum level of EM disturbance that can be present at a device, equipment or system in particular conditions.

Compatibility levels have a strong relation with emission limits and test levels: it is a disturbance level which can be maintained by implementing practicable limits on emissions and it is the level of disturbance from which, with a suitable margin, equipment operating in the relevant environment must have immunity.

**Emission limit** A specified maximum emission from a source.

Emission limits are set to ensure that actual disturbance levels do not exceed the compatibility level, apart from low-probability events that are accepted in EMC. Usually, a number of devices are installed in the same environment. Therefore, the limits must be specified in such a way, that when an expectable number of apparatus are acting together in the same environment all meeting the individual emission limits, the total emitted amount of disturbance does not exceed the compatibility level.

**Immunity level** The maximum level of a given EM disturbance on a particular device, equipment or system so that it remains functional at certain degree of performance.

The immunity level of a product is chosen so that it is above the compatibility

level of its normal operating environment, normally with a certain margin. Although the individual disturbances may be below the compatibility level, the combination of them can cause some apparatus to malfunction. Because the number of combinations is infinite, it is not possible to set compatibility levels for combinations of disturbances. When a certain combination is harmful for a certain product, that combination need be identified.

**Planning level** A planning level is a level of disturbance in a particular environment and in a specific area, adopted by those responsible for planning and operating that power supply network. It is used as a reference value for the limits to be set for the emissions from large loads and installations, in order to co-ordinate those limits with all the limits adopted for equipment intended to be connected to the power supply system. The planning level can not be higher than the compatibility level.

## 3.3 Examples

In principle, every electric or electronic equipment is able to generate EMI. In this section some typical examples will be given. One of the main causes of EMI in industry is the so-called ‘variable frequency drive’ (VFD). This device generates square waves of relatively high voltage (starting from approximately 220 V), resulting in a broad frequency spectrum. Therefore the signals generated by a VFD will be studied in this section.

### 3.3.1 Signals generated by a Variable Frequency Drive

Measurements are performed on an installation consisting of a VFD and a free-running motor. The phase voltages at both VFD- and motor-side are measured as well as the CM current in the cable between VFD and motor.

The goal of these measurements is to gain more insight in the kind and level of disturbance that can be generated by a frequency converter connected to a motor.

#### Description of measurements

The circuit describing the installation where the measurements are performed is given in figure 3.3.



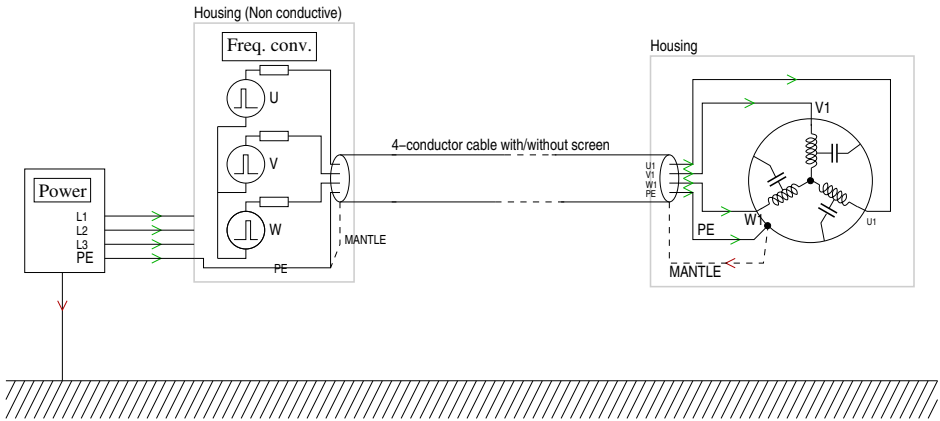


Figure 3.3: The frequency converter setup with the motor

### Driving frequency

The driving frequency is the frequency that can be set on the inverter and that has a direct influence on the rotational speed of the connected motor. The converter used in this experiment can generate frequencies ranging from 0.1 Hz to 440 Hz [45]. The effect of the driving frequency on the spectrum of the CM current in the three phase leads of the cable at the inverter side is derived. The used driving speeds are: 50, 25, 15 and 5 Hz but in the figure only the results of 50 Hz are shown. On this scale the results are equal for the other frequencies. Next to that, the CM current is measured while the driving speed was set to 0 Hz (no rotation of motor) and while the inverter was switched off (disconnected from the electricity supply). The resulting spectra are shown in figure 3.4.

The spectra of 5, 15, 25 and 50 Hz are approximately equal. That is as expected because they are mainly caused by the rising edge of the pulses generated. This rising edge is not changed if the driving frequency is changed. The time-domain signals used for the spectra are seen in the top of the figure.

The 0 Hz spectrum is sufficiently lower than the spectra with rotating motor, as expected. In this case no driving voltages are generated and no current is expected to flow in the phase conductors and in the motor.

It is striking that the spectrum of the case where the inverter is switched off is even lower. Even if the inverter is not driving the motor, there appears to be still some disturbance signal present. This must be caused by the micro controller in the inverter which is still running.

Next to the CM currents the driving voltages are measured at the driving frequency

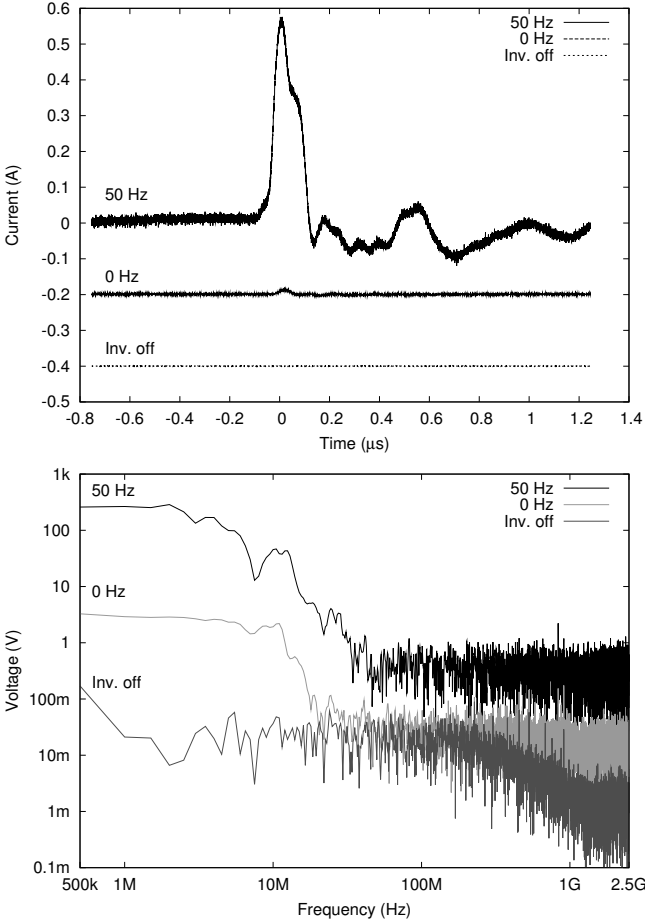


Figure 3.4: Top: the measured currents in time-domain. The lines for 0 Hz and for 'inverter off' are shifted downward for visibility reasons. In reality they are at the 0 A line as well. Bottom: Spectra (of the time domain signals at the left) resulting of different driving speeds. The used current probes are calibrated until 500 MHz, but at higher frequencies the differences are still visible.

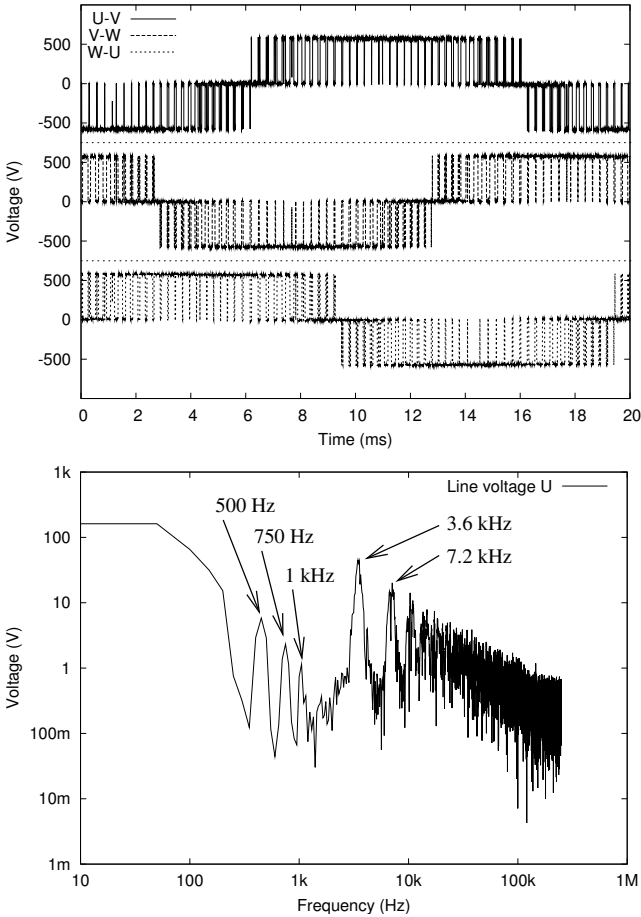


Figure 3.5: Top: voltages between the phases U, V and W of figure 3.3. Bottom: the spectrum of one of these voltages w.r.t. ground.

of 50 Hz. The voltages of the three phases are measured at the same time with a low sampling frequency so that an overview of the signal is obtained and the lower frequencies in the spectra can be seen. In figure 3.5 the pulse width modulation (PWM) voltages are seen together with the resulting (calculated) 50 Hz signal. In the bottom part of the figure the spectra of the voltages are given. In the spectra the 10<sup>th</sup>, the 15<sup>th</sup> and the 20<sup>th</sup> harmonic of the 50 Hz signal at 500, 750 and 1000 Hz respectively are clearly recognised. The next peak in the spectrum, which is much higher than those harmonics is at 3.6 kHz. That is the peak generated by the ‘sampling frequency’ of the inverter, which is 3.6 kHz: in the plot in the top part of the figure it can be seen that every 0.28 ms a new period of the PWM signal starts.

## Conclusion

If the inverter is driving a motor, the spectrum is at least 25 times higher (28 dB) than in the case that the motor is not rotating. This holds for the whole measured frequency range, until at least 500 MHz.

The difference with respect to the case where the inverter is switched off is even bigger.

It must always be taken into account that the inverter is generating signals until at least 500 MHz, even if the inverter is generating low frequencies. These signals have to be suppressed or screened.

### 3.3.2 Signals generated by a GSM telephone

In some cases, if a mobile phone is located close to a stereo set, it can cause disturbance in the stereo set that is audible as a sequence of pulses, during one or two seconds. These pulses are heard a couple of times per hour and just before the mobile phone starts to ring. This disturbance is caused by the transmission of control signals from the mobile phone to the base station as a response to the calling signal of the base station.

Most mobile telephones of the GSM type work in one of three bands: the 900 MHz band (890–915 MHz up link and 935–960 MHz down link), the 1800 MHz band (1710–1785 MHz up link and 1805–1880 MHz down link) and the 1900 MHz band (1850–1910 MHz up link and 1930–1990 MHz down link). The up link is used for communication from mobile phone to base station and the down link for the reverse direction. The 900 MHz and 1800 MHz bands are used in Europe, large parts of Asia, Africa and the Middle East. The 1900 MHz band is used in the United States and Canada.

In this example, the signals generated by a GSM mobile phone working in the

900 MHz band will be discussed [46].

### Modulation

The voice signal picked up by the microphone of the handset is converted to a digital signal by an AD converter. This digital signal consists of a stream of one's and zero's and is transmitted using Gaussian Minimum Shift Keying (GMSK) modulation, which is derived from frequency shift keying (FSK) [47]. The zero's are represented by a frequency deviation of 68 kHz from the carrier and the one's by the opposite deviation from the same carrier. Thus the frequencies representing the two bits are separated by 136 kHz. An example waveform of FSK is shown in figure 3.6. The change between a one and a zero is abrupt, causing a wide main lobe and relatively high side lobes of the transmitted signal. To minimize this effect, the input stream of ones and zeroes is filtered by a Gaussian filter resulting in a smoother signal and less abrupt phase changes in the transmitted signal. This, in turn, causes a smaller main lobe and lower side lobes, and thus less disturbance to other equipment.

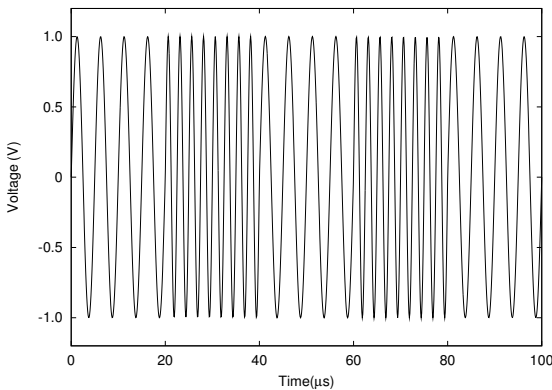


Figure 3.6: Wave form of FSK modulated signal. One frequency represents zero's and the other one's.

Next to this modulation, the communication signals of mobile phones are multiplexed so that one communication channel can be used by several users at the same time. This is done by applying Time Division Multiple Access (TDMA), which means that the handset can transmit in certain time slots. Each GSM channel can serve eight users simultaneously, so that a handset can transmit only  $1/8^{th}$  of the time. A handset can thus transmit its digital information during  $577 \mu s$  out of 4.615 ms. It can be concluded that, during a talk, a GSM handset transmits

bursts of signals with a duty cycle of 12.5 %.

## Power

The handset can transmit signals with a maximum power ranging from 13 dBm (20 mW) to 43 dBm (20 W), depending on the handset. The power is controlled by the base station to reduce interference between mobile phones which are found in different cells and that use the same communication channel. The base station sends messages to the handset to increase or decrease the transmission power in steps of 2 dB until the base station receives the same level of all handsets in its cell [48, 49]. As a result of this, a handset that is far away from the base station transmits at a higher level and is therefore able to cause more disturbance.

## 3.4 Definitions

### 3.4.1 Digital Fourier Transform

The digital Fourier transform (DFT) is supposed to be well-known:

$$X(k) = \sum_{n=0}^{N-1} x(n)e^{-\frac{2\pi i k n}{N}} \quad (3.1)$$

Where  $x(n)$  is the sampled time-domain signal,  $X(k)$  is its Fourier transform,  $N$  is the number of samples used and  $k$  is the digital frequency.

The reverse transform is given by:

$$x(n) = \sum_{k=0}^{N-1} X(k)e^{\frac{2\pi i k n}{N}} \quad (3.2)$$

So far, there are no confusions. However, the point is that, if (3.1) is filled in in (3.2), the original  $x(n)$  is obtained, *multiplied by  $N$* . This means that, somewhere in the two expressions, this factor  $N$  has to be taken into account. This can be done in a lot of different ways, for example by dividing the result of (3.1) or (3.2) by  $N$ , or by dividing the result of both by  $\sqrt{N}$ . If, within an algorithm, both transforms are applied, the end result can simply be divided by  $N$ , but, if only one of the transforms is used, a choice must be made.

In this thesis, the approach found in [50] is used, in which case the division by  $N$  is performed in the forward Fourier transform, so that equation (3.1) can be

rewritten as:

$$X(k) = \begin{cases} \frac{1}{N} \sum_{n=0}^{N-1} x(n) e^{-\frac{2\pi i k n}{N}} & , k = 0 \\ \frac{2}{N} \sum_{n=0}^{N-1} x(n) e^{-\frac{2\pi i k n}{N}} & , k > 0 \end{cases} \quad (3.3)$$





# Chapter 4

## Modelling of coupling paths

The end goal of the research is to find a methodology to optimise the cabling and wiring in buildings and installations with respect to EMC. This means that an answer has to be given to the question: “What cable has to be used and where do I have to install the cable in order to fulfil the EMC requirements of the installation?”. To be able to find an optimum, the following aspects need be known:

- The properties of cables that can be used in the installation.
- Which layouts can be used for the cables to be installed.
- The amount of coupling between every pair of cables in the installation in the possible layouts.

After that, the combinations of layout and kinds of cable have to be compared and the best one chosen, based on the procedure described in chapter 8.

This chapter is dealing with the calculation of the coupling of signals between different points in an installation via the cables. The calculation method is needed as a tool to determine differences between installation options. It is the basis needed for the optimisation process.

### 4.1 Introduction

Different approaches are possible to calculate the coupling between cables in an installation. There are three categories:

A The most accurate but also the most difficult and time consuming method is to solve all electric and magnetic fields analytically. This method is practically only usable to analyse small circuits or parts of circuits. It is also used to determine radiation patterns of antennas and the impedance of antennas as function of frequency. That approach can be used to predict the radiation of a circuit if the CM currents are known. For this reason CM currents are also referred to as antenna mode currents.

Analytical field solving can also be used to calculate inductances and capacitances of and between cables as well as impedances of conductors as function of frequency, where the skin effect plays an important role.

Solving the electric and magnetic fields can also be done numerically. Several methods in numerous computer programs are available to solve the fields given a certain source and geometry. This method discretizes space, whereby a finer discretization gives a more accurate result. For a complete installation, the discretization has to be such that a cable can be modeled as well as the geometry of the frame, which results in a very large number of cells. The method is especially useful when the problem has a complex geometry, and when the geometrical size of the problem is not much larger than a few wavelengths. The method is improved by applying different cell sizes and by optimizing the calculations.

B A simplification of these methods is the circuit theory, where circuits are described using sources, resistances, capacitances, inductances and controlled sources. Electric and magnetic fields are not directly visible in this method and traveling times are not taken into account. In other words, circuits are treated as if they are infinitely small.

All voltages and currents in a network are calculated in time- or frequency-domain. The geometrical size of the circuit is not taken into account. In case of small circuits, the voltages and currents can be calculated analytically. In case of large circuits, usually a numerical network solving program is used.

C To take into account the length of a cable or pair of wires, the transmission line method can be used. In that method the time needed for a voltage or current wave to travel from one location to another is taken into account. Again, this can be done analytically and numerically.

The method used in this thesis will be the numerical network theory, extended by the transmission line theory. The installation will be regarded as a set of networks all without geometrical size, connected by transmission lines which are coupled to each other. The approach is based on the assumption that the devices installed in the network are very small compared to the wavelength.

Throughout the text, as much as possible, direct or analytical calculation is applied.

Numerical modelling is used by the PhD student who is working on the same subject at the TU Eindhoven. However, one situation is also simulated using a numerical EM-field solving program, as will be seen in chapter 6.

## 4.2 Multi Conductor Transmission Line model

The model used to calculate the transfer of signals from one point in an installation to another point in the installation is the MTL model. In this model the sources and receptors (which is the installed equipment) are regarded as networks comprising of lumped elements and the cables are regarded as TLs connecting them. The approach is derived from [51] and is extended by a step-by-step procedure described in section 4.2.4.

### 4.2.1 Transmission lines

Although the theory of transmission lines is described in many texts, its most important characteristics are explained here briefly.

In case a transmission line (TL) is mentioned without the addition ‘multi conductor’, a transmission line with two conductors is meant. These two conductors are the forward and the return conductor.

In circuit theory the length of a conductor is not taken into account. This means that a current entering a conductor is leaving it *at the same time*. As a result, the current entering a conductor is always equal to the current leaving the conductor at the other side. However, in case the length of the conductor has to be taken into account, a current entering the conductor is leaving it at the other side  $l/v$  seconds later, where  $l$  is the length of the conductor and  $v$  the wave velocity. The order of magnitude of this velocity is  $10^8$  m/s. Two parallel conductors form a transmission line if the dominant mode of the transport of electro magnetic energy is the transversal electro magnetic mode, which means that the electric and magnetic field vectors are perpendicular to each other and to the direction of propagation. This is usually the case if the cross-sectional dimensions are much smaller than a wavelength.

To take into account the length of the conductor it is split into infinitesimally small parts, each of which have a length  $dl$ . Such a part, in turn, follows the rules of conventional circuit theory. All these parts together form the transmission line. An infinitesimal part of a TL is shown in figure 4.1. The four circuit elements in the figure,  $R'dz$ ,  $L'dz$ ,  $G'dz$  and  $C'dz$  describe the TL completely.  $R'dz$  is the

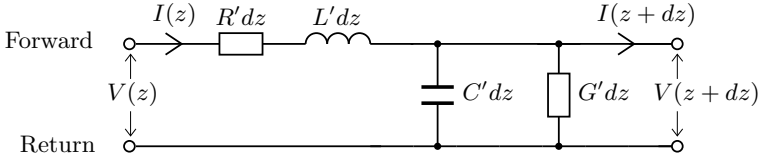


Figure 4.1: Infinitesimal part of a transmission line with length  $dz$ .

impedance of the two (forward and return) conductors together and is complex in case the skin-effect is taken into account.  $L'dz$  is the self inductance of the TL.  $G'dz$  is the conductance of the medium between the two conductors and  $C'dz$  is the capacitance between the conductors of the TL.

The circuit elements in the figure are the elements of an infinitesimal part, which means that they are the product of the per-unit-length parameter and the length  $dz$ . For example, the resistance  $R$  of this infinitesimal part is equal to the resistance per meter  $R'$  in  $\Omega/m$  multiplied by the infinitesimal length  $dz$ :  $R = R'dz$  in  $\Omega$ .

The series impedance can be expressed as  $Z' = R' + j\omega L'$  and the admittance as  $Y' = G' + j\omega C'$ . Using this the following relations can be given:

$$V(z + dz) = V(z) - Z'dzI(z) \quad (4.1)$$

$$I(z + dz) = I(z) - Y'dzV(z + dz) = I(z) - Y'dz\{V(z) + dV(z)\} \quad (4.2)$$

Differentiating with respect to  $z$  results in the following expressions:

$$\frac{dI(z)}{dz} = \frac{I(z + dz) - I(z)}{dz} = -Y'V(z + dz) = -Y'\{V(z) + dV(z)\} \quad (4.3)$$

$$\frac{dV(z)}{dz} = -Z'I(z) \quad (4.4)$$

Combining these two differential equations yields:

$$\frac{dI(z)}{dz} = -Y'(V(z) + dV(z)) = -Y'V(z) + Y'Z'I(z) \quad (4.5)$$

Differentiating again with respect to  $z$ , realizing that  $V(z) + dV(z) = V(z) - Z'I(z)$  and reorganizing terms results in the following second order differential equations:

$$\frac{dI^2(z)}{dz^2} + Y'Z'I(z) = 0 \quad (4.6)$$

$$\frac{dV^2(z)}{dz^2} - Y'Z'V(z) = 0 \quad (4.7)$$

Differential equation (4.6) is solved to find the current as a function of location along the line and (4.7) to find the voltage:

$$I(z) = I_0^+ e^{-\gamma z} - I_0^- e^{\gamma z} \quad (4.8)$$

$$V(z) = V_0^+ e^{-\gamma z} + V_0^- e^{\gamma z} \quad (4.9)$$

where  $\gamma = \sqrt{Y'Z'}$

### 4.2.2 Extension to multiple conductors

In this section the concept of TLs will be extended to multi conductor transmission lines (MTLs), having more than one conductor. A remark has to be made: An N-conductor MTL has N+1 conductors, because the return conductor is not separately counted, but implicitly expected to be present.

The calculation of voltages and currents in an MTL is performed in the same way as in 'normal' TLs. The difference is that the coupling parameters between the transmission lines will be taken into account.

In figure 4.2 the circuit of an infinitesimal part of an MTL is shown consisting of two conductors and a return conductor. The differences between an MTL and a TL are dealing with the coupling between the lines which is expressed by the components inside the dashed box in the figure:

- The capacitance  $C_{xy}$  between every combination of two TLs. This capacitance is directly related to the coupling between the transmission lines. In case one of the TLs is the inner conductor of a coaxial cable, the capacitances between this TL and the other TLs can be neglected most of the times.
- The mutual inductance  $M_{xy}$  between every two TLs. This inductance is also directly related to the coupling. This is often an important factor in the coupling.
- The conductance  $G_{xy}$  between every two TLs. This is a parameter of the insulation and can be neglected in almost all cases.
- The series impedance of TLs, depicted as  $R$  and  $L$  in figure 4.1, are the sum of the impedance of the forward and the return conductor. However, in MTLs, these impedances are mentioned separately. The reason is that the impedance of the return conductor is shared by all TLs and thus causes coupling between TLs while the impedance of the forward conductor does not. The impedance of the return conductor is a transfer impedance, because the current flowing in a TL causes a voltage across this impedance which appears as a source in the other TLs.

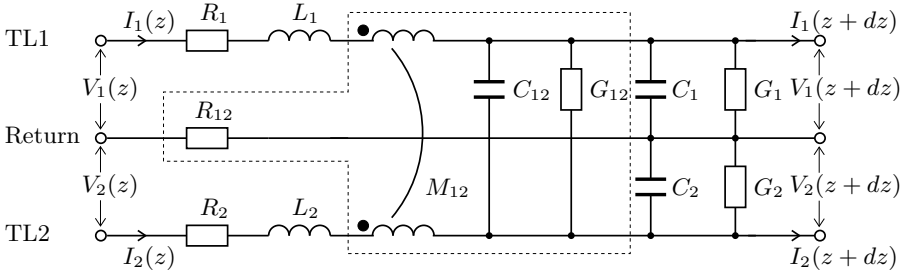


Figure 4.2: Infinitesimal part of an MTL with length  $dz$ . The parts inside the dashed box are related to the coupling.

The relations used to calculate the voltages and currents in this case are given by:

$$V_1(z + dz) = V_1(z) - Z_1 I_1(z) - j\omega M_{12} I_2(z) - R_{12} I_r(z) \quad (4.10)$$

$$V_2(z + dz) = V_2(z) - Z_2 I_2(z) - j\omega M_{12} I_1(z) - R_{12} I_r(z) \quad (4.11)$$

where  $I_r(z) = I_1(z) + I_2(z)$  is the current in the return conductor,  $R_{12}$  is the part of the transfer impedance caused by the impedance of the common conductor,  $Z_1 = R_1 + j\omega L_1$ ,  $Z_2 = R_2 + j\omega L_2$ .  $R_1$ ,  $R_2$  and  $R_{12}$  are complex in case the skin-effect has to be taken into account.

$$I_1(z + dz) = I_1(z) - Y_1 V_1(z + dz) - Y_{12} \{V_1(z + dz) - V_2(z + dz)\} \quad (4.12)$$

$$I_2(z + dz) = I_2(z) - Y_2 V_2(z + dz) - Y_{12} \{V_2(z + dz) - V_1(z + dz)\} \quad (4.13)$$

where  $Y_1 = G_1 + j\omega C_1$ ,  $Y_2 = G_2 + j\omega C_2$  and  $Y_{12} = G_{12} + j\omega C_{12}$ .

Similar expressions can be given if the number of transmission lines is increased. Equations (4.10)–(4.13) can be combined and expressed in matrix form as:

$$\frac{d}{dz} \begin{bmatrix} V_1(z) \\ V_2(z) \end{bmatrix} = - \begin{bmatrix} Z'_1 + R'_{12} & j\omega M'_{12} + R'_{12} \\ j\omega M'_{12} + R'_{12} & Z'_2 + R'_{12} \end{bmatrix} \begin{bmatrix} I_1(z) \\ I_2(z) \end{bmatrix} = - [Z'] [I(z)] \quad (4.14)$$

$$\frac{d}{dz} \begin{bmatrix} I_1(z) \\ I_2(z) \end{bmatrix} = - \begin{bmatrix} Y'_1 + Y'_{12} & -Y_{12} \\ -Y'_{12} & Y'_2 + Y'_{12} \end{bmatrix} \begin{bmatrix} V_1(z) \\ V_2(z) \end{bmatrix} = - [Y'] [V(z)] \quad (4.15)$$

Taking the derivative of (4.14) and filling in (4.15) results in:

$$\frac{d^2}{dz^2} [V(z)] = [Z'] [Y'] [V(z)] \quad (4.16)$$

Note the similarity with (4.7). The voltage and current along the MTL for mode  $m$  can be expressed as:

$$[V^m(z)] = [V_0^m(z)] e^{\pm\gamma_m z} \quad (4.17)$$

$$[I^m(z)] = [I_0^m(z)] e^{\pm\gamma_m z} \quad (4.18)$$

The  $\gamma_m$  and  $V_0^m$  are solutions to the following equation:

$$(\gamma_m^2 [U] - [Z'] [Y']) [V_0^m] = 0 \quad (4.19)$$

The matrix  $[U]$  is the unity matrix. The  $\gamma_m^2$  and  $V_0^m$  are the eigenvalue and eigenvector of the matrix  $[Z'] [Y']$ , which describes the MTL [52].

Now, the voltages and currents along the line can be described as the summation of an incident wave and a reflected wave:

$$[V(z)] = [V_i(z)] + [V_r(z)] = [S_v] [E(z)] [G_{i0}] + [S_v] [E(z)]^{-1} [G_{r0}] \quad (4.20)$$

$$[I(z)] = [I_i(z)] + [I_r(z)] = [S_I] [E(z)] [G_{i0}] - [S_I] [E(z)]^{-1} [G_{r0}], \quad (4.21)$$

where  $[S_v]$  is the matrix consisting of the eigenvectors  $[V_0^m]$  and  $[S_I]$  can be calculated by  $[S_I] = [Z']^{-1} [S_v] [\Gamma]$ . The matrix  $[\Gamma]$  is a diagonal matrix with the  $\gamma_m$  as its elements. The matrices  $[G_{i0}]$  and  $[G_{r0}]$  consist of the vectors of complex identities at the first end of the MTL, related to the incident and reflected waves.  $[E(z)]$  is the matrix describing the amplitude and phase relation between the points along the MTL, being a diagonal matrix with  $e^{-\gamma_m z}$  as its elements.

If we write  $[E(D)]^{-1} [G_{i0}]$  as  $[G_{rD}]$ , with  $D$  the length of the MTL, the voltages and currents at the first end and at the last end of the MTL can be written as:

$$[V(0)] = [S_v] ([G_{i0}] + [E_D] [G_{rD}]) \quad (4.22)$$

$$[I(0)] = [Y_c] [S_v] ([G_{i0}] - [E_D] [G_{rD}]) \quad (4.23)$$

$$[V(D)] = [S_v] ([E_D] [G_{i0}] + [G_{rD}]) \quad (4.24)$$

$$[I(D)] = [Y_c] [S_v] ([E_D] [G_{i0}] - [G_{rD}]) \quad (4.25)$$

Where  $[Y_c]$  is the characteristic admittance matrix of the MTL which can be calculated by  $[Y_c] = [S_I] [S_v]^{-1}$ .

The unknowns in these equations are  $[G_{i0}]$  and  $[G_{rD}]$ .

### 4.2.3 The interconnecting networks

The networks representing the equipment and the interconnections can be described using the following matrix notation:

$$[P] [V] + [Q] [I] = [E] \quad (4.26)$$

where  $[V]$  and  $[I]$  are vectors containing the voltages and currents at the nodes of the network. The vector  $[E]$  contains the sources in the network. The external nodes of the network coincide with the ends of the TMs. When at these locations the voltages and currents of the TMs are filled in, equation (4.26) can be solved resulting in the voltages and currents at the first ends and last ends of the TMs. Let us assume two networks connected by an MTL of length  $D$ . Network number 1 is connected to the first end of the MTL and network number 2 to the last end. Then, for the first end:

$$[P_1] [V(0)] + [Q_1] [I(0)] = [E_1] \quad (4.27)$$

end for the last end:

$$[P_2] [V(D)] + [Q_2] [I(D)] = [E_2] \quad (4.28)$$

After filling in (4.22)—(4.25) into (4.27) and (4.28), they can be written as:

$$\begin{pmatrix} [P_1] [S_v] + [Q_1] [Y_c] [S_v] \\ [P_1] [S_v] [E_D] - [Q_1] [Y_c] [S_v] [E_D] \end{pmatrix} \begin{pmatrix} [G_{i0}] \\ [G_{rD}] \end{pmatrix} + [E_1] \quad (4.29)$$

$$\begin{pmatrix} [P_2] [S_v] [E_D] + [Q_2] [Y_c] [S_v] [E_D] \\ [P_2] [S_v] - [Q_2] [Y_c] [S_v] \end{pmatrix} \begin{pmatrix} [G_{i0}] \\ [G_{rD}] \end{pmatrix} + [E_2] \quad (4.30)$$

These expressions, in turn, can be written in short as:

$$[A_1] [G_{i0}] + [B_1] [G_{rD}] = [E_1] \quad (4.31)$$

and

$$[A_2] [G_{i0}] + [B_2] [G_{rD}] = [E_2] \quad (4.32)$$

Now, by constructing the following combined matrices

$$[A_{total}] = \begin{bmatrix} [A_1] & [B_1] \\ [A_2] & [B_2] \end{bmatrix}, \quad [G_{total}] = \begin{bmatrix} G_{i0} \\ G_{rD} \end{bmatrix}, \quad [E_{total}] = \begin{bmatrix} E_1 \\ E_2 \end{bmatrix} \quad (4.33)$$

the system can be solved for  $[G_{total}]$ :

$$[A_{total}] [G_{total}] = [E_{total}] \quad (4.34)$$



### 4.2.4 Step-by-step procedure

Concluding, the solution is obtained in the following way, step by step:

1. Order the nodes of the networks in such a way that all nodes connected to a certain MTL are numbered consecutively. Order the nodes in the network at the other end of that MTL in the same way. Now, write down the  $[P]$ ,  $[Q]$  and  $[E]$  matrices for every network.
2. Choose the directions of the MTLs in such a way that every network is connected exclusively to first ends of MTLs or to last ends of MTLs. This makes implementation much easier. An MTL can be made to have two last ends or two first ends by inserting somewhere in the MTL a network merely consisting of interconnections. Now, write down the  $[Z']$  and  $[Y']$  matrices, as described in section 4.3.
3. Multiply the  $[Q]$  matrix of every network that is connected to last ends of TLs with  $-1$ .
4. Calculate the eigenvalues and eigenvectors of the matrix  $[Z'] [Y']$  for every MTL.
5. Construct an  $N \times N$  diagonal matrix  $[\Gamma]$  with the  $\gamma_m$  as elements.  $N$  is the number of conductors of the MTL. Do this for every MTL.
6. Construct a matrix  $[E_D]$  for every MTL, which is a diagonal  $N \times N$  matrix with elements  $e^{-\gamma_m D}$ , where  $D$  is the length of the MTL.
7. Calculate a matrix  $[Y_c]$  for every MTL
8. Calculate the  $[A_i]$  and  $[B_i]$  for every transmission line end and construct the matrices  $[A_{total}]$ ,  $[G_{total}]$  and  $[E_{total}]$ . Solve the equation for  $[G_{total}]$ , split  $[G_{total}]$  in  $[G_{i0}]$  and  $[G_{rD}]$ , and calculate the voltages and currents using (4.22)—(4.25).

## 4.3 MTL-parameter matrices

For the calculation procedure described in the previous section the MTL-parameter matrices  $[Z']$  and  $[Y']$  are needed. This section describes how to generate these matrices.

The impedance matrix  $[Z']$  can be written as the sum of the series resistance matrix  $[R']$  and the series inductance matrix  $[L']$  multiplied by  $j\omega$ :

$$[Z'] = [R'] + j\omega [L'] \quad (4.35)$$

The elements of the matrix  $[R']$  describe the series impedance in the TLs. The diagonal elements  $R_{xx}$  are the sums of the impedances in the two conductors of that respective TL. The off-diagonal elements  $R_{xy}$  are the impedances shared between TL $x$  and TL $y$ . If figure 4.2 is taken as an example, the matrix  $[R']$  is given by:

$$[R'] = \begin{bmatrix} R_1 + R_{12} & R_{12} \\ R_{12} & R_2 + R_{12} \end{bmatrix} \quad (4.36)$$

The off-diagonal elements of the matrix are all equal to  $Z_{12}$ . This impedance causes coupling from one TL to the other TLs. The matrix is symmetrical because the coupling between two TLs is reciprocal.

The impedance  $Z_{12}$  as well as the resistances  $R_1$  and  $R_2$  can be complex valued. For example, if the skin-effect has to be taken into account, these impedances will have an imaginary part that is approximately equal to the real part.

The matrix  $[L']$  can be written in the following way:

$$[L'] = \begin{bmatrix} L_1 & M_{12} \\ M_{12} & L_2 \end{bmatrix} \quad (4.37)$$

This matrix is also symmetrical because of reciprocity.

Like the impedance matrix, the admittance matrix  $[Y']$  can be written as the sum of the shunt admittance and the shunt capacitance multiplied by  $j\omega$ :

$$[Y'] = [G'] + j\omega [C'] \quad (4.38)$$

The matrix  $[G']$  can be written as follows:

$$[G'] = \begin{bmatrix} G_1 + G_{12} & -G_{12} \\ -G_{12} & G_2 + G_{12} \end{bmatrix} \quad (4.39)$$

While the matrix  $[C']$  is:

$$[C'] = \begin{bmatrix} C_1 + C_{12} & -C_{12} \\ -C_{12} & C_2 + C_{12} \end{bmatrix} \quad (4.40)$$

If the TL is homogeneous, both shunt conductance and capacitance can be calculated directly from the inductance by using the following formulas:

$$G = \frac{\sigma}{L} \quad (S/m) \quad (4.41)$$

$$C = \frac{\mu\epsilon}{L} \quad (F/m) \quad (4.42)$$

or, in matrix notation:

$$[G'] = \sigma [L']^{-1} \tag{4.43}$$

$$[C'] = \mu\epsilon [L']^{-1} \tag{4.44}$$

where  $\sigma$ ,  $\mu$  and  $\epsilon$  are the conductance, magnetic permeability and dielectric permittivity of the surrounding medium.

### 4.4 Application

The MTL method can be applied in situations where the cables and other conducting structures are oriented parallel to each other. In a real situation this is only true for parts of the cables. In that case all parts have to be considered separately. The MTLs are connected together by interconnecting networks containing normal circuit elements.

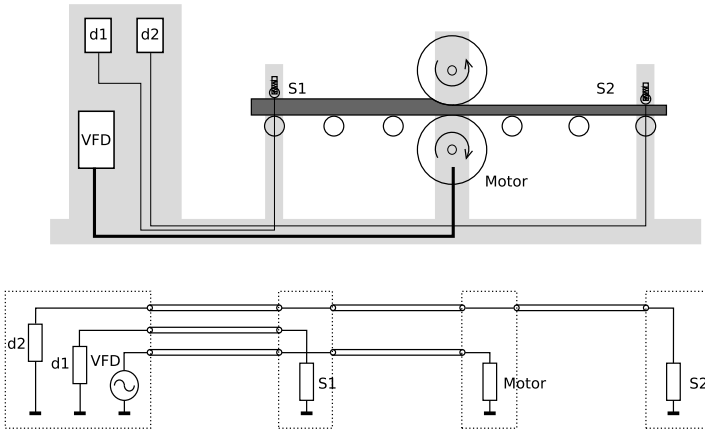


Figure 4.3: Example of an installation (top) and its MTL model (bottom).

The application of the MTL model will be explained by means of an example, see figure 4.3. In the top of this figure a sketch is given of a steel rolling installation with four distinct electrical parts, from left to right. The first part is a control cabinet with a variable frequency drive, denoted by 'VFD', and two sensor readouts, denoted by 'd1' and 'd2'. The second is a sensor to measure the thickness of the input steel plate, S1. The third part is the motor driving the rolls and the fourth part is a sensor to measure the thickness of the output steel plate, S2. The grey structure in the background is the steel frame the installation is mounted on.

In the bottom part of the figure the MTL model of this installation is drawn. Left the network representing the control cabinet. The VFD acts as a generator of CM disturbance currents and the sensor readouts, represented by their CM impedance, are the receptors of disturbance. Then, an MTL is drawn with three conductors: two sensor lines and a power cable between VFD and motor. Note that the return conductor is not drawn, although it is present. In the networks the connections to the return conductor are shown ( $\perp$ ).

On the right side of the three conductor MTL the second network is drawn with the CM impedance of the first sensor, S1. This network is also the end of one of the TLs. The two other TLs are going ahead to the third network where the CM impedance of the motor can be seen. From this network a single TL runs to the second sensor, S2.

In order to calculate the coupling between the circuits, the transmission line parameters have to be calculated.

In this case there is a clear and well defined conductor which is common to all TLs. That conductor is the steel frame of the installation, which is chosen to be the return for the TLs. Any other conductor can be chosen as return conductor, giving the same result.

The next step is to calculate the TL parameters. The series impedance is usually the easiest one. Because of the high relative permeability of steel, the skin-depth has to be taken into account. The series inductance of the TLs can be calculated easily as well. The mutual inductance is more complex. The steel plate can act as an electro magnetic mirror which has to be taken into account.

## 4.5 Distributed source

A cable can carry a CM current which causes a DM voltage in that cable via the transfer impedance. If the cable is short compared to the wavelength of the CM current, the CM current distribution in the cable will be flat. As a result, the DM voltage can be computed easily using the following formula:

$$U_{DM} = Z_t^l I_{CM} l \quad (4.45)$$

This formula can not be used if the CM current distribution is not flat in the cable, which is the case if the cable is not very short compared to the wavelength and if reflections occur on either side of the cable. In that case the voltage generated via the transfer impedance is a distributed voltage source. In figure 4.4 the model is seen.

Another situation in which a distributed source model is applied to calculate the DM voltage on a transmission line is when an external EM field couples to the

line, as described in [53, 54, 55].

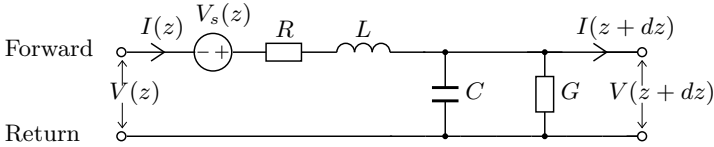


Figure 4.4: Infinitesimal part of a transmission line with distributed source  $V_s(z)$  of length  $dz$ .

## 4.6 Numerical modelling

In this part of the research no numerical modelling is used. However, the PhD student who is working at the TU Eindhoven on the same subject, is performing numerical simulations.

To simulate a complete installation numerically, which size can be hundreds or thousands of wavelengths, is a task which will take a huge amount of computer power. Therefore, the transmission line method is used in cases where possible. However, in cases where the transmission line method is not suitable, numerical simulations of (parts of) an installation have to be performed.

Numerical simulation is also a good method to determine the TL parameters, which can otherwise be very complex.

Numerical simulations can be used to determine TL parameters because of the complexity of analytical calculations in that case. It will be used next to measurements which have the same purpose.



# Chapter 5

## Coupling in a large-scale installation with underground cables

In the framework of the research several case studies have been performed, one of which will be described in this chapter.

In this case study the conducted interference produced by a VFD is measured, and the reduction of the disturbances by proper connection of the cable armour is determined. The work is a cooperation between the Technical University of Eindhoven and of the Technical University of Delft. The content of this section is published in short in a conference paper [56] and an IEEE transactions contribution describing the work in detail has been accepted for publication [57], number TEMC-128-2007.

### 5.1 Introduction

In a major project to establish proper EMC measures in large industrial installations [19], we want to come up with a data base of tested models for the design of large industrial electro technical installations with proper attention paid to EMC. It is desirable to put on all available metal for purposes of EMC, in order to improve the cost/benefit ratio. The section presents an example of a realised installation, where we predict ‘a posteriori’ the conducted emission from a variable frequency drive for an induction motor.



Figure 5.1: The trench with dozens of cables.

The model is based on available parameters or those that can be obtained from practical experience, and on parameters provided by additional dedicated measurements such as the transfer impedance of the cable. The aim is to assess the reduction of the conducted emission by the steel armour of a V0-YMvKas cable used as a shield. The code ‘V0-YMvKas’, describing the cable is explained in detail in [29]. The armour is primarily intended for protection against mechanical damage, such as intrusion of spades. Of course, shielded cables exist with much better performance. But still, the reduction by the armour is large enough not to be wasted.

The installation is a part of the waste-water purification plant ‘Dongemond’ located in Oosterhout (NL). The drives were installed in a control kiosk, and cables of the order of 100 m length connected drives and motors. The cables were buried in wet soil over most of their length; see figure 5.1. Safety regulations required armoured cables outdoor. The armours were treated as if they were a shield. Fol-



lowing good installation practise [8], the cable armour was clamped by a bracket to the grounded bare metal base plate on which the drive was mounted. At the motor end of the cable, a gland connected the armour to the motor chassis over the full armour circumference.

The switched-mode 7.5 kW variable frequency drive generates three-phase 400 V pulse width modulated signals at 3 kHz switching frequency. The motor has its windings in the usual delta configuration. The connection between the drive and this motor is an 85 m long V0-YMvKas cable with four 6 mm<sup>2</sup> solid copper leads. Three leads are used for the phases. The armour consists of 0.3 mm diameter steel wires in 8 bundles of 2 wires wound clockwise, and 8 bundles of 9 wires counterclockwise at the pitch of 38 mm and a weave angle of 47 degrees with respect to the cable axis; see figure 5.2. The open area between the 9-wire bundles is 0.8 mm wide. A 6 mm<sup>2</sup> straight bare copper litz is also embedded inside the armour as protective earth (PE) conductor. There is no further metal shield. The fourth lead in the cable is always connected in parallel with the PE litz at the cable ends.

We measured the output voltages and conducted interference produced by the drive. The net transient current of the three phase leads and the common mode current through the cable were determined at the drive and at the motor end of the cable by Fischer and Fluke current probes. The signals were recorded on digital scopes at each end (LeCroy and Tektronix); the triggers were synchronised by an optical fibre unit.

The model is based on a multi conductor transmission line (MTL) approach presented in [51], and also described in chapter 4. The transmission line (TL) which acts as source for the disturbances is composed of the three phase leads regarded as bundled single conductor and the armour plus PE and fourth lead regarded as return. The characteristic impedance and propagation speed of the internal TL were measured in the laboratory up to 10 MHz, as is to be discussed in Sect. 5.4. The measurements also provided the transfer impedance  $Z_t$  of the cable armour between the internal TL and a dedicated external circuit. At Dongemond, the external circuit is composed of the soil and the other cables in the trench, and we choose the source cable armour as common return. The excitation is distributed over the source cable length and occurs via the armour  $Z_t$ . We did not separately measure the soil properties like the conductivity  $\sigma_s$ , input for the determination of the parameters of the external circuit. First,  $\sigma_s = 10^{-2}$  S/m is a representative value for the wet soil in the western part of The Netherlands. The water table strongly influences the effective conductivity; it is maintained constant by the controlled drainage of the lands by mills. The cables lay at constant depth, except for a few meters at the ends. Second,  $\sigma_s$  enters the parameters as argument of a logarithm and little error is introduced by deviations from the actual  $\sigma_s$ . Third,

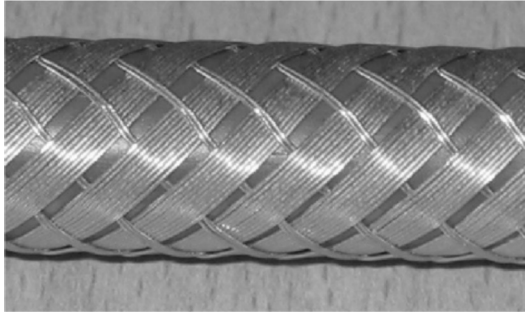


Figure 5.2: Photograph of cable armour, made of 0.3 mm diameter steel wires in 8 bundles of 2 wires wound clockwise, and 8 bundles of 9 wires counterclockwise.

the other cables in the trench are in parallel with the soil and take their share of the external current. These facts induce us to use constant TL parameters over the full length of the investigated cable. The ends are discussed in more detail in Section 5.7.

The goal of the investigation is three-fold: First we want to determine the disturbance levels in this installation. Second, we want to compare measurements with a model calculation. The model encounters several difficulties since several necessary details such as cable path or terminating impedances are only partially known. In addition, not all metal can be correctly included in the model, for instance reinforcement grids and bars of unknown interconnection. As a result, one has to make ‘educated guesses’ about their influence. The final goal of this experiment is to find out to what accuracy such estimates can serve to predict the coupling of interference originating in the drives to their environment, in spite of the uncertainties.

## 5.2 Choice of the various current loops

The circuits for the intended motor currents consist of the voltage sources U, V, and W in the drive, the three leads in the cable and the three phase windings of the motor (figure 5.3). These three currents are well balanced during the major part of the 3 kHz switching waveform, or in other terms for low frequencies. Long cables have large capacitances, which are to be charged/discharged by the drive output. Above a certain cable length, the manufacturer asks for a three phase choke (figure 5.3) to avoid activation of the internal overcurrent protection circuit, or to protect the drive against current surges. If a current flows through one of the

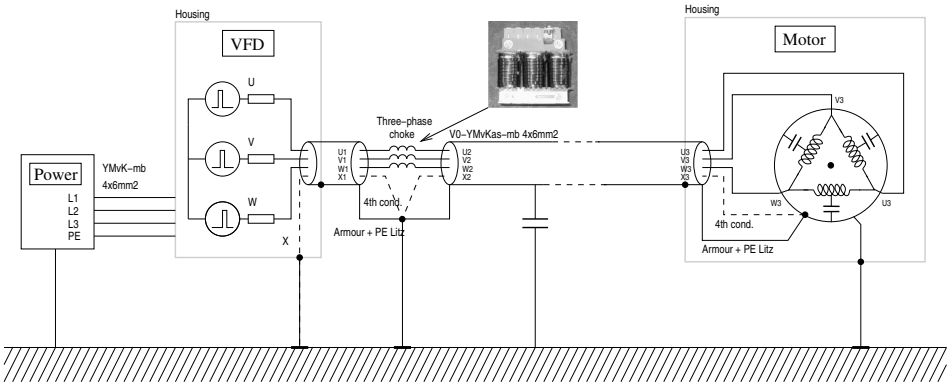


Figure 5.3: Setup of the installation. The inset is a photograph of the three-phase choke of the kind used in the installation.

leads and returns through the other two, the magnetic circuit closes in the core of the choke. The corresponding coupled inductance is typically about 1 mH, as has been found by measurement.

An unbalance in the three currents comprises a net current equally distributed over the three coil windings. The corresponding magnetic circuit closes via the large air gap of the surroundings. This occurs each time when one of the phases in the drive switches over between the negative and positive rail voltage. The average voltage of the three phases changes, and thereby the charge on the cable capacitances. The net current has  $\mu\text{s}$ -steep rise and fall edges, and is more intense when two phases switch simultaneously in the same direction, or when there is a jitter between phases in switching in opposite direction. Looking at the cable only, the return of this net current is the fourth lead in parallel with the PE litz and the cable armour.

For the analysis in this section, we then distinguish three current paths in the cable and its environment (figure 5.4): 1) the three phase leads considered as a bundle, 2) the soil with the other cables embedded and 0) the armour with the PE litz and the fourth lead. The choice of 1) is allowed, since the dominant interference is caused by the net current through the three phase leads. The three paths give two independent loops; transmission line TL1 comprises 1) and 0), whereas TL2 is made of 2) and 0). Instead of the usual choice of the soil, we have chosen 0) as common return. TL1 is terminated at the source end by the coil U2, V2, and W2 outputs bundled as single 'hot' terminal, and the local ground as 'cold' terminal. At the load end one finds the capacitances between the motor windings and its

chassis. Borrowing from common EMC language, one may consider TL1, source and load as the differential mode (DM) circuit with loop current  $I_{DM}$ . TL2 is then the common mode (CM) circuit. This name also indicates that the current in that loop is the algebraic sum of the currents through all conductors of the cable under discussion. A current probe around that cable will measure  $I_{CM}$ . The coupling between DM and CM circuit occurs via the transfer impedance, where we assume that the cable contribution is dominant. Although it is certainly important in the practical control room [58], we neglect in our model the CM current through other cables towards the drive, for instance the a.c. power leads.

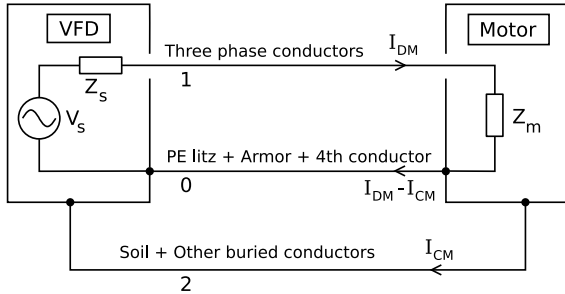


Figure 5.4: The CM and DM currents.

Figure 5.4 is a low frequency model. For frequencies where wavelength becomes comparable to the length, a transmission line model can be applied to take finite travel times into account.

### 5.3 Multi conductor Transmission Line approach

As mentioned in Sect. 5.2 we consider the parallel combination of armour, PE litz and fourth lead as reference conductor; it carries the current  $I_{CM} - I_{DM}$ . An infinitesimal section of the MTL is shown in the coupling model of figure 5.5, where only TL2 has been drawn. The quantities  $R'_x$ ,  $L'_x$ ,  $G'_x$  and  $C'_x$  are the per-unit-length transmission line parameters of TL $x$ . The coupling between TL1 and TL2 is represented by the circuit elements inside the dashed contour:  $R'_{12}$ ,  $L'_{12}$ ,  $G'_{12}$  and  $C'_{12}$ . The real and imaginary part of the transfer impedance are described by  $R'_{12}$  and  $L'_{12}$ , both depend on frequency because of the skin effect.

In the actual multi conductor transmission line (MTL) calculations we split the soil and the other cables and described them as individual TLs, numbered TL2 for the soil and up to TLN in figure 5.6. Network 1 describes the drive and choke, network 2 the motor. Both networks contain the connection to the return

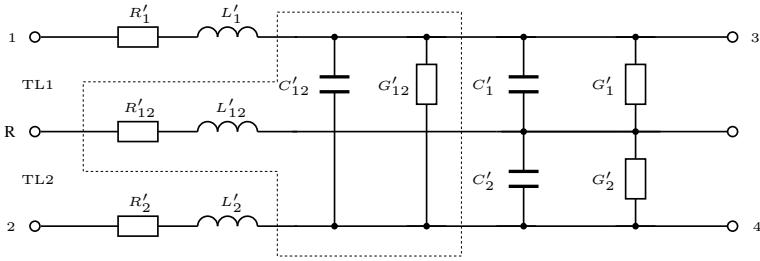


Figure 5.5: Infinitesimal transmission line part. TL1 is the bundle of three inner conductors and Return is the armour with the fourth conductor and PE litz. Here TL2 represents the soil and all other parallel cables.

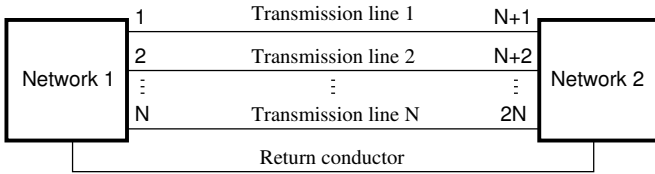


Figure 5.6: Model of the setup consisting of an  $N$ -conductor transmission line and two terminating networks, with node points numbered.

conductor.

We followed the approach of [51] to calculate the TL voltages and currents. The frequency response of the circuit is derived by assuming a 1 V sine wave voltage source at node 1 and calculating all voltages and currents at the frequencies of interest. The sample frequency used is 1.5 MHz and the number of samples is 256. The DM voltage generated by the drive is sampled, and converted to frequency domain via FFT, multiplied by the frequency response of the circuit, and finally transformed back to time-domain via IFFT.

## 5.4 Measurement of cable TL parameters

A 3.8 m long cable segment was tested in the laboratory. The cable was pressed in the corner of an aluminium L-shaped bar, see figure 5.7. The setup has two transmission lines: the inner circuit with three leads in parallel and the armour plus fourth lead and PE litz as return, and the outer consisting of the L and the return just mentioned. For both circuits we derived the transmission line parameters from the S-parameters measured with a vector network analyser (VNA) consisting of a

HP 4396A in combination with a  $S$ -parameters set HP 85046A. We limited the frequency band to 10 MHz. For the inner circuit or the cable itself, the reflection parameters  $S_{11}$  and  $S_{22}$  at the ports formed by nodes 1 and 3 were fitted to the following expressions [20]:

$$S_{11} = S_{22} = \frac{(\bar{Z}_0^2 - 1) \sinh(\gamma l)}{2\bar{Z}_0 \cosh(\gamma l) + (\bar{Z}_0^2 + 1) \sinh(\gamma l)}, \quad (5.1)$$

where  $\bar{Z}_0$  is the normalised characteristic impedance, which is  $Z_0/50$  and  $\gamma$  is the propagation constant given by:

$$\gamma = \alpha + j\beta = \sqrt{(R' + j\omega L')(G' + j\omega C')}. \quad (5.2)$$

Similarly, the transmission parameters  $S_{12}$  and  $S_{21}$  from node 1 to 3 and vice versa were fitted to

$$S_{21} = S_{12} = \frac{2\bar{Z}_0}{2\bar{Z}_0 \cosh(\gamma l) + (\bar{Z}_0^2 + 1) \sinh(\gamma l)}. \quad (5.3)$$

During these measurements the outer circuit was terminated at both ends into  $50 \Omega$  in order to reduce resonances. The same procedure is repeated for the the outer circuit on nodes 2 and 4, with the inner circuit terminated into  $50 \Omega$ . In this approach the coupling between the two circuits via the transfer impedance is neglected. The resulting TL parameters are given in Table 5.1 as characteristic impedance  $Z_0$ , propagation velocity  $v$  and  $\tan \delta$  for the damping. These parameters can be easily converted to the circuit parameters of figure 5.5. Please note that the parameters of the CM circuit (TL2) obtained here are different from the parameters in the actual installation with the cables in the soil.

### 5.4.1 Transfer parameters

The transfer impedance was obtained on a 1.2 m cable segment mounted in a similar L-shaped bar. Between 100 Hz and 1 MHz a sine wave generator ( $50 \Omega$

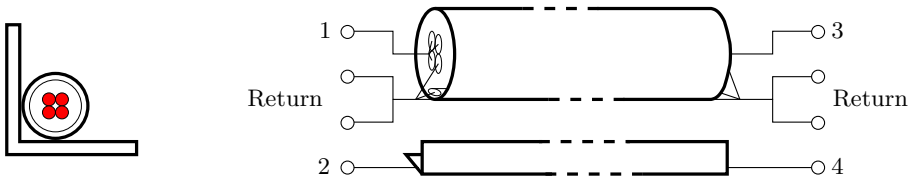


Figure 5.7: Setup to determine the transmission line parameters. Left: Cross-section of the setup. Right: Schematic representation; the numbers refer to the nodes in figure 5.6.

Table 5.1: Transmission line parameters derived by curve fitting of S-parameters.

Parameter	DM circuit (TL1)	CM circuit (TL2)
$Z_0$	18.5 $\Omega$	23.3 $\Omega$
$v$	$1.70 \cdot 10^8 \text{ m/s}$	$2.15 \cdot 10^8 \text{ m/s}$
$\tan(\delta)$	$10.2 \cdot 10^{-3}$	$24.2 \cdot 10^{-3}$
$L'$	127 nH/m	119 nH/m
$C'$	370 pF/m	220 pF/m

output) provided the current in one TL. The near end voltage induced in the other TL was measured by a lock-in detector over a 50  $\Omega$  termination; the far end of that TL was shorted. The resulting transfer impedance per meter length  $Z'_t$  is shown in figure 5.8. Guided by the observed behaviour as function of frequency, we fitted the  $|Z'_t|$  to the expression of the surface impedance  $Z'_s$  of a single equivalent round wire [59]

$$Z'_s(x) = R'_0 \frac{xJ_0(x)}{2J_1(x)}, \quad (5.4)$$

with  $R'_0$  the d.c. resistance of the wire and  $x = \sqrt{-jf/f_\delta}$ . Since the frequency variation of  $Z'_s$  only depends on  $R'_0$  and  $f/f_\delta$ , we do not specify the wire parameters further. However, for a single round wire of radius  $a$ , conductivity  $\sigma$  and magnetic permeability  $\mu$ , one would have  $R'_0 = 1/\pi a^2 \sigma$ . At the frequency  $f_\delta$  the skin depth  $\delta = \sqrt{2/\omega\mu\sigma}$  would be equal to  $a$ . The fitted parameters are  $R'_0 = 2.29 \text{ m}\Omega/\text{m}$  and the frequency  $f_\delta = 410 \text{ Hz}$ . The lower part of figure 5.8 shows that also the calculated phase of  $Z'_s$  is in good agreement with the measurements. Below 410 Hz the transfer impedance is about constant as determined by the parallel resistance of the PE litz, the fourth lead and the armour (1.34 m $\Omega$ ). In this measurement setup, the contact resistance of the connectors for the armour and PE litz add to  $R_0$ . Above 1 kHz the transfer impedance becomes proportional to the square root of the frequency, indicating a dominant surface skin effect. The near to constant phase angle of  $Z'_t$ , which is equal to  $\pi/4$  in good approximation, agrees with this interpretation. The low value of  $f_\delta$  indicates the predominance of the ferromagnetic armour in  $Z'_t$ . At frequencies between 300 kHz and 10 MHz the  $Z'_t$  has been determined with the VNA. In the region of overlap with the lower frequency data good agreement is observed. With open circuit terminations of inner en outer TL, the transfer admittance  $Y'_t$  has been determined. Below 10 MHz holds  $Y'_t = j\omega C'_{12}$  with  $C'_{12} = 0.23 \text{ pF/m}$ . With this low capacitance value, the coupling via  $Z'_t$  dominates the  $Y'_t$  contribution over the frequency range of interest. As a test, the measured  $Z'_t$  was used to calculate the transfer between both TLs in the setup with the 3.8 m long aluminium L-bar. Good agreement was obtained.

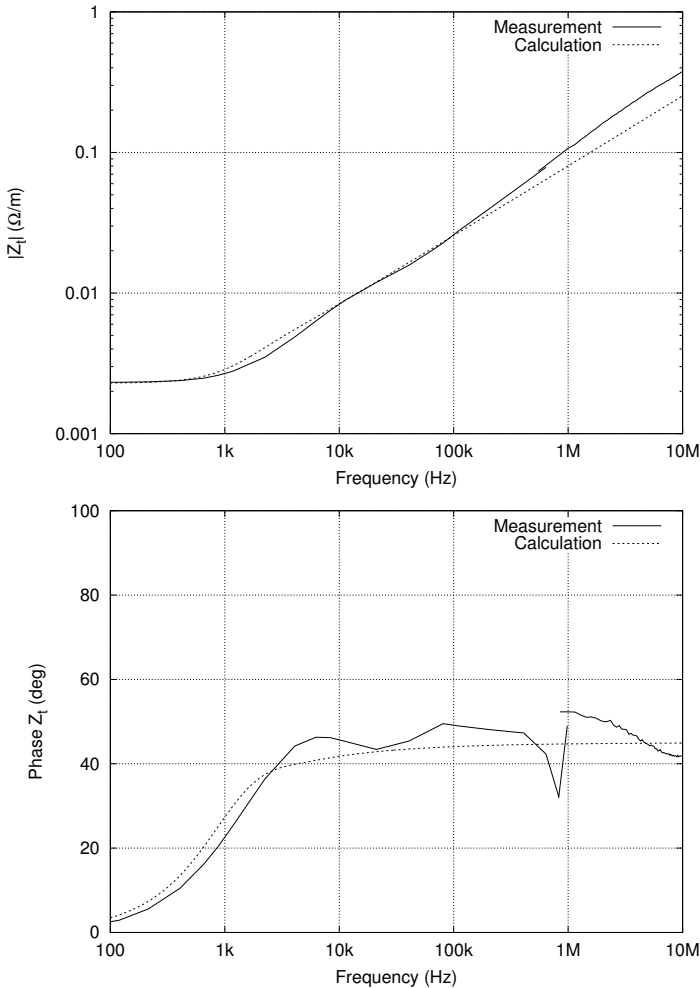


Figure 5.8: Measured amplitude and phase of the transfer impedance  $Z'_t$ . Below 100 Hz the phase rapidly tends to zero degrees. The graphs also show the  $Z'_t$  calculated from the fit to the low frequency data, extrapolated to 10 MHz. The deviations in phase just below 1 MHz are caused by the fact that two different measuring instruments are used, of which the one used below 1 MHz was at the top of its usable frequency range.



## 5.5 Modelling soil and other buried cables

As mentioned in Section 5.3, the soil is modelled as TL2 and the other buried cables as TL3 – TLN. We now present equations for the transmission line parameters in the form of per-unit-length impedance ( $Z'$  in  $\Omega/m$ ) and admittance ( $Y'$  in  $S/m$ ).

### 5.5.1 TL2

TL2 consists of the soil surrounding the cable as forward conductor and the armour of the cable as return conductor, separated by the PVC insulation of the cable. Expressions for the impedance and admittance of such a transmission line can be found in [60]. The impedance consists of the internal impedance of the soil  $Z'_g$ , the internal impedance of the armour  $Z'_i$  and the inductive reactance  $j\omega L'$  of the space occupied by the cable outer insulation. The internal impedance of the soil can be expressed analogous to (5.4) as:

$$Z'_g = R'_s \frac{x_s K_0(x_s)}{2K_1(x_s)}, \quad (5.5)$$

see e.g. [23, 61]. This expression can be approximated with excellent agreement by [62]:

$$Z'_g = \frac{j\omega\mu_0}{2\pi} \ln\left(\frac{1+x_s}{x_s}\right). \quad (5.6)$$

Here  $x_s = \gamma_s r_b$  and  $\gamma_s = \sqrt{j\omega\mu_s(\sigma_s + j\omega\epsilon_s)}$  is the propagation constant for a soil with conductivity  $\sigma_s$ , magnetic permeability  $\mu_s$  and electric permittivity  $\epsilon_s$ .  $R'_s = 1/\pi r_b^2 \sigma_s$  stands for the resistance per meter soil over the volume excluded by the cable. The outer radius of the cable including the insulation is  $r_b$ .

As mentioned in Sect. 5.1, the armour of the cable consists of  $8 \times 11$  parallel steel wires with a radius  $r_{sw} = 0.15$  mm (see figure 5.2). The pitch of the steel wire spiral is 38 mm. Combined with a radius of the armour  $r_a = 6.5$  mm, the total length of steel wire per spiral turn is 56 mm. If we neglect the interaction between neighbouring wires, the internal impedance is:

$$Z'_i = \frac{1}{8 \cdot 11} \frac{56}{38} Z'_s(x_{sw}), \quad (5.7)$$

with  $Z'_s(x_{sw})$  as in (5.4) with the parameters of the steel wires. Again, the ferromagnetic properties of the steel strongly increase  $Z'_i$  over a non-magnetic material like copper.

The self inductance of the space occupied by the cable outer PVC insulation is straightforward:

$$L' = \frac{\mu_0}{2\pi} \ln\left(\frac{r_b}{r_a}\right). \quad (5.8)$$

The total admittance is the series connection of the capacitance of the insulation gap and the admittance of the soil. The capacitance of the cable outer insulation is given by:

$$C' = \frac{2\pi\epsilon_i}{\ln\left(\frac{r_b}{r_a}\right)}. \quad (5.9)$$

In this equation  $\epsilon_i$  is the dielectric permittivity of the outer insulating. The admittance of the soil is approximated by

$$Y'_g \approx \frac{\gamma^2}{Z'_g}. \quad (5.10)$$

The upper part of figure 5.9 shows  $Z'_g$ ,  $Z'_i$  and  $j\omega L'$ , and the total series impedance  $Z'$ . One notes that the soil contribution mainly  $Z'_g$  determines  $Z'$  above 5 kHz. This cross-over frequency would be lower if the PE litz and 4th conductor would contribute to  $Z'_i$ . The lower part shows  $Y'_g$  and  $j\omega C'$  and total  $Y'$ . Here the cable insulation dominates in  $Y'$  over the frequency region of interest, i.e. below 750 kHz.

### 5.5.2 TL3 – N

The impedance of these TLs is consists of twice the  $Z'_g$  of the cable in the soil (5.5) and twice the  $Z'_i$  of (5.7). The additional coupling between the cables via the magnetic field in the soil can be expressed by a mutual impedance  $M'$  in  $-2j\omega M'$ . We followed the approach by [63, Eq. 4.44]:

$$M' = \frac{\mu}{2\pi} [K_0(\gamma d) - K_0(\gamma d_i) + W(\gamma d_i)], \quad (5.11)$$

where

$$W(\gamma d_i) = 2 \int_0^\infty \frac{e^{-2z\alpha} \cos(ud)}{\alpha + u} du. \quad (5.12)$$

In this equation,  $d$  is the distance between the cables,  $\alpha^2 = \gamma_s^2 + u^2$  and  $d_i = \sqrt{d^2 + 4z^2}$ , where  $z$  is the burial depth of the cables. Please note the change in variables with respect to [63]. We used  $d = 2$  cm and  $z = 1$  m. The integration of (5.12) has been carried out numerically up to an upper boundary  $u = 10$ . If we increased the upper boundary from  $u = 10$  to  $u = 100$  the relative change in  $W$  was  $10^{-8}$ , indicating sufficient convergence.

### 5.5.3 Coupling between TL2 and other buried cables

The coupling between TL2 and a nearby buried cable is a coupling of the electromagnetic fields in the soil (TL2) to the armour of an other cable. This coupling

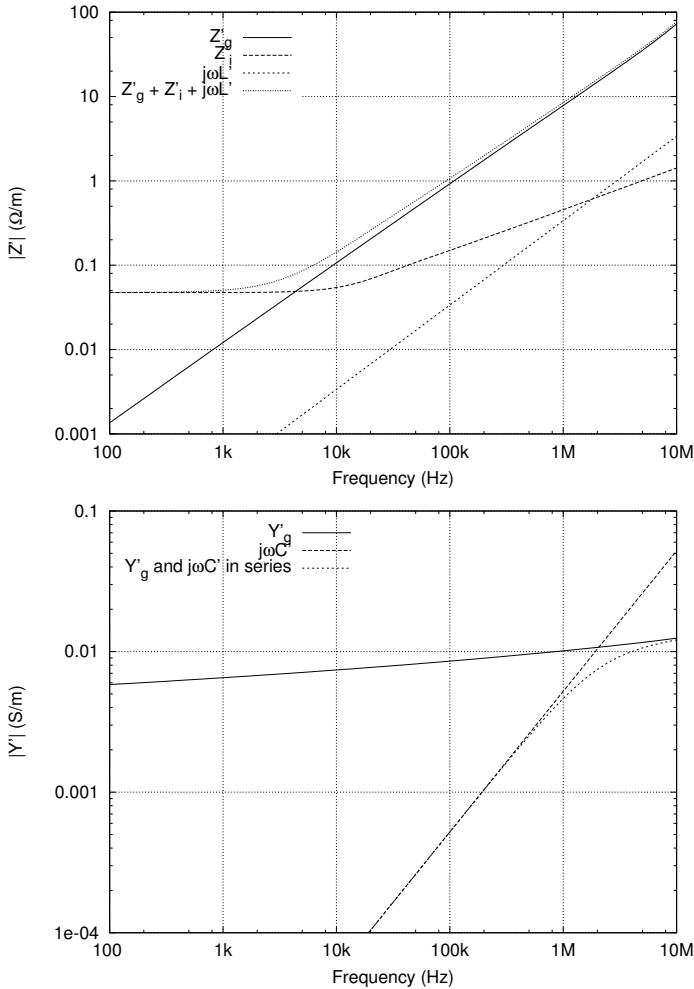


Figure 5.9: The contributions to the impedance (top) and to the admittance (bottom) by the cable and by the soil. The cable dimensions have been mentioned in the main text. The soil parameters were  $\sigma_s = 0.01$  S/m,  $\mu_s = \mu_0$  the magnetic permeability of vacuum and  $\epsilon_s = 10\epsilon_0$  with  $\epsilon_0$  the permittivity of vacuum. For the steel wire we used  $\sigma_{sw} = 10^7$  S/m and  $\mu = 500\mu_0$ , for the PVC cable insulation  $\epsilon_i = 4\epsilon_0$ .

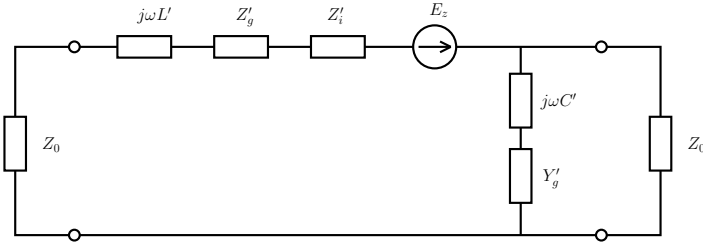


Figure 5.10: Infinitesimal part of transmission line formed by a buried cable in the soil.

is comparable to the coupling of lightning induced fields in the ground to buried cables which is described in [62]. Their model is valid until 30 MHz, which is far beyond our maximum frequency of 750 kHz, which makes their approach usable in our situation. The buried cable in the ground is modelled as a transmission line with a series voltage source  $E_z$ , see figure 5.10. The voltage of this source is equal to the tangential electric field at the location of the cable. The electric field parallel to the cable as a function of the distance to the cable,  $r$ , generated by the current  $I$  in the armour is given by:

$$E_z = \frac{\gamma_s I K_0(\gamma_s r)}{2\pi\sigma_s r_b K_1(\gamma_s r_b)}. \quad (5.13)$$

As can be derived from figure 5.10 the voltage per meter over the armour of the other buried cable is given by:

$$V = \frac{Z'_i}{Z'_i + Z'_c} E_z, \quad (5.14)$$

where

$$Z'_c = Z'_g + j\omega L' + Z_0 + \frac{Z_0(j\omega C' + Y'_g)}{Z_0 j\omega C' Y'_g + j\omega C' + Y'_g}, \quad (5.15)$$

and  $Z_0$ ,  $Z'_i$ ,  $Z'_g$ ,  $Y'_g$ ,  $L'$  and  $C'$  are equal to the parameters of TL2.

## 5.6 Simulation results for the actual installation

The DM current primarily depends on the TL1 parameters given above. The coupled inductance of the choke has been determined by interconnecting the three input terminals U1, V1, and W1 at one side and interconnecting the three output terminals U2, V2 and W2 at the other side. The inductance between the “1” and the “2” sides is 4.4  $\mu\text{H}$  over the frequency range of interest, as measured by an

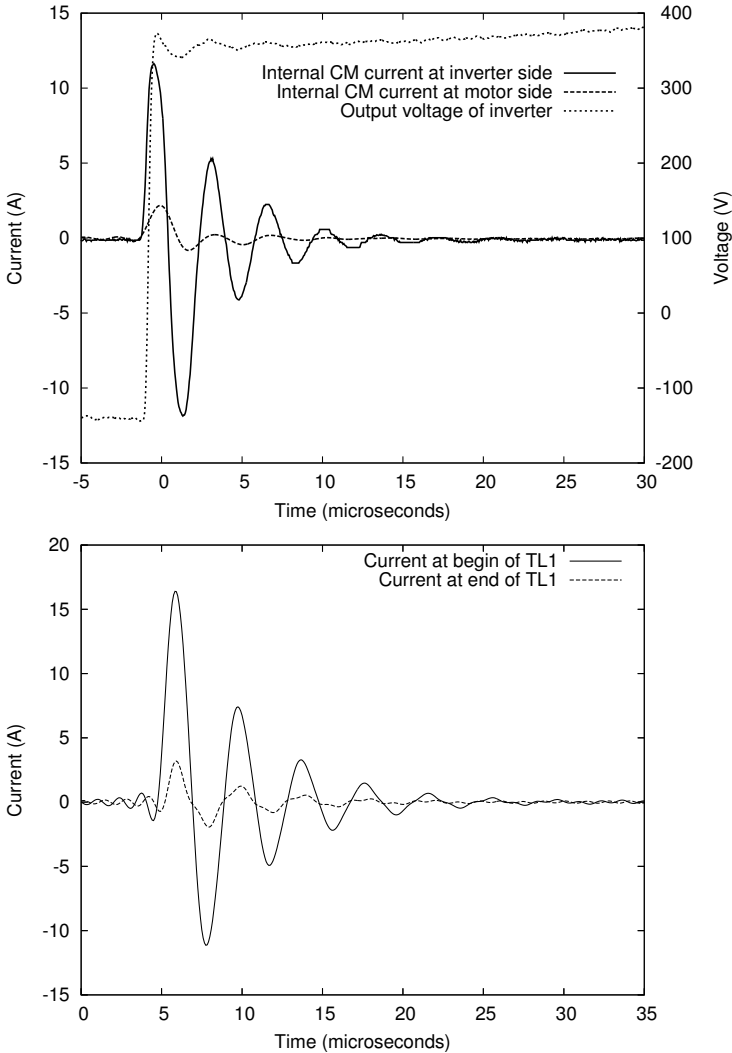


Figure 5.11: Time domain result of both the measurements (top) and the calculations (bottom). The plots give the results for the inner conductors, which is called TL1 in the simulations. The voltage step, causing the currents, is shown in the top plot.

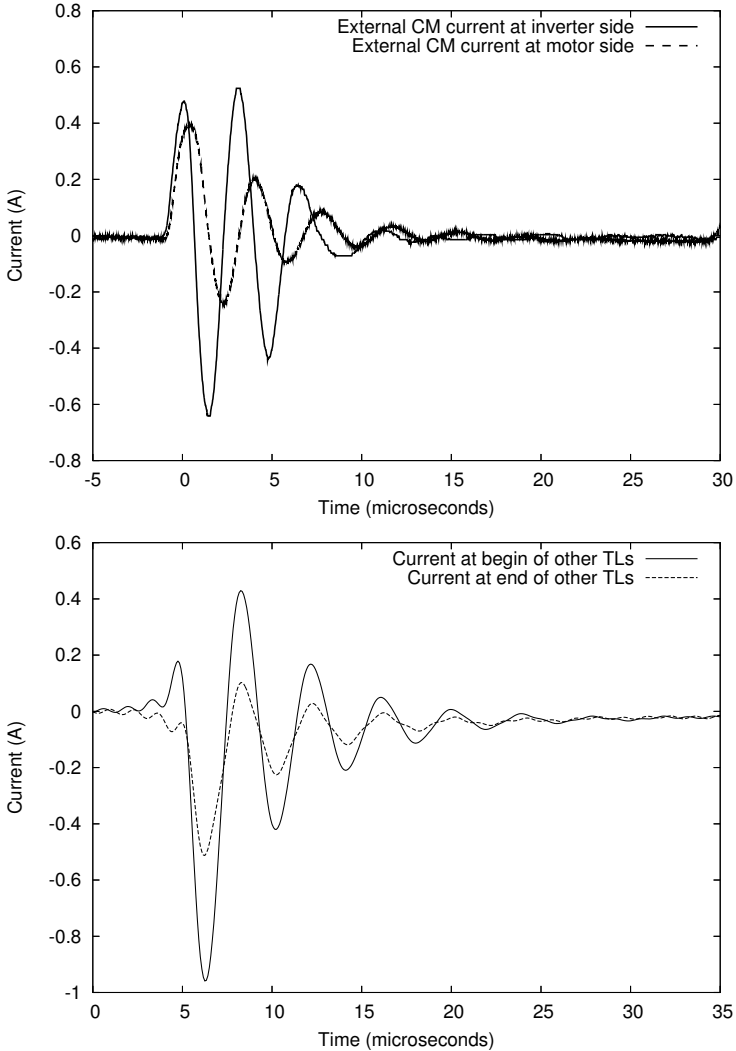


Figure 5.12: Time domain result of both the measurements (top) and the calculations (bottom). The plots give the results of the summation of the currents in all TLs except TL1.

Table 5.2: Simulated values of DM and CM currents at inverter- and motor side. The 300 kHz data assume a 1 V excitation at node 1. The simulated time domain data are the peak-to-peak values for a voltage rise at node 1 of 347 V.

		simulated			measured
$\sigma$ (S/m)		$10^{-2}$	50	$10^{-2}$	
#other cond. $n$		0	0	4	
300 kHz	TL1 begin	0.13	0.13	0.13	
	TL1 end	0.019	0.019	0.019	
	TL2-N begin	$1 \cdot 10^{-4}$	$6 \cdot 10^{-3}$	$7 \cdot 10^{-3}$	
	TL2-N end	$1.6 \cdot 10^{-5}$	$2.3 \cdot 10^{-3}$	$1.8 \cdot 10^{-3}$	
time domain	TL1 begin	25	25	26	23.4
	TL1 end	4.5	4.5	5.0	4.9
	TL2-N begin	0.021	1.4	1.5	1.12
	TL2-N end	0.004	0.5	0.6	0.6

Agilent 4263B impedance meter. The internal impedance of the inverter is assumed to be negligible compared to the choke impedance. The motor windings have a capacitance of 4.16 nF with respect to the chassis, as measured for the three phase windings together. With these parameters the lowest resonance frequency of TL1 and its terminations is in good agreement with the observed 300 kHz ringing found in the measurements (see figures 5.11 and 5.12). At this frequency the calculated ratio of the DM current at the drive to the DM current at the motor is about a factor of 5, as is also seen in the measurement results presented in Table 5.2. The time domain DM current has been calculated as the response to a slope limited voltage step of at node 1 (see figure 5.11). The supply voltage in the drive is 260 V for each polarity. In the selected data two phase switched simultaneously, which is equivalent to a source voltage at node 1 of  $2/3 \times 520 = 347$  V. The calculated DM current peak-to-peak value agrees well with the measurement.

The external TLs are modelled as parallel lines. However, in the actual installation these are less well known, because there are many possible current paths outside the TL1 cable of interest: the soil, other cables and the concrete reinforcement. To cope with this uncertainty we compare three situations, 1) TL1 is a single buried cable in the soil with a conductivity  $\sigma$  of  $10^{-2}$  S/m common for wet soil, and no other conductors in the neighbourhood, and 2) the other conductors simulated by an adapted soil conductivity of 50 S/m. In both cases we use the approximations for the TL2 impedance and admittance given by Vance [60, Ch. 4], and we assume that TL2 is terminated into a short circuit to the common return at both ends.

In Table 5.2 the following results have been summarised:

- The simulated time domain CM current for the common soil is too small by a factor of 150, so the other conductors must be taken into account.

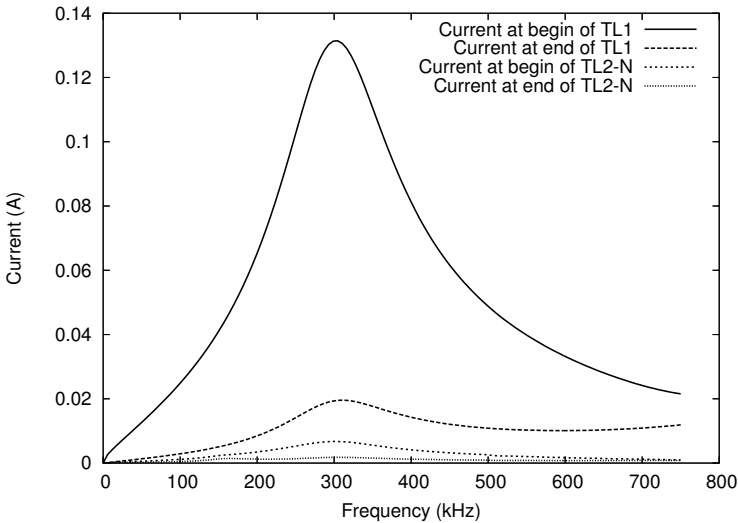


Figure 5.13: Frequency domain result of calculation of the TL currents for 1 V excitation at node 1. The ratio of the current at begin of TL1 to the current at the end of TL1 at 300 kHz is about 5. This is the simulation with four other buried conductors.

- The soil conductivity of 50 S/m gives reasonable agreement between the simulated and measured time domain CM current. Close to the drive, the ratio of the currents in TL1 and TL2 is about a factor of 20. The current ratio at begin and end of TL2 is about 2.5.
- If four other cables ( $n = 4$ ) are taken into account, see figure 5.14, the simulated currents are in reasonable agreement with the measured currents. Figures 5.11, figure 5.12 and 5.13 present the TL currents for this case.

## 5.7 Discussion

The prominent feature in the measured currents is the 300 kHz ringing frequency. The TL1 cable parameters and 4.16 nF capacitance at the motor end have been measured with an accuracy of the order of 1%. The actual length may vary by about 5 percent from the 85 m used in the calculation. The 4.4  $\mu$ H self inductance of the choke is essential to obtain agreement between measured and calculated resonance frequency and current amplitude.

The other cables are necessary in the model, to explain the observed CM current. The second model which relies on the soil alone, needs an unrealistically high



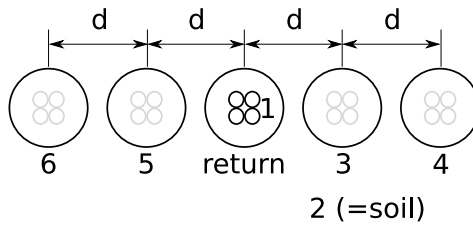


Figure 5.14: Arrangement of four other buried conductors. The numbers refer to the transmission line numbers. The distance  $d$  between the cables is 2 cm.

conductivity of 50 S/m.

The other cables in the ground are taken into account by regarding them as additional transmission lines which have the same length and follow the same path as TL1. All other motor drives are placed next to each other in the control kiosk. The motors are all connected to the local grounding which includes the concrete reinforcement. We assumed that this distributed grounding acted as a single connection for the CM current. Further modelling would require detailed information about all connections, which was not available.

As figure 5.1 shows, the many parallel cables form a spaghetti cluster, rather than a strictly parallel set of cables. In principle, a statistical model should have been more adapted to describe the TL3 and higher. Such models have been proposed, see e.g. [64]. However, we checked the sensitivity of the calculations results to the number of parallel cables. An increase of the number of cables in our model from 4 to 6 did barely alter the CM current. We did not measure the individual CM currents through the other cables.

The accuracy of the soil parameters is less important, because the soils carries only a small current and because these parameters enter the calculations primarily as part of the argument of a logarithm.

The four leads of the TL1 cable are positioned in a square arrangement. The symmetry is reflected in the current/voltage patterns of the four normal transmission modes. The PE litz inside the shield then destroys the precise fourfold symmetry of the configuration, complicating the mode patterns. Slight differences in propagation speed and damping between the modes might be expected. We therefore measured the effective TL parameters with the cable connected as in the practical situation: three phase leads bundled and the fourth lead grounded to PE litz and armour. Over the frequency band below 1 MHz, the differences in mode propagation are not important. If the measurement and modelling would be extended to higher frequencies, such differences would certainly have to be accounted for. The measurements were performed with eight bits resolution. The spectra did not

show sufficiently clear high frequency features to warrant a detailed analysis.

The transfer impedance  $Z'_t$  has been measured in the same configuration, three leads combined, and the fourth lead plus PE litz connected to the shield at the ends. It is to be expected that the  $Z'_t$  depends on the shape of the outer return, and on the position of PE litz with respect to the external conductor. Also the position of the fourth lead varies over the length, since the inner leads spiral around the cable axis. We checked the variation of  $Z'_t$  with the L-bar (Sect. 5.4) replaced by a 20 cm wide copper foil at a few distances up to 5 cm, and with the cable rotated over its axes. The  $Z'_t$  values remained to within 15% equal to the data of figure 5.8.

With its total coupled inductance of  $4.4 \mu\text{H}$ , the choke is not very effective to reduce the net current through the three phase leads. Another approach makes a more effective use of the fourth lead: install a balancing transformer with four windings on a single yoke with closed magnetic circuit. Such a transformer forces the net current through the three phase leads to return through the fourth lead. This approach relieves the requirements on the armour or a shield, but does not necessarily make these superfluous. The transformer has indeed been used in a practical situation [65] with good result.

## 5.8 Conclusion

The results of a field measurement in a complex industrial installation have been presented. A careful connection of a steel armour – as if it was a high quality shield – reduces the interference by about a factor of 20 (95% of the disturbing current is flowing back in this shield in stead of in other cables).

The calculated differential mode and common mode currents agree well with measurements. The armour of the neighbouring cables provide a low impedance path for the common mode currents. The soil is less important as CM return in this installation.

In the model the other buried conductors are short-circuited to the return conductor at the begin and end of the TLs. This appears to be a good approximation although in reality the other TLs are longer than the one under consideration.

# Chapter 6

## Case studies of parts of installations

In the previous chapter the most extended case study performed in the framework of the research has been described. In this chapter, four case studies are described related to parts of installations. Some of the case studies are related to coupling between cables, others to EMC parameters of cables. The purpose is to show applications of the modelling and measurement methods described in this thesis.

The first case study deals with cross coupling between two wires with a common return path. This well controlled experiment is used to check the implementation of the modelling method described in chapter 4.

The transfer impedance, which is an important parameter describing the quality of cables in terms of EMC, is measured as well as calculated in the third case study of a coaxial cable and in the fourth example of a two-conductor non-coaxial cable.

In the final case study the measurement of the CM current distribution in a single conductor cable is measured.

### 6.1 Two conductors parallel to a metal plate

*Goal: if a cable carries a CM current, what current will flow in a nearby cable? This current, in turn, causes a DM voltage in that cable.*

In this section the crosstalk between two wires is measured and calculated. The two wires are located parallel to each other and both are parallel to a metal plate. So, the setup can be regarded as a combination of two TLs, where each TL consists

of a copper wire as one conductor and the steel plate as the other conductor. Thus, the plate is a common conductor to both TLs.

First the TL properties of one TL are calculated and compared with measurements. After that the TL parameters necessary for calculating the crosstalk are derived. These parameters are needed to calculate the coupling between the two TLs using the MTL approach described in chapter 4. Next to the MTL calculation, the crosstalk is calculated using CST Studio Suite (TM) 2008, an EM simulation program, based on the finite integration technique (FIT) [66, 67]. Finally the calculated results are compared with measurements, both in frequency- and time-domain.

### 6.1.1 Asymmetrical transmission lines

The asymmetrical TLs dealt with in this section consist of a round copper wire as the one conductor and a steel plate as the other conductor. In figure 6.1(a) the setup is shown. The TL under consideration is the one connected to the vector network analyser (VNA). The other TL is loaded with  $50 \Omega$  at both sides during the measurements.

The metal plate that acts as common return is made of steel and has a thickness of 1 mm. Its width is 20 cm. At both sides a part of the plate of 5 cm is bended under an angle of  $90^\circ$  to give strength to the plate. At both ends a part of the plate of 4 cm is bended under an angle of  $90^\circ$  to mount BNC-connectors. The inner conductors of these connectors are connected to the solid copper wires which have a radius of 1 mm. The wires are both at a height of 20 mm above the steel plate. The wire of the TL under consideration is at a distance of 20 mm from the edge of the plate while the other is at the centre of the plate and thus the distance between the wires is 8 cm.

The TL parameters  $L'$  and  $C'$  of these lines can be calculated using the formula's given in, among others, [21]. The inductance per unit length is:

$$L' = \frac{\mu}{2\pi} \cosh^{-1} \left( \frac{h}{r} \right) \quad (H/m) \quad (6.1)$$

In this expression,  $h$  is the distance between metal plate and centre of the wire and  $r$  is the radius of the wire. The capacitance per unit length is given by:

$$C' = \frac{2\pi\epsilon}{\cosh^{-1} \left( \frac{h}{r} \right)} \quad (F/m) \quad (6.2)$$

If the dimensions are filled in according to figure 6.1,  $C' = 15.1 \text{ pF}/m$  and  $L' = 0.74 \text{ } \mu\text{H}/m$ .

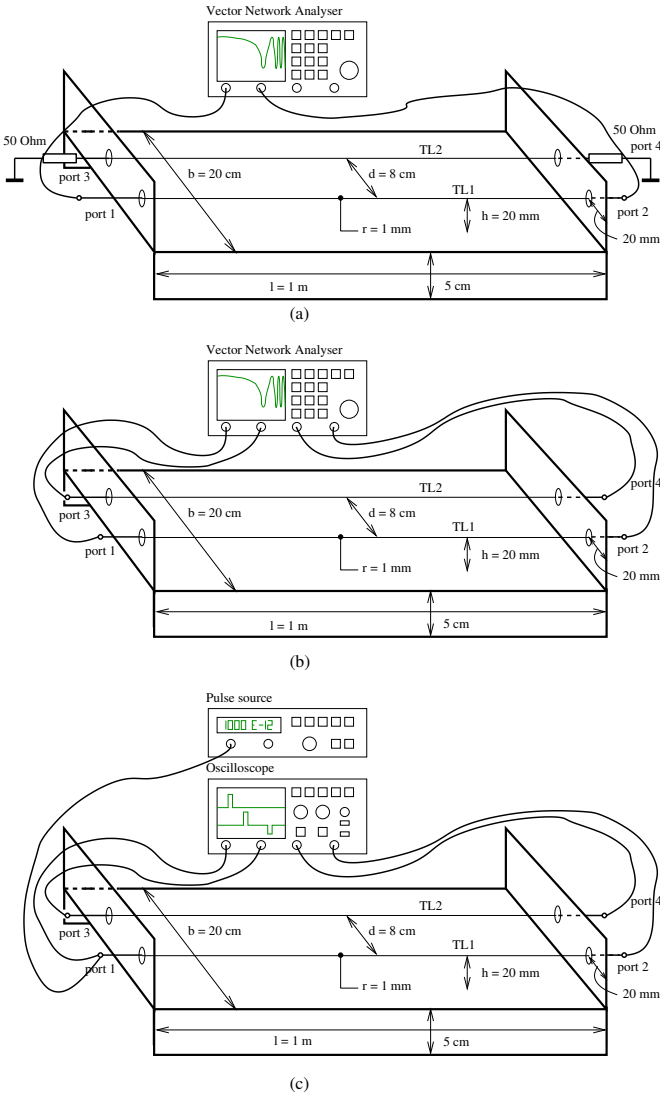


Figure 6.1: Steel plate with copper wires used in the experiment. (a) Measurement setup for S-parameters of single transmission line. (b) Measurement setup for measuring the crosstalk in frequency domain. (c) Setup for measurement of crosstalk in time domain.

The third TL parameters,  $R'$ , is the sum of the impedance of the metal plate  $Z'_{plate}$  and that of the copper wire  $Z'_{wire}$ .

The skin effect has to be taken into account if the skin depth is smaller than the cross-sectional dimensions of the conductors. At the lowest measurement frequency, 300 kHz, the skin depth, expressed as

$$\delta = \frac{1}{\sqrt{\pi f \mu \sigma}} \quad (m) \quad (6.3)$$

is 0.12 mm. for copper and 0.01 mm. for steel. The permeability of steel is in the range of 800–1100 [68]. In this case a relative permeability of 800 is used. The conductivity  $\sigma_s = 10 \cdot 10^6 S/m$  for steel and  $\sigma_c = 60 \cdot 10^6 S/m$  for copper. So, in this case the skin-effect has to be taken into account. As a result,  $R'$  will be complex and dependent on frequency. Assuming a uniform current distribution on the surface of the wire with a depth equal to the skin-depth, the impedance of the wire is approximated as:

$$Z'_{wire} = \frac{1+j}{\sigma_c 2\pi r \delta_c} = \frac{(1+j)\sqrt{\omega\pi 2 \cdot 10^{-7} \mu_r \sigma_c}}{2\pi r \sigma_c} \quad (\Omega/m) \quad (6.4)$$

In this formula  $\sigma_c = 60 \cdot 10^6 S/m$  is the conductivity of copper,  $\delta_c$  is the skin depth of copper and  $\mu_r = 1$  is the relative permeability of copper. The impedance of the plate will be approximated as follows: The current is supposed to be distributed uniformly in a layer with thickness  $\delta_s$  and width  $b=20$  cm, as indicated in figure 6.1. In reality, the current will be concentrated under the copper wire resulting in a higher impedance of the plate. In appendix B an approximation will be given, taking into account the current distribution. The impedance is expressed as:

$$Z'_{plate} = \frac{1+j}{\sigma_s b \delta_s} = \frac{(1+j)\sqrt{\omega\pi 2 \cdot 10^{-7} \mu_r \sigma_s}}{\sigma_s b} \quad (\Omega/m) \quad (6.5)$$

The fourth TL parameter,  $G'$ , which is the conductance of the surrounding air, is zero.

The before mentioned transmission line parameters are used to calculate the characteristic impedance  $Z_0$  and propagation constant  $\gamma$ :

$$Z_0 = \sqrt{\frac{Z'}{Y'}} = \sqrt{\frac{R' + j\omega L'}{G' + j\omega C'}} \quad (\Omega) \quad (6.6)$$

$$\gamma = \sqrt{Z'Y'} = \sqrt{(R' + j\omega L')(G' + j\omega C')} \quad (m^{-1}) \quad (6.7)$$

The characteristic impedance and the propagation constant are, in turn, used to calculate the S-parameters and compare them to the parameters measured with

the network analyser [20]. The reflection is given by:

$$S_{11} = S_{22} = \frac{(\bar{Z}_0^2 - 1) \sinh(\gamma l)}{2\bar{Z}_0 \cosh(\gamma l) + (\bar{Z}_0^2 + 1) \sinh(\gamma l)} \tag{6.8}$$

where  $\bar{Z}_0$  is the normalised characteristic impedance, which is  $Z_0/50$ . Similarly, the transmission parameters  $S_{12}$  and  $S_{21}$  are given by:

$$S_{21} = S_{12} = \frac{2\bar{Z}_0}{2\bar{Z}_0 \cosh(\gamma l) + (\bar{Z}_0^2 + 1) \sinh(\gamma l)} \tag{6.9}$$

The result of the measurement as well as of the calculation is shown in figure 6.2. From the figure it is clear that they agree well, which means that, in this case, this calculation of TL parameters is sufficient.

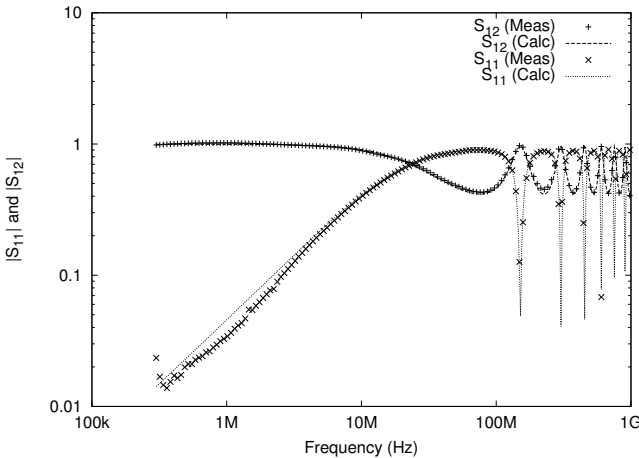


Figure 6.2: Comparison of measured and calculated S-parameters of figure 6.1(a).

### 6.1.2 Symmetrical transmission line

The two conductors together also form a TL. Although this TL is not used in the calculation of the crosstalk between the two conductors, its characteristics are determined here to show an effect that is not observed in the other TLs at the frequencies where the measurements are performed.

In this case the steel plate is *not* part of the transmission line. Nevertheless, it has influence on the TL parameters because it acts as a mirror to the electric fields.

The inductance and capacitance per unit length, without taking the steel plate into account, are given by:

$$L' = \frac{\mu}{2\pi} \ln \left( \frac{d^2}{r_1 r_2} \right) \quad (H/m) \quad (6.10)$$

$$C' = \frac{2\pi\epsilon}{\ln \left( \frac{d^2}{r_1 r_2} \right)} \quad (F/m) \quad (6.11)$$

Filling in the distance between the wires  $d = 8 \text{ cm}$  and radii of the wires  $r_1 = r_2 = 1 \text{ mm}$  results in:  $C' = 6.34 \text{ pF/m}$  and  $L' = 1.75 \text{ } \mu\text{H/m}$ .

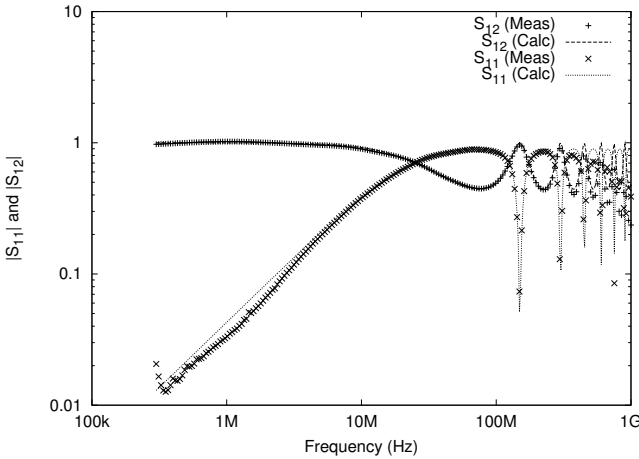


Figure 6.3: Measurement and calculation of balanced S-parameters of situation of figure 6.1(b).

If the steel plate is taken into account by regarding it as a perfect mirror, the inductance between the two copper conductors at heights  $h_1$  and  $h_2$  above the plate, can be calculated as:

$$L' = \frac{\mu}{2\pi} \ln \left( \frac{d}{r_1} \right) + \frac{\mu}{2\pi} \ln \left( \frac{d}{r_2} \right) - \frac{\mu}{2\pi} \ln \left( \frac{d'}{2h_1} \right) - \frac{\mu}{2\pi} \ln \left( \frac{d'}{2h_2} \right) \quad (H/m) \quad (6.12)$$

The heights of the copper conductors above the return plate are both equal to 2 cm. In this case:  $h_1 = h_2 = h = 2 \text{ cm}$  (see figure 6.1). The distance between a conductor and the image of the other conductor is  $d' = \sqrt{d^2 + (2h)^2}$ . The first two terms on the right hand side express the self inductance in case the steel plate is absent. These two terms together are equal to (6.10). The last two terms are



related to the flux contribution of the images of the two conductors where the steel plate acts as a mirror. The expression can be rewritten as:

$$L' = \frac{\mu}{2\pi} \ln \left( \frac{4h^2 d^2}{4h^2 r^2 + d^2 r^2} \right) \quad (H/m) \tag{6.13}$$

Calculating the transmission line parameters based on this equation results in an inductance of  $L' = 1.43 \mu H/m$  and a capacitance of:

$$C' = \frac{\mu\epsilon}{L'} \quad (pF/m) \tag{6.14}$$

which results in  $7.78 pF/m$ .

The measurements of the S-parameters is done by the ‘balanced’ option of the vector network analyser. In this case all four ports are used, see figure 6.1(b). The analyser makes combinations of two ports, resulting in two balanced ports. The two ports on the left side form one balanced port and the two ports on the right side form the other balanced port.

In figure 6.3 the result of the measurement of the balanced transmission properties are shown. In the same figure the calculated S-parameters are shown, where the TL parameters are used with the steel plate taken into account. Note that for the calculation the  $\bar{Z}_0$  in eqs. (6.8) and (6.9) must be  $Z_0/100$  because in case of a balanced measurement the internal impedance of the VNA is  $100 \Omega$  in stead of  $50 \Omega$ .

The measured S-parameters are deviating clearly from the calculated ones above 300 MHz, where the emission of energy from the line can no longer be neglected. At this frequency the distance  $d$  between the lines is approximately  $(1/12)^{th}$  of a wavelength:  $d = 0.08 \lambda$ . In [69], where the antenna behaviour of an open-wire transmission line is researched, the emission is 0.1% at the frequency where  $d = 0.02 \lambda$  and 1.3% where  $d = 0.07 \lambda$ .

## Conclusion

The MTL approach is applicable in the frequency range where the maximum distance between the conductors does not exceed  $(1/12)^{th}$  of a wavelength.

### 6.1.3 Coupling between the two lines in frequency-domain

In order to calculate the coupling between the two lines four more TL parameters are needed: The mutual inductance and capacitance between the two TLs, the conductance between them and the transfer impedance caused by the common return.

In the calculation of the mutual inductance between the two lines the steel plate is taken into account as a mirror, like in the case of the balanced TL:

$$M'_{12} = \frac{\mu}{2\pi} \ln \left( \frac{\sqrt{d^2 + 4h^2}}{d} \right) \quad (H/m) \quad (6.15)$$

Filling in results in  $M'_{12} = 22.3$  nH/m. The mutual capacitance between the two lines is expressed as:

$$C'_{12} = \frac{\mu\epsilon}{M'_{12}} \quad (F/m) \quad (6.16)$$

Filling in results in  $C'_{12} = 498$  pF/m.

The conductance between the two lines is ignored again because the medium between the two lines consists of air.

The last parameter influencing the coupling is the transfer impedance. The transfer impedance in this case is equal to the impedance of the common return path which is the metal plate. In the equation to calculate the impedance given in (6.5) the current is assumed to flow uniformly over the width of the plate. However, the current tends to concentrate under the copper conductor, which effect increases with frequency. This results in a higher impedance than calculated by (6.5), about three times higher at 1 GHz in our case. In appendix B a description is given how to take the current distribution in the metal plate into account. Equation (B.3) is used to calculate the impedance of the metal plate.

The coupling between the two TLs can now be calculated using the MTL approach outlined in chapter 4. The parameters calculated in section 6.1.1 and the current section are used. The measurement is performed with the setup sketched in figure 6.1(b).

Next to the MTL calculation, the coupling is calculated using an EM-simulation program. The BNC connectors are modelled as coaxial structures with an inner conductor radius of 1 mm, an outer conductor inner radius of 2.3 mm and vacuum isolation, making it a 50  $\Omega$  coaxial waveguide. The length of the BNC connector model is 20 mm, extending out of the metal plate. The calculated S-parameters are referenced to the ends of the BNC-connectors. The EM-simulation is based on a time-domain calculation. The frequency-domain result is calculated via DFT. Thus the package gives results in both frequency- and time-domain. Both results are compared to MTL-calculations and measurements. The results of measurements and calculations in frequency-domain are given in figures 6.4 and 6.5.

### 6.1.4 Coupling between two lines in time-domain

To check the calculations a measurement is performed in time domain where TL1 is used as the line carrying a signal that is coupled to TL2. The setup is shown

in figure 6.1(c). A very short pulse (length  $\approx 2$  ns) is generated at the beginning of TL1. The voltages at the four connections of the setup are measured: at begin and end of TL1 and at begin and end of TL2.

The result of the measurements as well as of the calculations are shown in figure 6.6 and 6.7.

It can be seen that the amplitudes of the calculated pulses and the time difference between them show good agreement with the measurements.

In the measurements, after each pulse an oscillation can be seen which does not appear in the calculations. The oscillation has a half-period of approximately 1.4 ns, which corresponds to a travelling distance in free space of 20 cm. This is equal to the width of the metal return plate.

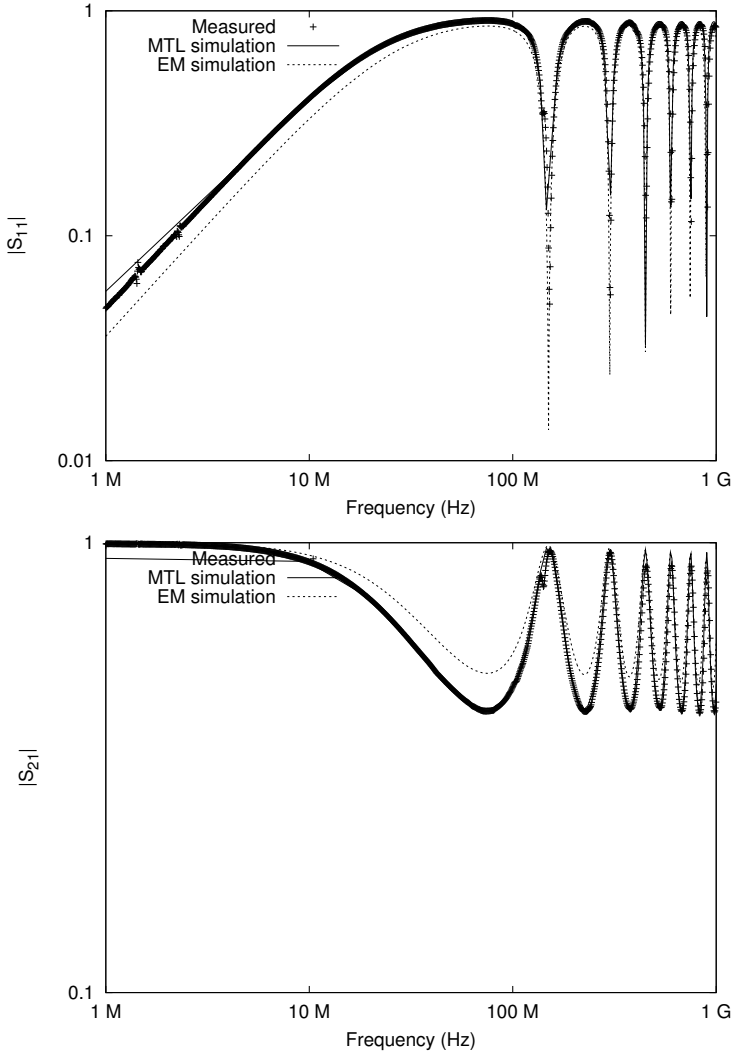


Figure 6.4: S-parameters in frequency-domain. Top: the reflection parameters. Bottom: the transmission parameters.

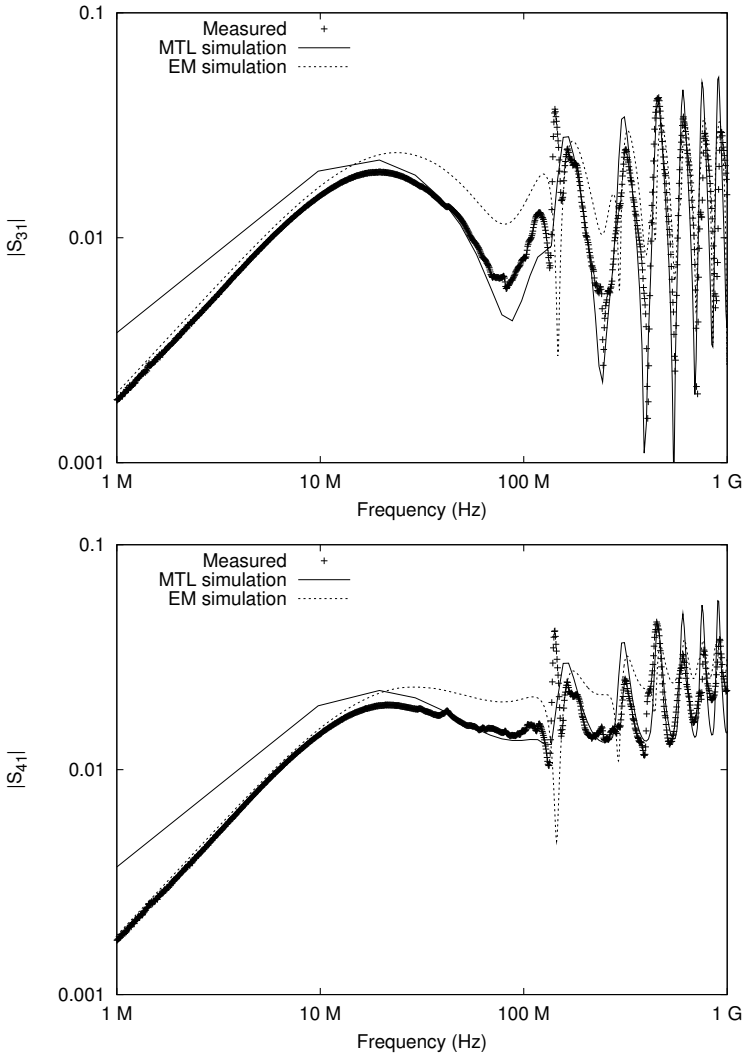


Figure 6.5: S-parameters in frequency-domain. Top: coupling to the near end. Bottom: coupling to the far end.

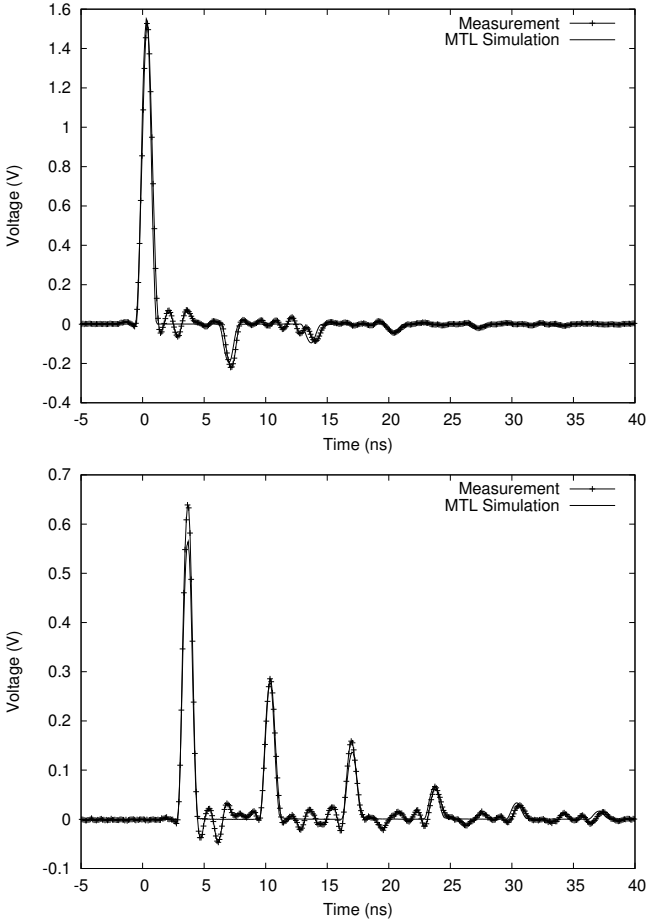


Figure 6.6: The short pulse at the beginning and end of TL1. The time difference is 3.3 ns, which is equal to the time needed to travel 1 m at the speed of light.

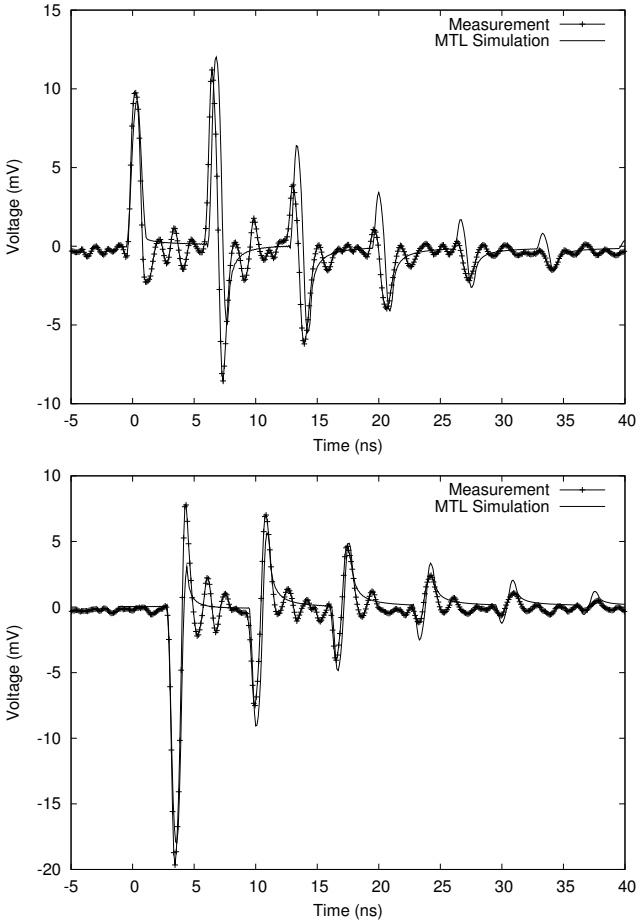


Figure 6.7: The voltages at begin and end of TL2 as a result of the coupling.

### 6.1.5 Influence of line matching

Using the described model, the coupling between the lines is predicted under different load conditions of the lines. Referring to (6.6), (6.1) and (6.2), the characteristic impedance is approximated by:

$$Z_0 = \sqrt{\frac{L'}{C'}} = \frac{1}{2\pi} \sqrt{\frac{\mu}{\epsilon}} \cosh^{-1} \left( \frac{h}{r} \right) \quad (\Omega) \quad (6.17)$$

Filling in the before mentioned geometrical parameters results in a characteristic impedance of  $Z_0 = 221 \Omega$ . The following four situations are calculated:

1. Both lines are not matched, but loaded with  $50 \Omega$  at both ends, which is the situation described in the preceding sections. This is taken as a reference case.
2. The source line is matched with  $221 \Omega$  at both ends (in stead of  $50 \Omega$ ), while the receptor line is loaded with  $50 \Omega$  at both ends.
3. The source line is loaded with the original  $50 \Omega$  at both ends and the receptor line is matched with  $221 \Omega$  at both ends.
4. Both source and receptor lines are loaded with the matching resistance of  $221 \Omega$  at both ends.

The resulting  $S$ -parameters for these four situations are shown in figure 6.8.

The plots can be split in two frequency ranges. For the frequencies below 10 MHz, the cables do not show resonances and in this range it can be easily concluded which situation gives the best results (the smallest coupling), i.e. the case where both lines are matched at both sides. Above 10 MHz, reflections are becoming important and above 100 MHz a lot of resonances occur. These frequencies will change with the length of the cable. In the resonance area, the effect of the matching can be predicted only after accurate modelling and calculation.

One striking effect will be brought to attention: At certain frequencies there will be an effect in the receptor TL that is dependent on the direction of the energy transport in the source TL. At 150 MHz, where the length of the MTL is equal to half a wavelength, the coupling to the near end of the receptor TL is a factor 30 lower than to the far end, where near and far are the positions relative to the location where the energy enters the source TL. This effect is used in directional couplers which are used in microwave engineering. The same effect appears at every odd multiple of this frequency.



### **Conclusions**

From the parts of the plots below 10 MHz some general conclusions can be drawn:

- There will be less coupling between two TLs if one or both of the lines are matched.
- Matching the receptor line results in more reduction of the coupling than matching the source line. The difference is 1.66 times, in this case.
- The reduction in coupling is maximal if both lines are matched. In this case the coupling shows directional effects.

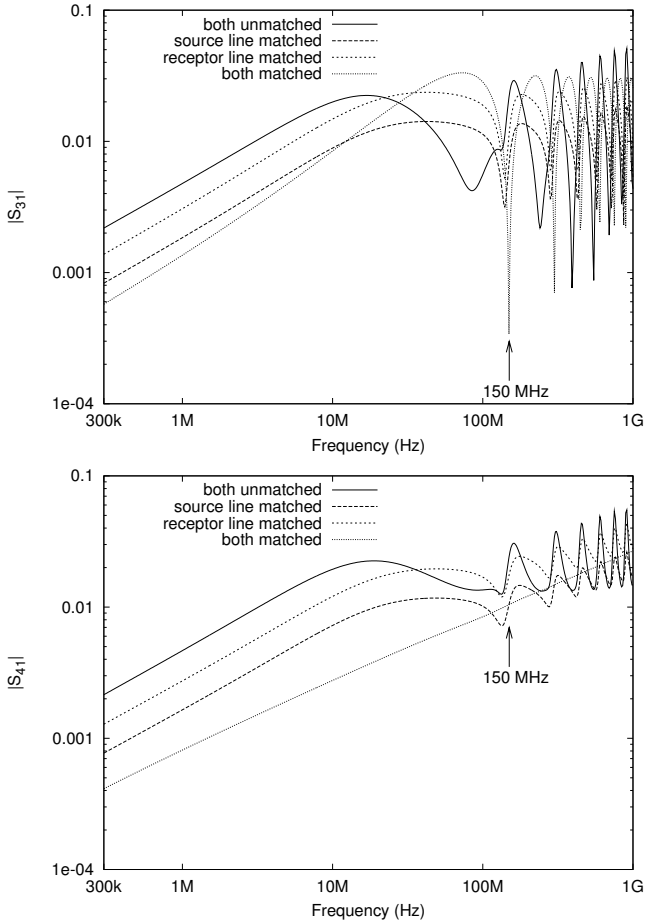


Figure 6.8: Different matching configurations.  $S_{31}$  is the coupling to the near end of the receptor line and  $S_{41}$  to the far end.

## 6.2 Transfer impedance of V0-YMvKas cable

This case study is dealing with the determination of the transfer impedance of a low voltage power cable consisting of four solid inner conductors with a cross-section of  $2.5 \text{ mm}^2$  each, and a steel armour. It is the same kind of cable as used in chapter 5, but this one has conductors with a smaller cross-section. Parallel to the steel armour a stranded copper conductor is found, see figure 6.9. This

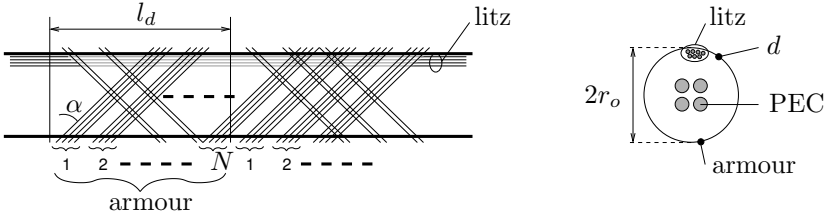


Figure 6.9: Left: Sketch of the shield of the cable.  $N$  is the number of parallel braids,  $l_d$  is the period of the braids and  $\alpha$  is the braid angle. Right: Cross-section of the V0-YMvKas cable.

conductor is intended for safety reasons and has the same nominal cross-section as one of the inner conductors, i.e.  $2.5 \text{ mm}^2$ . The nominal cross-section, which is the cross-section given by the manufacturer, “identifies a particular size of conductor, but is not subject to direct measurement” [70]. Thus, the physical cross-section is not necessarily equal to the nominal cross-section and is chosen such that the DC resistance of the conductor is not larger than the prescribed DC resistance for a cable of the given nominal cross-section [71]. The DC-resistance of one conductor is  $7.41 \text{ m}\Omega/\text{m}$ , as given by the manufacturer [72]. The transfer impedance will be estimated by calculation and derived by measurement. Two cases will be investigated, reflecting the two ways in which the cable can be used: one with the four inner conductors together as the DM conductor and a return consisting of the armour and the litz in parallel. This case represents situations with cables with only three inner conductors, where the litz alone is used as PE conductor. The other case will be with three inner conductors as the DM conductor and the return consisting of the fourth inner conductor parallel to the armour and the litz. This is the common way the cable is used. In the latter case the fourth inner conductor acts as a protective earth conductor (PEC).

### 6.2.1 Approximation and Measurement

As a first step, the impedance of the PEC, of the steel armour and of the copper litz are calculated, as well as the impedance of the combinations of two or three

of them parallel. The copper inner conductors, and thus the PEC, have a radius  $r_{PEC}$  of 0.86 mm and a conductivity  $\sigma_{copper}$  of  $58 \cdot 10^6$  S/m. The DC resistance is given by:

$$R'_{DC,PEC} = \frac{1}{\pi r_{PEC}^2 \sigma_{copper}} = 7.4 \text{ m}\Omega/\text{m} \quad (6.18)$$

The armour consists of 88 steel conductors, each having a radius  $r_{sw}$  of 0.15 mm. Due to the rotation, the length of the conductors per meter of cable is

$$\frac{\sqrt{l_d^2 + (2\pi r_o^2)^2}}{l_d} = 1.15 \text{ m}.$$

The conductivity of steel  $\sigma_{iron}$  is  $10 \cdot 10^6$  S/m. The DC resistance is thus given by:

$$R'_{DC,armour} = \frac{1.15}{\pi r_{sw}^2 \sigma_{iron} 88} = 18.4 \text{ m}\Omega/\text{m} \quad (6.19)$$

The litz consists of 40 copper conductors, each having a radius  $r_{lw}$  of 0.125 mm. The DC resistance of the copper litz is thus:

$$R'_{DC,litz} = \frac{1}{\pi r_{lw}^2 \sigma_{copper} 40} = 8.8 \text{ m}\Omega/\text{m} \quad (6.20)$$

The resistance of armour and litz parallel is thus  $6.0 \text{ m}\Omega/\text{m}$  and of armour, litz and PEC parallel is  $3.3 \text{ m}\Omega/\text{m}$ . The impedance of a round conductor, taking into account the skin-effect, is given by [60]:

$$Z' = \frac{j\gamma J_0(j\gamma r)}{2\pi r \sigma J_1(j\gamma r)} \quad (\Omega/\text{m}) \quad (6.21)$$

where  $\gamma$  is the propagation constant in the conductor,  $r$  is the radius of the conductor,  $\sigma$  is the conductivity of the conductor and  $J_n$  are the Bessel functions of the first kind and  $n^{th}$  order. The impedance of armour, PEC and litz are given in figure 6.10, as well as the impedance of the parallel connection of armour and litz and of the parallel connection of armour, PEC and litz.

The transfer impedance is expected to be close to the parallel connections of the two or three conductors at low frequencies because for these frequencies the inductance of the CM current loop does not play a significant role.

At high frequencies, the inductance of the CM loop via the armour is smaller than via the litz, causing the CM current to flow mainly in the armour. As a result, it is expected that the transfer impedance is close to the parallel connection at low frequencies and close to the impedance of the armour at high frequencies.

Next to calculation, the transfer impedance of the cable has been measured. The result of the measurement together with the result of the calculation is shown in figure 6.11.

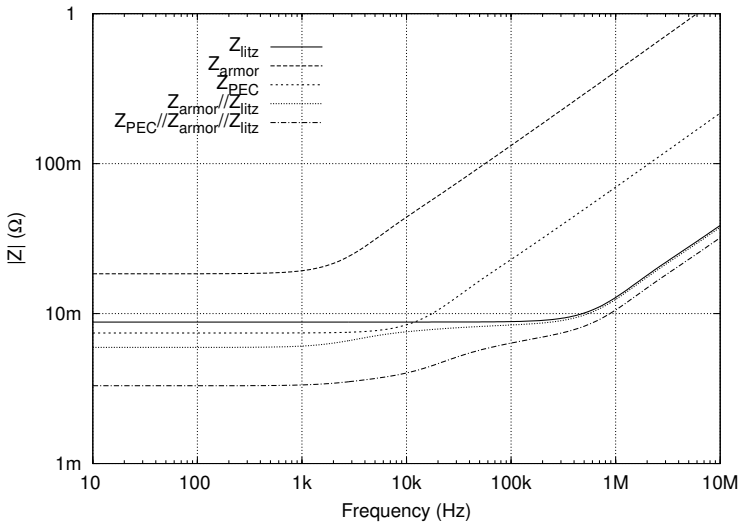


Figure 6.10: The impedance of the three return conductors  $Z_{litz}$ ,  $Z_{armour}$  and  $Z_{PEC}$  individually and the parallel connection of two of them ( $Z_{armour} // Z_{litz}$ ) and of three of them ( $Z_{PEC} // Z_{armour} // Z_{litz}$ ).

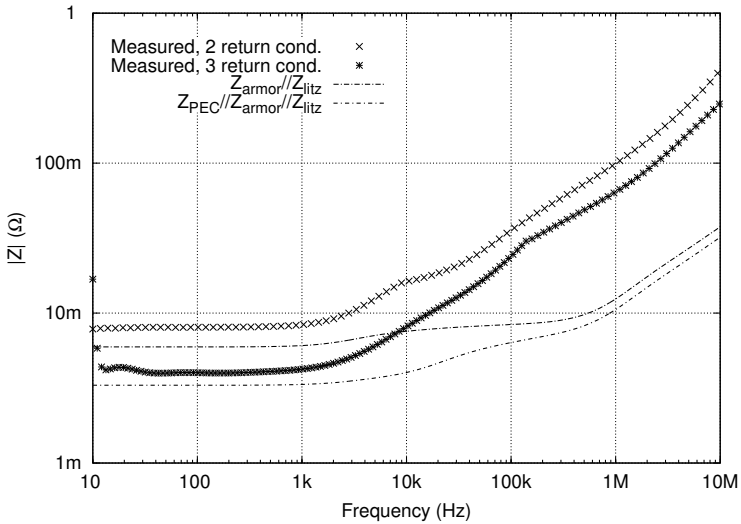


Figure 6.11: Measured transfer impedance of two return conductors and of three return conductors and the calculation of the impedance of the parallel connection of two and of three conductors.

From the plot it can be concluded that the transfer impedance can not accurately be calculated by taking the parallel connection of the return conductors.

### 6.2.2 Influence of current distribution

As a second step the distribution of the current over the three return conductors is measured (see figure 6.12).

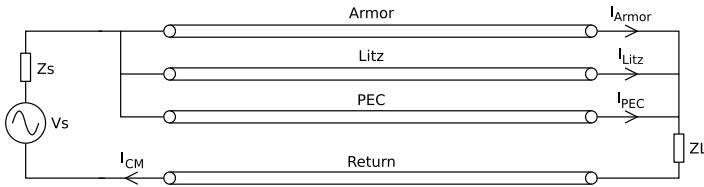


Figure 6.12: The currents in the V0-YMvKas cable.

In figure 6.13 the result is shown. The currents are plotted as a percentage of the total CM current. The plots show that at low frequencies most of the current flows in the PEC and the smallest current flows in the armour. At high frequencies the situation is the opposite, as expected.

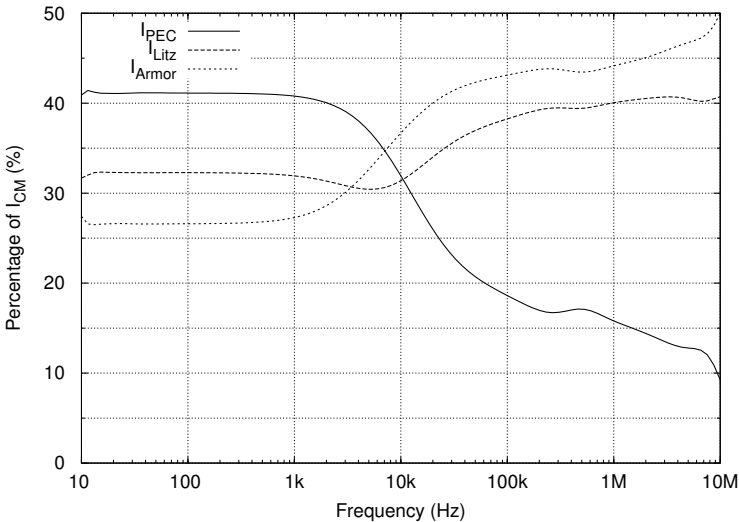


Figure 6.13: Current distribution between the three return conductors.

The current fractions can be used to calculate the DM voltage in the three return conductors together in the following way:

$$U_{DM} = \frac{U_{PEC} + U_{litz} + U_{armour}}{3} \quad (V) \quad (6.22)$$

The voltage in one of the conductors, e.g. the PEC, is calculated as:

$$U_{PEC} = I_{PEC} Z_{PEC} \quad (V) \quad (6.23)$$

The CM current is the sum of the currents in the return conductors:

$$I_{CM} = I_{PEC} + I_{litz} + I_{armour} \quad (A) \quad (6.24)$$

Thus, the transfer impedance will be calculated as:

$$Z'_t = \frac{U_{DM}}{I_{CM}l} = \frac{I_{PEC}Z_{PEC} + I_{litz}Z_{litz} + I_{armour}Z_{armour}}{3(I_{PEC} + I_{litz} + I_{armour})l} \quad (\Omega/m) \quad (6.25)$$

for the case with three return conductors and

$$Z'_t = \frac{U_{DM}}{I_{CM}l} = \frac{I_{litz}Z_{litz} + I_{armour}Z_{armour}}{2(I_{litz} + I_{armour})l} \quad (\Omega/m) \quad (6.26)$$

for the case with two return conductors. The result of these calculations is shown in figure 6.14.

From the figure it can be concluded that, if the current distribution is taken into account, the transfer impedance can be calculated accurately. This current distribution is not equal to the current distribution resulting from the parallel switching of the three conductors. In order to calculate the current distribution, the electro magnetic interaction between the conductors should be taken into account, which is a recommendation for further research.

### 6.2.3 Conclusion

The Transfer impedance of a V0-YMvKas cable can not be accurately calculated by simply taking the parallel switching of the three return conductors.

To calculate the transfer impedance of a V0-YMvKas cable, the interaction of the return conductors has to be taken into account.

The current distribution over the conductors has a strong influence on the transfer impedance.

Using the PEC of a V0-YMvKas cable as return reduces the transfer impedance. In the studied case, the reduction is a factor 1.8 over the frequency range from 10 Hz until 10 MHz.

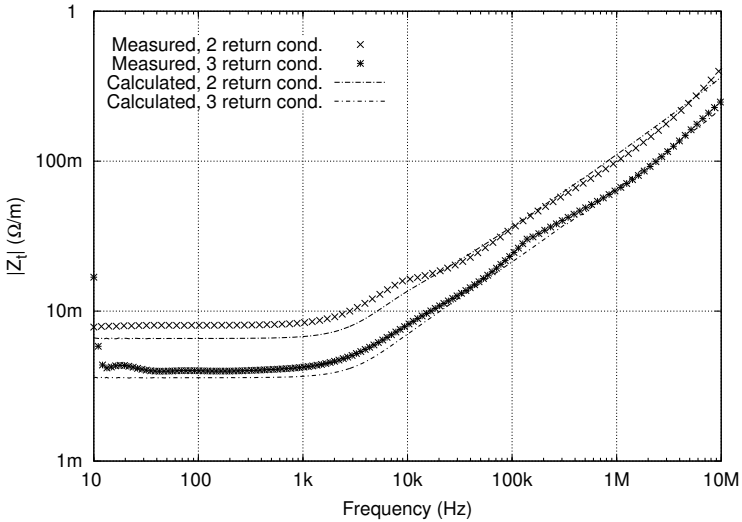


Figure 6.14: Measured transfer impedance and calculated transfer impedance based on the measured individual return conductor currents and calculated individual return conductor impedances.

The measurement of the separate currents in the three conductors shows that towards higher frequencies, the current tends to flow more and more in the outer screen. The current fraction in the PEC, which is at the centre of the cable, is decreasing with frequency.



## 6.3 Transfer impedance of symmetrical cables

This example is dealing with symmetrical cables. The transfer impedance of symmetrical cables is different from the transfer impedance of asymmetrical cables, like coax cables. In the latter case the CM current is flowing in *one* of the conductors. That conductor is, in case of coax cables, the outer conductor. Measurement methods are developed to measure the  $Z_t$  of coaxial cables [31, 73]. In the case studied here, the CM current is floating in *both* conductors, none of which is connected to ground. It is assumed that half the CM current is flowing in one conductor and half of it in the other conductor. The goal is to find the transfer impedance in case one conductor has a different diameter than the other conductor.

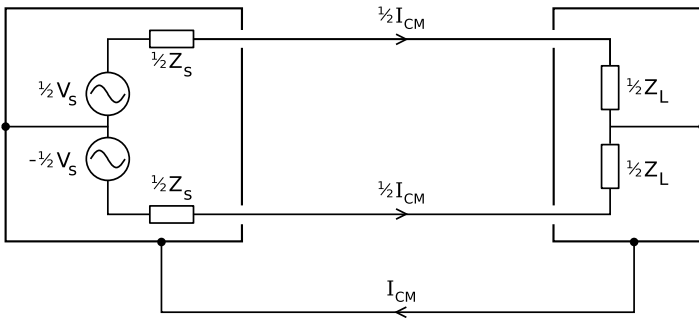


Figure 6.15: A symmetrical connection between a balanced source ( $\pm\frac{1}{2}V_s$ ) and load ( $2 \times \frac{1}{2}Z_L$ ). The CM current is assumed to be equally distributed over the two conductors of the symmetrical line between source and load.

The cable type under consideration consists of two separate conductors installed in a pipe or conduit. This type of cables occurs in low voltage installations for illumination and connection of computers, household appliances, and so on. In domestic installations in the Netherlands, all wires have a cross section of  $2.5 \text{ mm}^2$  except the live wires between a switch and a load, which have a cross section of  $1.5 \text{ mm}^2$ . In this case the difference between the conductors is relatively large. The measurements have been performed to check the model so that it can be used to calculate the transfer impedance of cables in other situations where the diameters of the conductors are not equal.

Simulations related to comparable situations are performed before [74]. In that case the asymmetry of the cable was in the location of the wires with respect to each other and in the non-homogeneity of the surrounding medium.

The transfer impedance is expressed as:

$$Z_t = \frac{V_{DM}}{I_{CM}l} \quad (\Omega/m) \quad (6.27)$$

where  $l$  is the length of the cable.  $I_{CM}$  is the sum of the currents in the two conductors and  $V_{DM}$  is the voltage between the conductors, caused by  $I_{CM}$ .  $V_{DM}$  will be zero if the two conductors are equal, in contrast to coaxial cables, where  $V_{DM}$  is zero if the screen is closed and has a zero impedance.

### 6.3.1 Measurement setup

In [32, 75] a measurement set-up is described to measure the transfer impedance of non-coaxial cables. For that set-up a special probe, described by MacFarlane [12] was needed to perform the measurements without disturbing the symmetry of the cable under test (CUT). Such a probe was successfully built, but its usable frequency range is limited to approximately 40 MHz. Measurements are performed with these probes as well [32]. These measurements are repeated using a four port VNA with which it is possible to perform balanced measurements. This option will be used to measure the DM voltage without disturbing the symmetry of the CUT. In this case the MacFarlane network used to split CM and DM currents is not needed, which increases the frequency range and the accuracy of the measurement.

#### Description of the set-up

A schematic of the set-up can be seen in figure 6.16.  $V_s$  is the source of the VNA with  $Z_s=50 \Omega$  internal impedance. The Voltmeters  $V_1$  and  $V_2$  are ports of the VNA which are used as inputs in this case, together forming a balanced measurement port with internal impedance of  $100 \Omega$  ( $2 \times 50 \Omega$ ). TL1 and TL2 are the two conductors of the CUT.

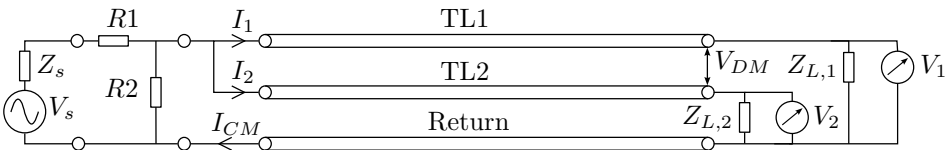


Figure 6.16: Measurement set-up with balanced measurement option.

The network consisting of  $R1$  and  $R2$  is an impedance matching network to match the  $50 \Omega$  of the source to the CM characteristic impedance of the CUT, which is the parallel switching of the two TLs formed by the two conductors and their

returns, respectively. The return conductor in this set-up is a flat copper foil. The two conductors of the cable are located on top of the foil, as seen in figure 6.17.

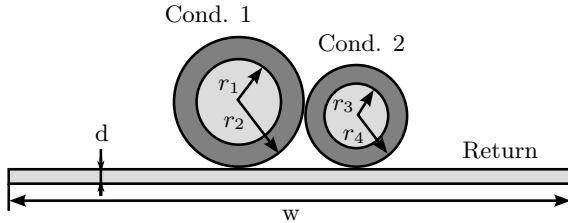


Figure 6.17: Cross-section of the CUT with return conductor.

The parameters  $r_1-r_4$  in the figure are the radii of the conductors and of the insulators. The horizontal bar at the bottom of the figure is the return conductor.

**Flatness of the current distribution**

The CM current in the CUT is assumed to have a flat current distribution, which means that it is equal for every point along the CUT. This is important because equation (6.27) is only valid if the current  $I_{CM} = I_1 + I_2$  is equal along the whole line.

The flatness of the current distribution is dependent on the matching at both ends of the TL. A measure for the matching is the reflection coefficient, which should be as low as possible. If the reflection coefficient at one end of the cable is zero over the frequency band of interest, the reflection must also be zero at the other end. The flatness of the current distribution can be described by the standing wave ratio (SWR) which is the ratio of the maximum current or voltage to the minimum current or voltage on the TL:

$$SWR = \frac{V_{max}}{V_{min}} = \frac{1 + |\Gamma|}{1 - |\Gamma|} \tag{6.28}$$

If the SWR is 1, the current distribution is uniform over the length of the TL. The reflection coefficient  $\Gamma$  can be measured directly using a VNA with S-parameter measurement options. The  $S_{nn}$  parameter is the reflection coefficient measured at port  $n$ , where  $n$  is 1, 2, 3 or 4 in case of the four-port VNA used for these measurements.

The measured SWR is shown in figure 6.18. This SWR is measured in the CM circuit of the setup by the port of the VNA which delivers the CM current. That is the port indicated by  $V_s$  and  $Z_s$  in figure 6.16. The SWR is close to 1 at low

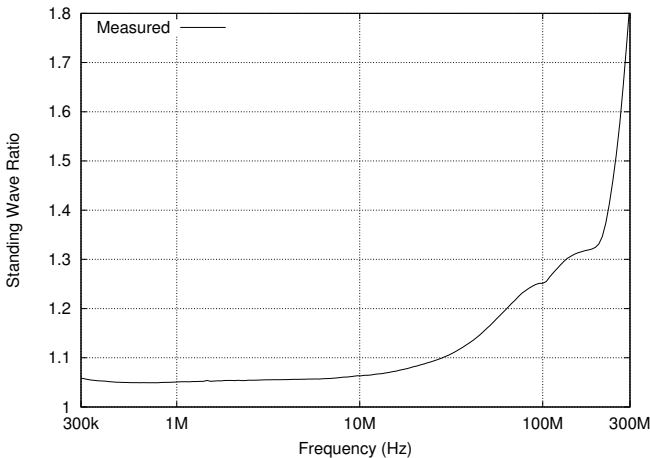


Figure 6.18: The CM standing wave ratio in the measurement setup.

frequencies and increases with increasing frequency. At 300 MHz it is increased to 1.8, which means that the maximum deviation from the average current is approximately 30%.

### Measurement results

The measurements are performed using a Rohde & Schwartz ZVB VNA. The frequency range used was from 300 kHz until 2 GHz. The cable used consists of two insulated copper wires, one with a cross-sectional area of  $1.5 \text{ mm}^2$  and the other with an area of  $2.5 \text{ mm}^2$ . In the figure three lines are shown. The line “Zero measurement” is the result of a measurement where a short circuit connection is placed at the location of the “VDM” indication in figure 6.16. The line “ $Z_t$  measurement” is the actual measurement of the transfer impedance.

In an ideal case the result of the zero measurement is negligibly small, but in our case the zero measurement is in the same order of magnitude as the actual measurement. Therefore the zero measurement is subtracted (in the complex domain) from the actual measurement, resulting in the third line in the figure 6.19, indicated by “Corrected  $Z_t$ ”. Thus, the zero measurement is used for calibration. The resulting transfer impedance is approximately a straight line until 300 MHz, as expected based on the calculation result which will be described in section 6.3.3. The deviations at frequencies higher than 300 MHz are caused by imperfections in the layout and by parasitic inductances and capacitances in the set-up. To make measurement of the transfer impedance above 300 MHz possible, two aspects have

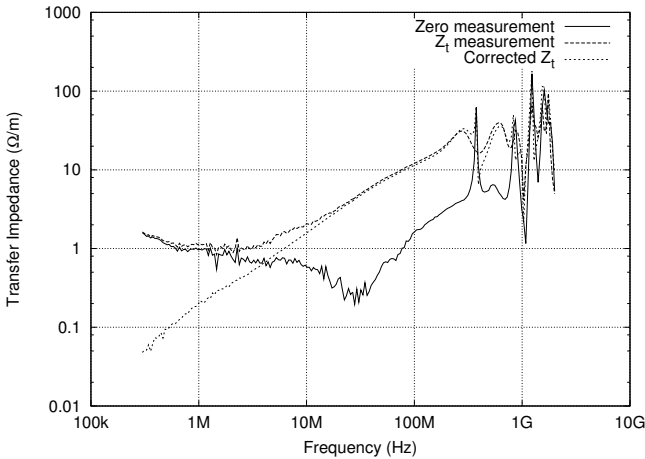


Figure 6.19: Measured result of two different wires of  $1.5 \text{ mm}^2$  and  $2.5 \text{ mm}^2$ .

to be improved: 1) The matching of the CM TL to the source, resulting in a flat current distribution at frequencies above 300 MHz and 2) the matching of the DM TL to the load. The first improvement can be done by a better approximation of the characteristic impedance of the CM transmission line and choosing more exact matching resistors. Next to that resistors can be used that are designed for higher frequencies. The second improvement is more difficult because two resistors of  $50 \Omega$  should be inserted in series with TL1 and TL2 and those two resistors should be equal to within  $1 \text{ m}\Omega$ .

### 6.3.2 Calculation

Next to measuring the transfer impedance of cables, it will be calculated. The calculation is done using the MTL approach described in [21, 51]. The MTL consists of two transmission lines, as shown in figure 6.20. The part of the circuit between '1' and '3' is transmission line 1 (TL1) and the part between '2' and '4' is TL2. The return conductor, consisting of the copper plate, is the horizontal line between the two TLs indicated by 'R'.

One TL consists of the  $2.5 \text{ mm}^2$  conductor and the return plate and the other of the  $1.5 \text{ mm}^2$  and the return plate. The radii of the conductors (see figure 6.17) are measured and given by:  $r_1 = 0.89 \text{ mm}$ ,  $r_2 = 1.58 \text{ mm}$ ,  $r_3 = 0.67 \text{ mm}$  and  $r_4 = 1.33 \text{ mm}$ . The insulating material is PVC with a relative permittivity of 2.9. Because the space between the conductors and between conductor and return is filled only half with the insulating material and half with air, the relative

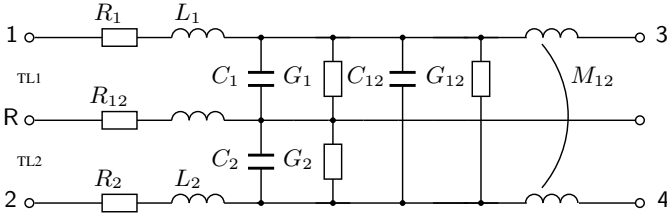


Figure 6.20: Infinitesimal part of multi conductor transmission line.

permittivity must be between that of the insulating material and that of air. The average of the two is  $0.5 \times (2.8 + 1) = 1.9$ . The width of the copper return plate  $d = 32$  mm and the thickness  $w = 0.7$  mm. The per-unit-length impedance  $R'_1$  and  $R'_2$  of the conductors are:

$$R'_{cond} = \frac{1}{\pi r^2 \sigma} + \frac{(1 + j) \sqrt{10^{-7} f \mu_r \sigma}}{\sigma r} \quad (\Omega/m) \quad (6.29)$$

where  $r$  is the radius of the respective conductor,  $\sigma$  is its conductivity and  $\mu_r$  is its permeability. The impedance of the return conductor is:

$$R'_{12} = \frac{1}{dw\sigma} + \frac{(1 + j) \sqrt{\pi^2 f^4 \cdot 10^{-7} f \mu_r \sigma}}{\sigma w} \quad (\Omega/m) \quad (6.30)$$

which is also expressed in  $\Omega/m$ . In this expression,  $w$  is the width of the copper plate and  $d$  the thickness. The inductance is given by:

$$L' = 2 \cdot 10^{-7} \cosh \left( \frac{r_{insul}}{r_{cond}} \right) \quad (H/m) \quad (6.31)$$

where  $r_{insul}$  is the distance between the centre of the conductor and the return conductor,  $r_2$  for conductor 1 and  $r_4$  for conductor 2. The radius of the conductor,  $r_{cond}$ , is  $r_1$  for conductor 1 and  $r_3$  for conductor 2 (see figure 6.17). The mutual coupling between the conductors is given by:

$$M'_{12} = \frac{\mu}{2\pi} \ln \left( \frac{\sqrt{(r_1 + r_4)^2 + 4r_1 r_4}}{r_2 + r_4} \right) = \frac{\mu}{4\pi} \ln \left( 1 + \frac{4r_2 r_4}{(r_2 + r_4)^2} \right) \quad (H/m) \quad (6.32)$$

The capacitances between conductor and return and between the conductors can be calculated from the self- and mutual inductances, respectively, by using (6.14).  $G_1$ ,  $G_2$  and  $G_{12}$  are assumed to be zero in this example. These TL parameters are used to calculate the voltages and currents on the TLs as a function of frequency. The DM voltage is calculated as the difference between the voltages at the end of TL1 and TL2. The CM current is the sum of the currents in TL1 and TL2.

Calculated result

The transfer impedance is calculated in the range from 10 Hz to 2 GHz. The result of the calculation is shown in figure 6.21.

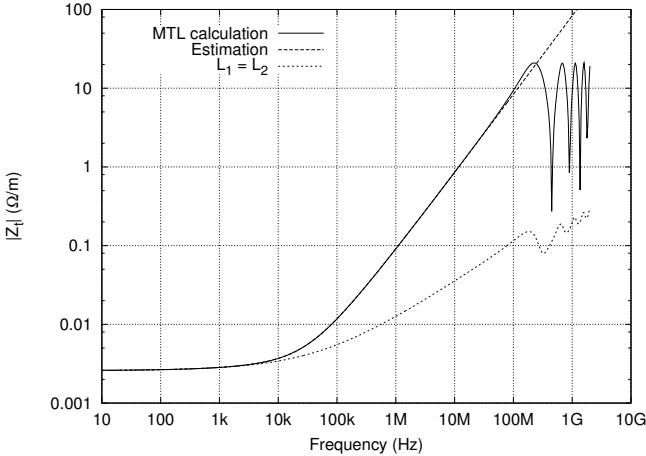


Figure 6.21: Calculated transfer impedance as function of frequency of two wires of 1.5 mm<sup>2</sup> and 2.5 mm<sup>2</sup>.

The upper boundary is the same as the measurement boundary and the lower boundary is chosen to have a simple check: The transfer impedance at 10 Hz is supposed to be equal to the transfer impedance at DC, because nor skin effect nor inductance play a significant role at these low frequencies. The DC transfer impedance is given by:

$$Z'_{t,DC} = 0.5(R_{1,DC} - R_{2,DC}) = 0.5 \left( \frac{1}{\pi r_1^2 \sigma} - \frac{1}{\pi r_2^2 \sigma} \right) \quad (\Omega/m) \quad (6.33)$$

which is 2.6 mΩ/m in this case. The result of the MTL model at 10 Hz is equal to 2.6 mΩ/m, the DC value. The transfer impedance is proportional to the difference in impedance between the two conductors and can be estimated as:

$$Z'_t = Z'_{t,AC} + 0.5j\omega(L_1 - L_2) = \frac{Z_{1,AC} - Z_{2,AC} + j\omega(L_1 - L_2)}{2} \quad (\Omega/m) \quad (6.34)$$

where  $Z'_{1,AC}$  and  $Z'_{2,AC}$  are the impedances of the conductors, taking into account the skin-effect.  $Z'_{t,AC}$  is the contribution to the  $Z_t$  caused by  $Z'_{1,AC}$  and  $Z'_{2,AC}$ .  $L_1$  is the self inductance of TL1 and  $L_2$  of TL2. At frequencies above 300 MHz the transfer impedance is deviating from the straight line, caused by reflections in the Tls.

The third line in figure 6.21 shows the  $Z_t$  in case the inductances of the two lines are equal:  $L_1 = L_2$ . In that case the transfer impedance is proportional to the difference in  $Z'_{1,AC}$  and  $Z'_{2,AC}$ . Due to the skin-effect, the  $Z_t$  is proportional to the square root of the frequency from  $f = 300$  kHz.

### 6.3.3 Comparison of measurement and calculation

The result of the calculation and of the measurement are shown together in figure 6.22.

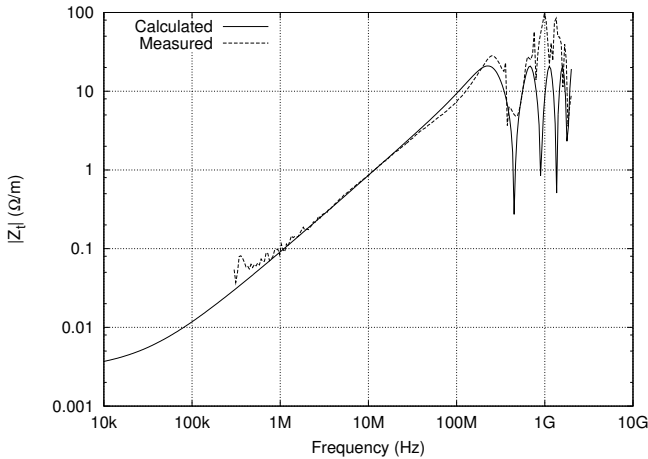


Figure 6.22: Result of measurement and calculation.

The plot can be divided in three parts:

**$f < 1$  MHz** In this area the signal to noise ratio is too small to perform a consistent measurement. The calculations are assumed to be correct at frequencies below 300 kHz because at these frequencies the parasitic capacitance and inductance do not play an important role.

**$1$  MHz  $< f < 200$  MHz** In this area the calculated transfer impedance agrees very well with the measured transfer impedance.

**$f > 200$  MHz** At these frequencies the reflections are dominant, both in the calculations and in the measurements.



### 6.3.4 Changing load conditions

The load conditions of a balanced TL vary in real situations. If the circuit the TL is connected to is a balanced circuit, the two loads,  $Z_{L,1}$  and  $Z_{L,2}$  in figure 6.16, will be equal. In the measurement these loads were both equal to  $50 \Omega$ . In this section the influence of other loads will be calculated.

First the balanced situations will be calculated with  $Z_{L,1} = Z_{L,2} = 5 \Omega$  and with  $Z_{L,1} = Z_{L,2} = 500 \Omega$ . The results of both calculations are shown in figure 6.23.

The next situation is an unbalanced one. The two loads are chosen such that  $Z_{L,1}$  is equal to the characteristic impedance of TL1, which is  $54.7 \Omega$  and  $Z_{L,2}$  is equal to the characteristic impedance of TL2, which is  $49.1 \Omega$ . This results in a lower transfer impedance. This lower transfer impedance is caused by the fact that the currents in the two TLs are no longer equal.

The difference between the currents as a percentage of the average current in the TLs is shown in figure 6.24. The currents are equal below 10 MHz in the balanced case and they differ by more than 10% in the unbalanced case. Between 10 MHz and 100 MHz the currents in the balanced case start deviating as well.

### 6.3.5 Conclusion

The following conclusions can be drawn:

1. Calculation and measurement of the transfer impedance agree very well.
2. At frequencies where the CM current in the cable is not resonating, the transfer impedance is proportional to the impedance difference between the two lines, if the CM current is equally distributed between the two conductors.
3. Cables consisting of wires of different diameters have a non-zero transfer impedance and thus form a coupling path for EM disturbance. The transfer impedance is dependent on the load conditions.
4. The transfer impedance of a cable with two conductors of different diameters can be decreased by loading the two transmission lines with their characteristic impedances.

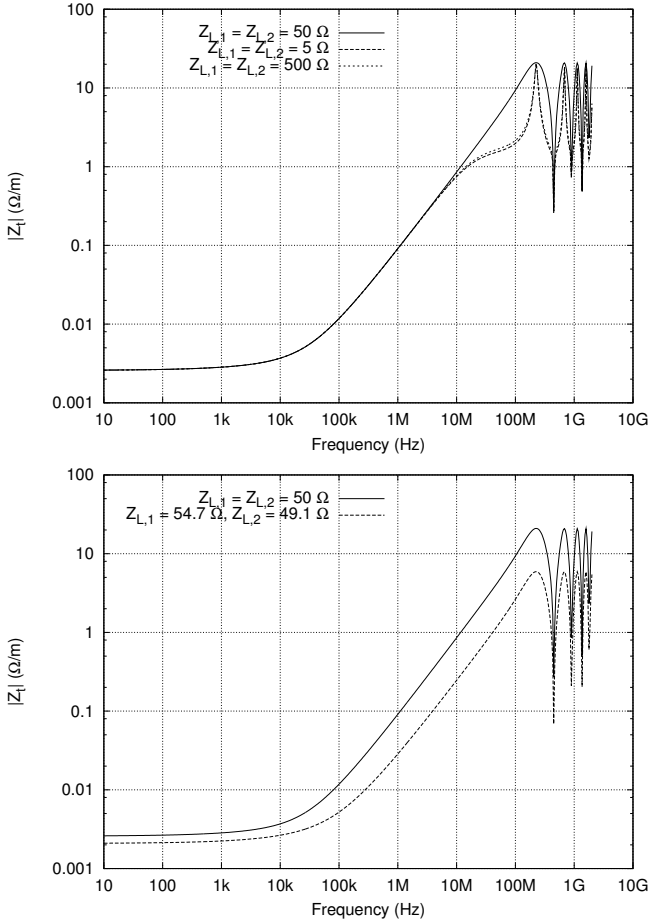


Figure 6.23: Result of calculation with different loads  $Z_{L,1}$  and  $Z_{L,2}$ . Top: loading with 50  $\Omega$ , 5  $\Omega$  and 500  $\Omega$ . Bottom: loading with 50  $\Omega$  and loading with matched impedances.

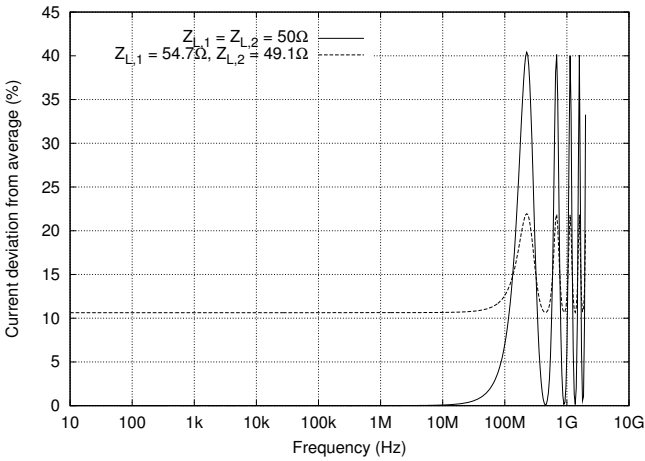


Figure 6.24: The deviation of the currents  $I_1$  and  $I_2$  from the average current  $0.5(I_1 + I_2)$  with different loads  $Z_{L,1}$  and  $Z_{L,2}$ .

## 6.4 Common mode current distribution

If a pulsed electro magnetic field is present, e.g. generated by a lightning strike, a conductor starts to resonate. It is assumed that the frequency of the resonance is caused by the length of the conductor and by the way it is connected to other conductors. The resonance appears in the form of an AC current. This current is a CM current in case there is talk of a cable or set of conductors. In case of a conductor connected to ground, the current distribution will look like a quarter period of a cosine function with its maximum at the ground side and its minimum at the floating side. To verify this assumption a measurement is performed.

For the measurement a 5 m. long single, round, copper conductor with a cross section of  $2.5 \text{ mm}^2$  is used which is connected to the copper grid which is immersed in the concrete floor of the laboratory and which extends at least 10 m. in all directions around the measurement setup. The pulses are generated with a portable impulse generator, generating pulses comparable to lightning impulses ( $1.2 \mu\text{s}$  rise time and  $50 \mu\text{s}$  decay time) at a rate of 25 pulse/s. The impulse generator is connected to a loop consisting of a copper conductor with an area of approximately  $10 \text{ m}^2$  at a distance of 3–4 m. The return of the loop is the copper grounding grid. The open circuit output voltage of the impulse generator is approximately of 100 V. The spectrum generated by these pulses has its maximum around 300 kHz. From this frequency the spectrum is decreasing with increasing frequency.

The current is measured every 20 cm. using a spectrum analyser and a current transformer surrounding the conductor.

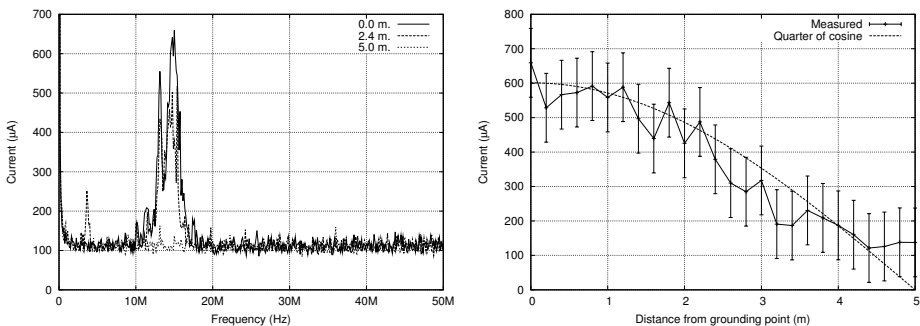


Figure 6.25: Left: Spectra of the current measurements at three locations. At the grounding point (0.0 m.), in the centre (2.4 m.) and at the floating end (5.0 m.). Right: The current at  $f = 15 \text{ MHz}$  as function of location.

At every location the spectrum of the current from 9 kHz to 50 MHz is measured. Three of these spectra are plotted in figure 6.25 (left). In these spectra a peak

is observed at 15 MHz. If this peak is directly related to the spectrum of the source signal, than there must be larger peaks at lower frequencies because above 300 kHz the spectrum of the source is decreasing with frequency. However, this is not the case, so the 15 MHz peak must have another origin. At 15 MHz, the conductor is exactly a quarter wavelength long, so the conductor is resonating at this frequency. The measured currents at 15 MHz are taken from the spectra and plotted as function of the location in the right side of the figure. A cosine function is also plotted as reference. It is clear that the current distribution does indeed show the shape of a quarter period of a cosine.

The measured currents are close to the noise level of the spectrum analyser (Agilent E4422B [76]), which is between -113 dB and -119 dB at the used bandwidth of 1 kHz. These values correspond with a possible deviation in the current between 80 and 160  $\mu\text{A}$ . The noise level is indicated by the error bars in the figure, and can clearly be seen in the spectrum in the figure.

A three-dimensional representation of the current distribution is shown in figure 6.26.

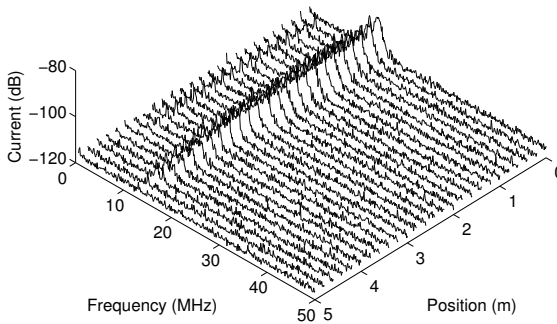


Figure 6.26: Current distribution in the 5 m wire as function of both frequency and position

Another measurement is performed with a conductor of 1.5 m length. This conductor is floating at both ends. Its expected resonance will be a half-wave resonance at 100 MHz. The resonance observed is at a slightly lower frequency, which may be caused by small capacitances from the ends to the environment, which makes the conductor seem to be slightly longer. The same phenomenon is known from antennas. In figure 6.27 the result is shown. In this case the noise floor is between 0.4 and 0.8  $\mu\text{A}$ , because a low-noise 26 dB amplifier was used together with the same spectrum analyser as during the previous measurement. The noise contribution of the amplifier is ignored. Although the measurements are suffering from a lot of noise because the currents are very small, the half-wave shape can be seen

in the distribution.

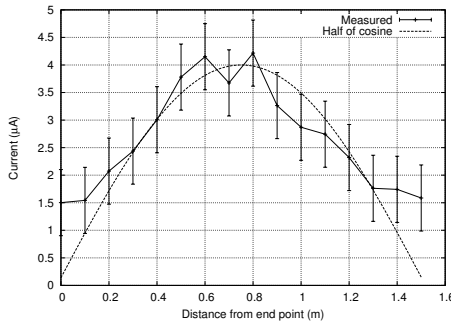


Figure 6.27: The current at  $f = 97.6$  MHz as function of location. The current is measured every 10 cm.

## Conclusion

From these experiments it can be concluded that a cable can carry resonant CM currents with a frequency determined by the length of the cable and the way it is connected. These currents can be triggered by a pulse, which does not necessarily have a peak at this resonance frequency.

If connected equipment is sensitive to pulses at this frequency, a bandstop filter can be used, tuned to this frequency, or a cable of another length can be used to shift the resonance to another frequency.

# Chapter 7

## Buildings and Installations

In the previous chapter several case studies are described of measurements performed in a laboratory where the properties of the environment are very well known. The case study of the cable in the soil showed that it is possible to successfully calculate the disturbance currents in case guesses have to be made. In this chapter it is investigated whether the location and interconnection of conducting structures in a building can be predicted.

In chapter 1 a description is given of the three aspects of EMC: the source of disturbance, the coupling path and the receptor of the disturbance. Buildings and installations are considered to be a part of the coupling path.

The cables connected to source and/or receptor are an important path for the disturbance signals. All other nearby cables can also have influence on the coupling path or be a part of it.

Buildings and installations, which are defined later in this chapter, can act as coupling path or have influence on the coupling path in one of the following ways:

1. It can provide a conductive path.
2. It can be part of a transmission line
3. It can act as an antenna. If a current is flowing in a metal part of a building, for example a steel bar, than as a result an electro magnetic field is generated which can propagate to a receptor somewhere else. On the other hand, when a varying electro magnetic field is present at a steel bar, a resulting current will flow in the bar.
4. It can act as a shield that blocks or attenuates electro magnetic fields.

The first two are dealing with conductive coupling while the latter two deal with radiative coupling.

In order to deal with all aspects of buildings and installations that are of importance to EMC in a clearly-structured way, they are divided in separate construction elements. These elements form the building blocks of the building or installation. The construction elements are treated individually; the following aspects will be considered:

1. Where can conducting materials be expected within the construction element?
2. Are these conducting materials connected to each other and how?
3. Are the dielectric properties of non-conductive materials important and why and to what extent?
4. Are conducting parts of one construction element connected to those of other elements and, if yes, how are they connected?

In this chapter an investigation of the properties of buildings and installations which are of relevance to EMC is described. The investigation is performed as a literature research combined with interviews of civil engineers.

## 7.1 Buildings

This chapter describes the situation with regards to buildings in the Netherlands. As already mentioned in chapter 1, buildings can be defined as: *A structure with a roof and walls, such as a house or factory* [4]. The construction elements considered regarding to buildings are:

1. Foundation
2. Skeleton
3. Floors
4. Walls
5. Roofs

Every building consists of (some of) these construction elements. Next to these elements, buildings can have a lot of other elements like windows, pillars, stairs, etc.



### 7.1.1 Foundation

The foundation of a building is the lowest part of a building, usually invisible, that acts as a support for the whole building. It has the shape of large bars located under, amongst others, walls, pillars and large area floors of the building.



Figure 7.1: Left: Corner of foundation reinforcement. It can be seen that the reinforcement of the foundation is one big cage. The thick vertical rod in the middle of the pile (see arrow) is for grounding purposes. Right: Two ways of connecting reinforcement, welding or using iron wire.

Modern buildings have a foundation of reinforced concrete. The reinforcement has the shape of long, welded, cages which are welded together or tied together with iron wire [77]. Thus, the whole foundation can be considered a conductive cage immersed in concrete, see figure 7.1.

Next to the foundation itself sometimes piles are used. They can be made of concrete, steel or wood. Concrete piles have reinforcement which consists mainly of vertical, isolated, steel wires. These wires are not, or only coincidentally, connected to the metal cages of the foundation. In some cases an additional steel rod is found in the pile for safety grounding purposes. The down end of such a rod is making contact to the soil with an area equal to the cross section of the rod. The top end is connected to a copper wire which protrudes out of the concrete where it is connected to the safety grounding system. The grounding rod and copper wire can be seen in figure 7.1. Steel piles are hollow steel pipes which are filled with concrete after driving the piles.

### 7.1.2 Skeleton

Buildings with a steel skeleton usually have floors of concrete. The walls can be made of any material.

All parts of the skeleton are mechanically connected to each other. In most of the cases they will be electrically connected as well, although coatings can prevent a good connection.

The concrete floors can be made in two ways: 1) In the factory (prefab). In that case the reinforcement of the floors is not connected to the steel skeleton. 2) The floor is poured on-site. In that case the reinforcement is connected to the steel skeleton. An example of a steel skeleton, where the floors are installed already, is found in figure 7.2.



Figure 7.2: Example of a steel skeleton of a building.

### 7.1.3 Floors

Floors are the horizontal planes of a building. Floors and ceilings are not treated separately in this thesis because they are in fact the same element of the construction. A ceiling can be considered the bottom part of a floor.

Most of the floors are made of concrete. The reinforcement of the concrete commonly has the shape of a cage although, especially in the case of residential housings, it sometimes is just a mesh near the top surface of the concrete together with rods in one direction at the bottom surface of the concrete.

Floors can be poured on-site or can be delivered as prefab elements. In the first case

the reinforcement is connected to the reinforcement of adjacent poured concrete elements. In the latter case the reinforcement is not connected to anything. See also figure 7.3.

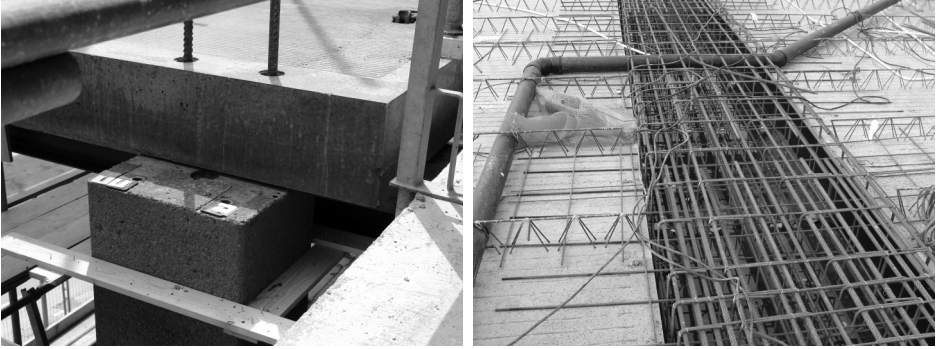


Figure 7.3: Left: Connection of a prefab floor to a column. The reinforcement of both elements are not in contact with each other. Right: A floor of which the upper part will be poured on-site. All reinforcement seen in this picture will be connected together additionally by meshes, rods and iron wire.

In high-rise buildings, of more than three layers, there is always a ‘core’ of the construction. This core gives the building its horizontal strength. It can be, for instance, an elevator tube. The core always has integral reinforcement from bottom to top of the building. All floors adjacent to the core have their reinforcement connected to that of the core [78].

Sometimes floors are reinforced with fibres instead of steel bars [79, 80]. These fibres are usually chopped steel fibres with a thickness  $\leq 1\text{mm}$  and a length of 1-6 cm. The individual fibres are not connected to each other and have arbitrary orientation. They are supposed to be evenly distributed in the concrete. This reinforcement has the advantage that the tensile strength is increased in all directions. Fibre reinforcement is rarely used.

#### 7.1.4 Walls

Walls are the vertical planes which act as support for the floors and as a separation between the rooms.

Concrete walls are always reinforced, except in some low-rise residential housing, where there is sometimes only a band of reinforcement. In case of locally poured concrete, the reinforcement is connected to adjacent reinforcement. In case of prefab walls the reinforcement is not connected to anything.

Masonry walls can be reinforced, especially in areas with a relatively high risk of earthquakes. It is quite often used in low-rise houses in Asia and South America. In North America, Australia and New Zealand and other places it is often used [81].

Industrial buildings can exist of a steel skeleton and can have walls that are made of steel plates, sometimes combined with an outer wall of other material e.g. masonry, concrete plates or synthetic material.

### 7.1.5 Roofs

Roofs are not always reinforced, especially tilted roofs. Tilted roofs have a steel or wooden skeleton covered with stone-like material. Flat roofs of industrial buildings are often made of metal plates on a steel skeleton.

### 7.1.6 EM properties of concrete

The electro magnetic properties of concrete are important in case the reinforcement act as a conductor of a transmission line (TL). The behaviour of the TL is influenced by the magnetic permeability, the permittivity and the conductivity. Concrete is a non-magnetic material, so the magnetic permeability is  $4\pi 10^{-7} H/m$ . In the framework of research to radar systems used to penetrate the concrete for non-destructive integrity checking, the dielectric properties of concrete is measured by several research groups. It is found that the dielectric constant is dependant on the water saturation level where it is 4 in case of dry concrete and 8.2 if the concrete is saturated [82] (measured at 1.5 GHz).

The type of aggregate also influences the dielectric permittivity [83], where it can be between 3.6 and 5 in the range from 50 MHz to 1.5 GHz.

The permittivity is decreasing with frequency in an exponential way, between 500 MHz and 3 GHz in a slab of concrete that is partially dried. The permittivity can also vary with depth, if the moisture content changes with depth. The conductivity of the concrete is increasing with frequency in the range between 500 MHz and 3 GHz [84].

From these studies it can be concluded that the relative permittivity of concrete ranges at least from 6 to 12.

### 7.1.7 Remarks

Although the most commonly used materials used in buildings are described in this chapter, it is not relevant within the context of this thesis to describe every

possible material and combination of materials used in buildings.

The statements in this chapter apply to the vast majority of situations. However, one must be aware of the fact that sometimes exceptions occur, for example in some cases not all parts of the reinforcement of on-site poured concrete are connected to each other. Also, sometimes the reinforcement of a prefab element is electrically connected to nearby reinforcement.

## 7.2 Installations

A description of an installation can be derived from the definitions given in chapter 1: “A particular combination of several types of apparatus and, where applicable, other devices”.

From this description it is clear that an installation always consists of several apparatus. Next to that it consists nearly always of cables connecting the apparatus either to each other or to the outside world, e.g. the power supply network. Most of the times the apparatus are mounted in a framework. The construction elements of installations are:

- A Apparatus. The apparatus in the installation are both source of disturbance and receptor of disturbance at the same time. However sometimes one aspect is dominant, e.g. in case of a motor which is more probable to be a source of disturbance while it can hardly be upset by signals of other sources. The apparatus, or especially its cabinet, can act as part of the framework.
- B Cables. Used to guide power or signals from one location to another location. They often form an important path for the disturbance signals. Three kinds of cables can be separated: 1) Cables between apparatus in the installation. 2) Cables between the installation and something external to the installation, e.g. cables connected to an electricity distribution or telephone network. 3) Cables that run through or very close to the installation but are not connected to the installation itself. They are running from and to something external to the installation.
- C Framework. Everything needed to give mechanical support to the installation. This can be bars, pipes, plates, cabinets, grids, etc. Often the framework is the part of the installation that is most visible. Cable conduits are considered to be part of the framework.  
The framework of an installation is of interest to EMC as far as it is conductive. For this reason only metal parts of the framework are taken into account. The metal parts can be connected to each other by welding or by using screws, nuts and bolts.

Installations can appear in countless different ways. That makes it nearly impossible to say something general about installations.

Examples of installations dealt with in this thesis are industrial installations and laboratory installations.

## 7.3 Conclusion

A literature research is performed to the presence of conducting materials in buildings and installations. In case of buildings metals are often invisible, especially if they are covered with concrete. However, the location of metals in the concrete can be predicted to a certain extent. If it is known whether the concrete is poured on-site or delivered in the form of prefab elements, than it is known if the reinforcement is connected or not. In case of steel skeletons and steel coverings, the situation is clear.

However, for installations the situation is more complicated because the framework of an installation can be made of anything in any shape.

# Chapter 8

## Optimization procedure

The original title of the project is: “Optimizing cabling and wiring in buildings and installations”. The optimization referred to in this title is with respect to EMC. The cabling and wiring are the cables used in buildings and installations to connect electrical equipment to the power supply and to each other. The buildings and installations are the environments where the cables and wires are installed. That excludes environments like cars, ships and airplanes, which are different due to the fact that they form a big common ground plane to the entire installation which makes modeling different.

### 8.1 Optimum with respect to EMC

To find the optimum of an installation with respect to EMC, the information needed is covered by the following three points:

1. It must be defined what is the optimum.
2. The current status with respect to the optimum must be known.
3. Knowledge is required of the actions which should be taken to move from the current status in the direction of the optimum.

EMC is defined as: “*The ability of an equipment or system to function satisfactorily in its electro magnetic environment without introducing intolerable electro magnetic disturbances to anything in that environment*”. From this, a definition of the optimum should be derived. Referring to the three aspects of EMC mentioned in chapter 1 (figure 1.1 on page 2), the optimum can be split in three optima, related to these three aspects:

- The *disturbance source* should generate as little disturbance as possible. The theoretical optimum can be reached by eliminating the generation of disturbance.
- The *coupling path* should provide a coupling as weak as possible for the disturbance signals. If there is no coupling path, the optimum is reached.
- The *receptor* should have the lowest possible sensitivity to disturbance signals. A receptor that is not sensitive at all to disturbance is the optimum receptor, in terms of EMC.

These aspects are not independent. Changing the coupling path from source A to receptor B may change the coupling path from A to C as well.

The optimum with respect to EMC is reached if one or more of the above optima is reached. Note that reaching one optimum is already sufficient: if there is no disturbance signal, the amount of coupling and the sensitivity of the receptor to disturbance signals does not matter any more. If there is no coupling path, a disturbance signal, no matter how strong, will never reach the receptor. If the receptor is insensitive, disturbance signals will have no influence.

It is not very likely to obtain the theoretical optimum for one of the aspects, although it can be approached in some cases. If, for example, a glass fiber waveguide is used to transport signals optically, there is no detectable electro magnetic coupling to other cables.

In this research project the optimization of the *coupling path* is investigated. As a result the disturbance sources and the receptors are regarded as given. To make a further restriction the research is narrowed to cables and wires and the way they are installed. That means that the optimization intended in this research is to find a coupling between cables as small as possible.

## 8.2 Additional conditions for optimization

In the design of the cabling and wiring of a building or installation there are a number of limiting conditions that have to be taken into account. These conditions are related to the following fields:

**Economy** This is a factor that nearly always plays a role, and in most cases an important role. Customers usually want an installation that fulfills their requirements as much as possible at the lowest possible price.

**Environment** Environmental effects are getting increasing attention over time. This also has consequences for electrical installations and influences the choice of materials and the energy consumption of the equipment used.



**Reliability** This is an important factor, especially in certain environments like health care and military, where it is a critical factor.

**Safety** This aspect plays an important role e.g. in industrial installations where there is a danger of explosion. In such an environment much attention is given to prevent ignition of explosive gasses or fluids. Safety aspects of cables can be the inflammability and protection against mechanical impact.

**Ease of installation** The level of difficulty of the installation of an installation or parts of it can have influence on the end result. If this level is high, the time needed to realize the installation will be relatively long, resulting in higher cost and probably more mistakes. It may also have – positive or negative – influence on the maintainability of the installation.

**Maintainability** Installations need to be serviced on a regular basis. The service friendliness or maintainability of the installation is an important factor at service time.

**Availability** The availability of the materials needed can also be an issue, both at the time of construction and afterwards when parts may have to be replaced.

**Sustainability** This aspect is related to the environmental aspect, although it is more general. A product is sustainable if it has as little as possible negative consequences for later generations.

An installation can be optimized with respect to one of these aspects. For example the installations used in a hospital for monitoring the condition of patients are optimized with respect to reliability and safety. Optimizing one aspect may be at the cost of one of the other aspects. If an installation needs to be extremely reliable it will be very expensive, which can be sub-optimal from an economic point of view.

In this research a method is developed to optimize an installation with respect to EMC, while taking into account one or more of the aspects mentioned above.

## 8.3 Description of the procedure

In the previous section a definition is given of the optimum of an installation with respect to EMC.

In this section, the other two aspects will be discussed: first, the current status and, secondly, what to do to go from the current status in the direction of the optimum.

To know the current status a measure is needed to express it. This measure must also be usable to describe the optimum and to compare different situations quantitatively.

The measure used in this research is the Risk Priority Number  $RPN$  which describes the risk resulting from a certain coupling. Changing a parameter in the installation, for example rerouting a cable, in general has influence on several  $RPN$ s. To judge the EMC performance of the complete installation, all these  $RPN$ s have to be taken into account. The score of the installation is  $RPN_{max}$ , which is the maximum  $RPN$ .

### 8.3.1 Optimization steps

The steps to be taken to optimize the installation with respect to EMC are outlined in figure 8.1.

In the following sections the different steps in the procedure are explained.

#### Find sources and receptors

A list has to be made of all sources of EMI that can have influence on the installation and of receptors of EMI. Note that sources and receptors outside the installation have to be taken into account as well.

#### Coupling risk analysis

In theory, of all combinations of source and receptor the transfer function has to be calculated. However, this is not very practical and really time-consuming. For that reason, one has to make a decision which combinations of source and receptor should be treated first. To make such a decision possible, the combinations have to be ranked. For this ranking a method called “coupling risk analysis” (CRA) is developed, which is based on the “failure mode, effects and criticality analysis” [85].

A semi-quantitative way of ranking failure modes is called “Failure Mode and Effect Analysis”, FMEA, which can be extended to FMECA where the ‘C’ stands for criticality. The methods are equal, except that in the latter the severity of the failure modes is quantified in a more fine-grained manner. The method is quantitative because each failure mode is given a number that can be used to rank the failure mode. The higher the number, the more serious the failure mode. On the other hand, the numbers are based on a qualitative judgement of the different aspects, hence the addition ‘semi’. This analysis can be used to rank the different combinations, where, in stead of failure modes, the couplings are analysed.

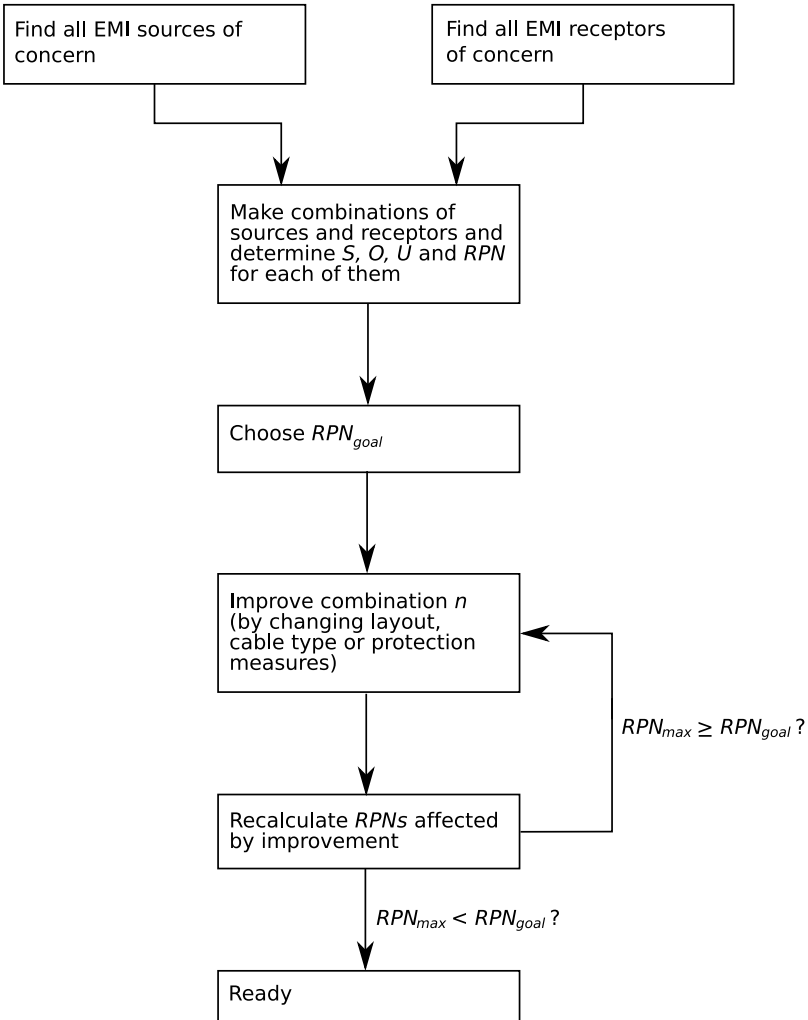


Figure 8.1: Flow diagram to reach the goal of an installation in terms of EMC performance.

For every coupling the effect of the disturbance has to be determined. Next to that, the following ranking numbers have to be determined:

- The severity of the disturbance of the receptor. How serious is the result of the disturbance? The severity of a certain disturbance is expressed by a dimensionless number  $S$ . The higher the number, the more severe the effect. To define the severity of a certain coupling, in depth background knowledge is needed of the installation as well as of the purpose of the installation. The  $S$  is given a value based on experience and can not be calculated deterministically. So, it is semi-quantitative and will depend in some cases on which expert is consulted. An example of severity ranking is given in table 8.1.
- The probability,  $O$ , that this disturbance occurs. This probability can be calculated if details are known about the disturbance signal: how often does it appear and at what times, what is the state of the receptor when this disturbance appears.
- The unpredictability,  $U$ , describing the inability to predict this kind of disturbance.

The numbers  $S$ ,  $O$  and  $U$  are then multiplied to calculate the Risk Priority Number,  $RPN$ :

$$RPN = S \times O \times U \quad (8.1)$$

The higher the  $RPN$ , the higher the risk caused by this coupling. After calculating the  $RPN$  for each coupling, they can be ordered from high to low risk couplings. FMECA, where this procedure is based on, assumes that the failure modes are independent. However, the couplings are not fully independent of each other. One source can disturb several receptors and one receptor can be disturbed by several sources. In the CRA method the dependencies are taken into account by adding a matrix which will be called dependency matrix. The rows of the matrix indicate the receptors and the columns the sources. The  $RPNs$  of the combinations are the elements of the matrix. If one source is a serious threat to several receptors, there will be multiple high  $RPNs$  in the column of that source. In that case changes should be made to the cabling of that source, because then multiple couplings with a high risk are treated at the same time.

### Improve combination

Improving one coupling path is done by rerouting the cable, by applying a conduit or by replacing the cable by one with a (better) screen (remember that this thesis is dealing with the *cabling* and that the sources and receptors are considered given). Three different situations can be distinguished:

- The source is relatively strong. In that case it is best to take measures at the cable(s) connected to the source. Putting these cables in a conduit or replacing them by better cables is the most preferable option, because transfer functions of other combinations with this same source will also benefit. Rerouting the cable is only advisable if it is sure that other receptors will not receive more disturbance as a result. Possible future extensions of the installation should be kept in mind if rerouting a cable.
- The receptor is relatively sensitive. In this case the best option is to put the cables of the receptor in a conduit or to replace them. Rerouting is less preferable for the same reason as above.
- The combination of source and receptor is bad. In this case, if nor the source is relatively strong nor the receptor is relatively sensitive, it does not really matter which measure is taken to improve. Rerouting the cables can be a good option, but replacing a cable or placing it in a conduit can also be a good option, although it is likely to be more expensive.

## 8.4 Example

To explain the method, an example will be given. Consider an installation which is part of a production line. The installation under consideration is built around a digital controller with digital input and output ports and an Ethernet connection that is used to monitor the process from a distance. The controller has an analog input as well that is used to read the very small signal generated by a sensor. The power supply of the controller is the 240 V, 50 Hz power which is available locally. Another part of the installation is an electro mechanic valve with a solenoid which is controlled by a DC signal. Finally, a broadcast transmitter is located nearby the factory. In figure 8.2 a schematic overview of the installation is given.

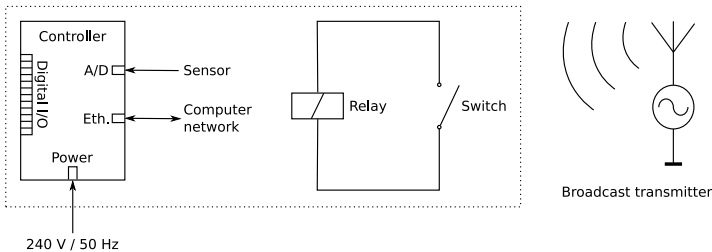


Figure 8.2: Example installation of a part of a production line. Parts outside the dashed box form part of the environment.

The controller ports taken into account in this example are the power supply port, the Ethernet port and the A/D port. Next to that the relay and the broadcast transmitter are considered.

As a first step, the possible receptors of disturbance will be determined. They are four:

1. The A/D port of the controller
2. The Ethernet port of the controller
3. The power supply port of the controller
4. The relay

The second step is to define the possible sources of disturbance. There are four possible sources in this case:

1. The Ethernet port of the controller
2. The relay which generates an EM pulse at switching time.
3. The power supply network, which is generating a 50 Hz electric field.
4. The broadcast transmitter.

The severity ranking used in this example is derived from table 8.1. For the probability of occurrence and the unpredictability no table is presented, but they are ranked from 1 – 10, where 1 indicates a low probability of occurrence and rank 10 means that the occurrence is certain. For unpredictability the ranking is also from 1 – 10, here rank 1 indicates an almost certain prediction while rank 10 means that it is nearly impossible to predict.

The resultant *RPN* is given in table 8.2. The zeroes in the *Severity* column mean that the disturbance in question does not have any negative influence, while a zero in the *Occurrence* column means that that disturbance never occurs.

There are three *RPNs* that are large compared to the others, viz. 64, 60 and 48. These three disturbance couplings should be treated first. The highest one, 64, is related to the power port of the controller, which is relatively insensitive to continuous and modulated signals, but very sensitive to pulses caused by switching the relay. These pulses can cause a reset of the controller, in which case the production process has to be restarted, causing loss of production. This disturbance coupling can be treated by changing the cabling of the source or of the receptor, because both are involved in this coupling only. That can be seen in the dependency matrix found in table 8.3, where the other *RPNs* for this receptor are small as well as the other *RPNs* of the source.

Table 8.1: Severity ranking of EMI consequences for an installation in a production plant

$S$	Severity	Criteria
5	Very high	Loss of lives or injury
4	High	Production stopped. Service needed to enable start of production again.
3	Moderate	Production slowed down or production with loss of quality. Extra effort needed to meet production specifications.
2	Low	Production possible at normal speed, but extra effort needed.
1	Very low	Some parts not necessary to the production process need to be replaced or reset at some time. E.g. bulbs at non-critical places.
0	None	Everything remains functioning with no or negligible interruption.

The other two high  $RPNs$  (60 and 48) are on one row in the dependency matrix, which means that they are related to one receptor, which is the A/D input of the controller. These high  $RPNs$  are caused by two different sources, viz. the Ethernet port and the broadcast transmitter. In this case it is advisable to change the cabling of the receptor, because then both couplings are addressed at the same time. Moreover, the broadcast transmitter can not be changed.

Table 8.2: RPN matrix

Receptor	Kind of disturbance	Effect of disturbance	S	O	U	RPN	Source of disturbance
Controller, power port	Modulated signal	Distorted power signal	1	3	2	6	Broadcast transmitter
	Modulated signal	Distorted power signal	1	1	4	4	Controller, Ethernet port
	Pulse	Controller reset	4	2	8	64	Relay
Controller, Ethernet port	Continuous wave	More bit errors	2	9	1	18	50 Hz power supply
	Modulated signal	More bit errors	2	8	2	32	Broadcast transmitter
	Pulse	Minimal	0	2	8	0	Relay
Controller, A/D port	Continuous wave	Wrong measurement	3	9	1	27	50 Hz power supply
	Modulated signal	Wrong measurement	3	8	2	48	Broadcast transmitter
	Modulated signal	Wrong measurement	3	5	4	60	Controller, Ethernet port
Relay	Pulse	Negligible	0	2	8	0	Relay
	Continuous wave	Unintended switching action	3	1	1	3	50 Hz power supply
	Modulated signal	Unintended switching action	3	0	3	0	Broadcast transmitter
	Modulated signal	Unintended switching action	3	0	3	0	Controller, Ethernet port



Table 8.3: Dependency matrix

		Source			
		Controller, Ethernet port	Relay	50 Hz power supply	Broadcast transmitter
Receptor	Controller, power port	4	64	-	6
	Controller, Ethernet port	-	0	18	32
	Controller, A/D port	60	0	27	48
	Relay	0	-	3	0



# Chapter 9

## Conclusions and recommendations

### 9.1 Conclusions

A multi conductor transmission line approach has been applied successfully to calculate the couplings between cables in an installation. This is a necessary condition to reach the end goal of the project: “optimizing cabling and wiring in buildings and installations with respect to EMC”. In several case studies we have shown that measurement and calculation of coupled signals using this approach agree very well. The “coupling risk analysis” has been developed to obtain knowledge of which coupling in an installation is bearing which risk. This knowledge is needed to determine at which priority each coupling should be treated.

These two fundamental aspects are needed to optimize the cabling and wiring of an installation with respect to EMC.

The general conclusions from this thesis are as follows:

- The armour of a V0-YMvKas cable, although merely designed for mechanical protection, should be connected at both ends to reduce common mode currents.
- In cases of parallel cables, the multi conductor transmission line model can be applied successfully to calculate the coupling between the cables, in the frequency range where the wavelength is larger than 12 times the maximum distance between the conductors.
- Using the multi conductor transmission line approach to model the transfer

impedance of a symmetrical cable with conductors of different diameters, the differential mode disturbance caused by a common mode current can be calculated accurately.

- The length and connection of a cable or conductor determine the resonance frequency at which the CM current will resonate in case of a present EM pulse. The cable length must be chosen so that this resonance frequency is not equal to a sensitive frequency of the equipment.
- In large installations in buildings many coupling paths between source and receptor are possible. The coupling risk analysis procedure has been developed to prioritize the optimization order for the different coupling paths.

Referring to the subjects mentioned in chapter 1 on page 7, the following conclusions can be drawn:

#### A Coupling between cables

- 1 The steel armor of V0-YMvKas cables, although not intended for EMC purposes, can reduce the disturbance coupling to nearby cables. In the example of a buried cable in chapter 5, the reduction is approximately a factor 20.
- 2 The multi conductor transmission line model is suitable to determine both common mode and differential mode currents in a real installation, where educated guesses are made of the electrical properties of the surroundings. This is shown in the example of coupling via buried cables, found in chapter 5.
- 3 The common mode current in a cable buried in the soil can be increased by nearby, parallel buried cables.
- 4 The choke installed between a variable frequency drive and the load connected to that drive is not very effective to suppress common mode currents. A transformer which forces the net current in the three phase conductors to flow back in the fourth conductor, could be more effective.
- 5 The common mode current caused by the switching actions of a variable frequency drive due to simultaneous switching in the same direction of two phases is higher than the common mode current of a single switching action. This is caused by the fact that the common mode voltage step is twice as high.
- 6 Coupling between two transmission lines is decreased if one of the lines is matched and minimized if both of them are matched, see section 6.1.

#### B Transfer impedance of non-coaxial cables (section 6.3)

- 1 Cables consisting of wires of different diameters have a non-zero transfer impedance and thus form a coupling path for EM disturbance.
- 2 This transfer impedance can be accurately calculated using the multi conductor transmission line approach.
- 3 This transfer impedance is proportional to half the difference between the impedances of the individual lines.
- 4 This transfer impedance depends on the load conditions.

C Conductive structures in buildings and installations (chapter 7)

- 1 If the concrete of a building is poured on-site, the individual pieces of concrete reinforcement can be considered electrically connected to each other.
- 2 If a building is made of prefab concrete elements, the reinforcement in these elements can be considered electrically floating.
- 3 The relative dielectric permittivity of concrete lies between 6 and 12.
- 4 The framework of an installation consists of variable kinds of materials, the conductivity and interconnection of which has to be determined for every single installation.

D Resonance of common mode currents in conductors (section 6.4)

- 1 A conductor which is connected to ground is resonating at a frequency where the wavelength is four times the length of the conductor, in case an electro magnetic pulse is present.
- 2 An electrically floating conductor is resonating at a frequency where the wavelength is equal to twice the length of the conductor, in case an electro magnetic pulse is present.
- 3 These resonances can be triggered by a pulse. The spectrum of this pulse does not need to have a peak at the resonance peak of the cable.
- 4 If equipment is very sensitive to certain frequencies, the cable lengths connected to it must be chosen such that they are not equal to a quarter or to half of the wavelength of that sensitive frequency.

E EMI signals (chapter 3)

- 1 The lower part of the spectrum generated by a variable frequency drive is dependent on the driving frequency and the higher part is dependent on the rise time of the individual pulses of the pulse width modulation signal.
- 2 The signal generated by a variable frequency drive is not necessarily zero if the connected motor is not rotating. The signal generated by a commercially available drive was 28 dB lower in case of a motor which was not running.

F Optimization method (chapter 8)

- 1 See the general conclusions.

## 9.2 Recommendations for future work

The method described to compute the coupling between cables relies on the availability of knowledge about the transmission line parameters of the cables under consideration. During the research much effort was needed to calculate these parameters. A step forward will be to develop (or collect from literature) expressions that give these parameters, or a good approximation to these parameters. These expressions should be kept at hand to decrease the time needed to calculate the coupling in a given situation.

Measurements and calculations of couplings are done in two different installations: One industrial installation with cables buried in the soil and one installation in the laboratory. Further to the latter investigations an experiment with additional influence of concrete reinforcement would be recommended.

The VO-YMvKas cable used has a steel armor. This armor can be part of a transmission line for common mode currents. In the example of the cables in the soil, the cable is regarded as a transmission line, together with the surrounding soil. If such a cable is used in an installation where the return path for the common mode current is a nearby metal bar or plate, the transmission line behaviour may be influenced by the fact that the armor of the cable consists of *rotating* steel wires. This might cause the transmission line to be non-uniform, which makes calculations more complicated. Research is needed into this effect.

With reference to the current distribution in section 6.2, it is advised to measure the current distribution over the three conductors (armour, PEC and litz) in the VO-YMvKas again, but now with the inner conductors as return. It is expected that a larger portion of the current will flow in the PEC conductor. The goal is to assess if this effects the transfer impedance.

Furthermore, modelling and calculation of the current distribution over the three conductors is recommended in order to accurately model the transfer impedance of VO-YMvKas and similar cables.

# Abbreviations

AM	Amplitude Modulation
CM	Common Mode
CRA	Coupling Risk Analysis
CUT	Cable Under Test
CW	Continuous Wave
DC	Direct Current
DFT	Digital Fourier Transform
DM	Differential Mode
EM	Electro Magnetic
EMC	Electro Magnetic Compatibility
EMI	Electro Magnetic interference
EMVT	Electromagnetische Vermogens Techniek
EFT	Electrical Fast Transient
ESD	Electro Static Discharge
EUT	Equipment Under Test
FFT	Fast Fourier Transform
FIT	Finite Integration Technique
FM	Frequency Modulation
FMEA	Failure Mode and Effect Analysis
FMECA	Failure Mode Effect and Criticality Analysis
FSK	Frequency Shift Keying
GSM	Groupe Spéciale Mobile (original abbreviation) or Global System for Mobile Communications
GSMK	Gaussian Minimum Shift Keying
IEC	International Electrotechnical Committee
IEEE	Institute of Electrical and Electronics Engineers
IFFT	Inverse Fast Fourier Transform
IOP	Innovatief Onderzoeks Programma
MTL	Multi conductor Transmission Line
NA	Network Analyser

NEC	Numerical Electromagnetics Code
PE	Protective Earth
PEC	Protective Earth Conductor
PVC	Polyvinyl Chloride
PWM	Pulse Width Modulation
RF	Radio Frequency
RMS	Root Mean Square
RPN	Risk Priority Number
TDMA	Time Division Multiple Access
TL	Transmission Line
VFD	Variable Frequency Drive
VNA	Vector Network Analyser



# Appendix A

## Calculation of MTL

An implementation in Matlab (TM) is given of the MTL calculation method described in chapter 4. The code follows the steps in that description. The example deals with an installation consisting of two networks connected by two transmission lines having a common return. A sketch is given in figure A.1.

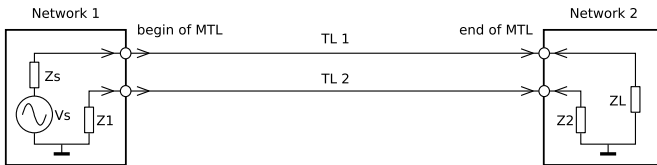


Figure A.1: Example installation

In the figure the two networks are given as well as the MTL. The direction of the MTL is indicated. At network 1 the current reference directions for the network and for the MTL coincide while at network 2 they are opposite. For the voltages the references are equal in both cases.

In listing A.1, the matrices  $P_1$ ,  $Q_1$  and  $E_1$  describe network 1, while  $P_2$ ,  $Q_2$  and  $E_2$  describe network 2. Because of the current reference directions, the matrix  $Q_2$  is negated.

The TL parameters are used to construct the matrices  $R$ ,  $L$ ,  $G$  and  $C$ . The interpretation of these parameters is described in section 4.2.2.

The code has to be executed for every frequency step needed and the results have to be saved in memory. If the time domain response to a certain signal has to be calculated, the following steps have to be performed:

1. Calculate the Fourier transform of the input time-domain signal.
2. Calculate the response of the circuit in frequency domain.
3. Multiply both results to obtain the frequency-domain response to the given signal.
4. Perform an inverse Fourier transform which yields the time domain response to the time domain input signal.

Listing A.1: The Matlab listing

```

%-----
P_1 = eye(N);
Q_1 = [Zs 0;
       0  Z1;];
E_1 = [Vs; 0;];

P_2 = eye(N);
% negation of Q_2 at end of TL!
Q_2 = -1 * [ZL 0;
            0  Z2;];
E_2 = [0; 0;];

%-----
% Combine TL parameters to complex TL-parameter matrices:

R = [R_1+Z_12  Z_12;
     Z_12      R_2+Z_12;];
L = [L1  M12;
     M12  L2;];
G = [ G1+G12  -G12;
     -G12     G12+G2;];
C = [ C1+C12  -C12;
     -C12     C12+C2;];

Z = R + j*omega*L;
Y = G + j*omega*C;

%-----
% Find eigenvalues gamma_square and -vectors V_0 of Z*Y:

[S_v gamma_square] = eig(Z*Y);

%-----
% Put gamma's in matrix Gamma:

```

```

Gamma = eye(N);
for i=1:N
    Gamma(i,i) = sqrt(gamma_square(i,i));
end

%-----
% Fill matrix E_D:

E_D = eye(N);
for i=1:N
    E_D(i,i) = exp(-Gamma(i,i)*D);
end

%-----
% Compute Y_c:

Y_c = inv(S_v * inv(Gamma) * inv(S_v) * Z);

%-----
% Calculate A_i and B_i for every node:
% negate Q_2 because of current direction!

A_1 = P_1*S_v + Q_1*Y_c*S_v;
B_1 = P_1*S_v*E_D - Q_1*Y_c*S_v*E_D;
A_2 = P_2*S_v*E_D + Q_2*Y_c*S_v*E_D;
B_2 = P_2*S_v - Q_2*Y_c*S_v;

A_total = [A_1 B_1; A_2 B_2];
E_total = [E_1; E_2];

%-----
% Solve for G and split G in G_i0 and G_rD:

G_total = A_total\E_total;

G_i0 = G_total(1:N);
G_rD = G_total(N+1:2*N);

%-----
% Calculate voltages and currents for every node:

VO = S_v*(G_i0 + E_D*G_rD);
IO = Y_c*S_v*(G_i0 - E_D*G_rD);
VD = S_v*(E_D*G_i0 + G_rD);

```

$$ID = Y_c * S_v * (E_D * G_{i0} - G_{rD} \quad );$$

%-----

# Appendix B

## Impedance of metal return plate

In section 6.1 the current in a conductor is flowing back in a nearby metal plate parallel to the conductor. In a printed circuit board where the current in a track flows back via a ground plane a similar situation exists. In an installation where a cable is installed nearby a metal plate, they can together behave like a transmission line. In all cases the impedance of the ground plane is needed for an accurate prediction of the current in the ground plane. This appendix gives an expression of that impedance and shows the current distribution in the plane.

In figure B.1 a sketch is given of the situation. The current in the conductor is flowing back in the metal plate. The distance between the center of the conductor and the surface of the plate is  $h$  and the radius of the conductor is  $r$ .

In [9] a derivation is given for the electric field in the metal plane, which is derived from [86] and [87]:

$$E_y = - \int_0^{\infty} F(\alpha) \cos(\alpha x) e^{z\sqrt{\alpha^2 + j\omega\mu\sigma}} d\alpha \quad (\text{B.1})$$

The parameter  $\mu = \mu_0\mu_r$  is the magnetic permeability of the plate and  $\sigma$  is the conductance of the plate.  $x$  and  $y$  are the coordinates corresponding to the coordinate system in the figure.  $\omega$  is the angular frequency and equal to  $2\pi f$ . In order to calculate the electric field, the function  $F(\alpha)$  has to be found, which is done via the calculation of the magnetic fields and filling in the boundary conditions (the magnetic field in and above the plate must be continuous):

$$F(\alpha) = \frac{I}{\pi} e^{-\alpha h} \frac{j\omega\mu}{\sqrt{\alpha^2 + j\omega\mu\sigma} + \mu_r\alpha} \quad (\text{B.2})$$

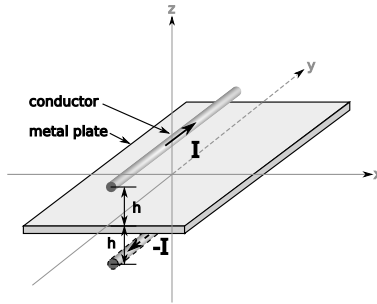


Figure B.1: Conductor with metal plate as return. The current  $I$  is mirrored in the plate, as shown by the image current  $-I$ .

$I$  in this equation is the current flowing in the conductor. The impedance of the plane per unit length can be expressed as:

$$Z' = \frac{E_z}{I} \quad (\Omega/m) \tag{B.3}$$

The current in the plane tends to be concentrated under the current carrying conductor, which effect is more pronounced at higher frequencies. In figure B.2 the electric field at the surface of the plate ( $z = 0$ ) is shown for three different frequencies.

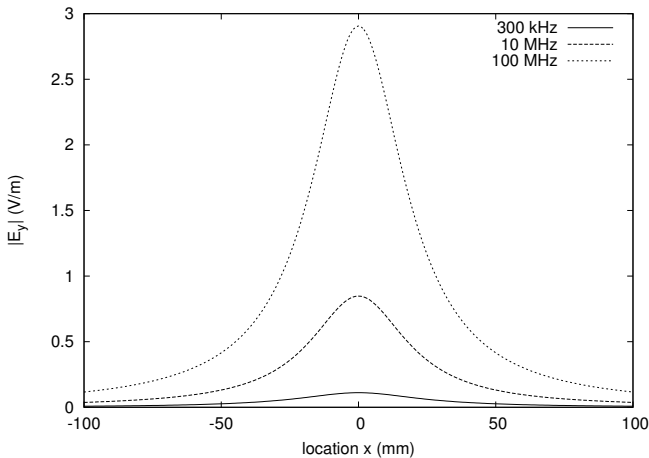


Figure B.2: The E-field at the surface of the metal plate as a function of the location along the x-axis.

The field is calculated using a numerical integration where the upper boundary is chosen to be  $10^4$ . Increasing the upper boundary did not change the results significantly.





# Appendix C

## Legislation

Standards are developed to make trade easier by eliminating technical barriers. When a number of countries have the same standards which products manufactured in that country have to meet, than a product manufactured in one country meets also the standards in the other countries. In the EU (European Union), CEN, CENELEC (Comité Européen de Normalisation Electrotechnique, the European electro technical standardization committee, composed of members of electro technical committees of 28 European countries) and ETSI are working on the harmonization of the standards throughout the EU.

By the IEC (International Electro technical Committee) a number of standards are developed, amongst others a series of EMC (Electro Magnetic Compatibility) standards. These standards describe both electro magnetic emission limits and electro magnetic immunity levels products have to meet. Emission limits are limits which may not be exceeded by the disturbance level of equipment. Immunity levels are disturbance levels equipment have to be able to withstand without too much loss of performance. That means that the equipment has to maintain operational after, or even during the disturbance.

In 1989 the first EMC directive (89/336/EEC) is passed [88] which has come into force the 1<sup>st</sup> of January 1992. The 20<sup>th</sup> of July 2007 this directive has been repealed and replaced by a new directive (2004/108/EC) [7]. The new directive ‘greatly simplifies regulatory procedures and reduces costs for manufacturers, while increasing information and documentation on products for inspection authorities’ [89].

The Directive refers to Harmonized Standards, ‘which reflect the generally acknowledged state-of-the-art as regards electro magnetic compatibility matters in the European Union’ [7]. An apparatus is presumed to conform to the EMC Di-

rective, if it meets these Harmonized Standards. Next to that it is possible to demonstrate conformity to the EMC Directive by other means.

Electric or electronic apparatus can bear the so-called CE-marking which is shown in figure C.1. For a product bearing this marking there are no restrictions with regards trading within the European Economic Area. The CE-marking shows that the product meets *all* applicable standards of the European Union. This means that this mark can show conformity to both EMC and other standards [90].

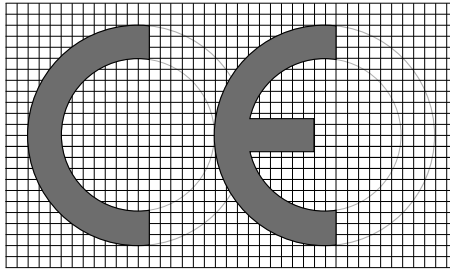


Figure C.1: The CE-marking. Usually applied without grid and circles. The vertical dimensions may not be less than 5 mm [7].

By applying the CE-marking the manufacturer of the product states that the product complies, amongst others, to the EMC Directive. It does not need to be verified by third parties.

# Bibliography

- [1] D. J. Groot Boerle. EMC and functional safety, impact of IEC 61000-1-2. In *2002 IEEE International Symposium on Electromagnetic Compatibility*, volume 1, pages 353–358, Aug 2002.
- [2] C. R. Paul. *Introduction to Electro Magnetic Compatibility*. John Wiley & Sons, Hoboken, New Jersey, 2nd edition edition, 2006. ISBN 0-471-75500-1.
- [3] IEC 50161. International electrotechnical vocabulary, chapter 161: Electromagnetic compatibility, 1990.
- [4] Catherine Soanes and Angus Stevenson, editors. *The Oxford Dictionary of English*. Oxford University Press, 2nd edition edition, 2005. ISBN 0198610572.
- [5] European Commission. Guidelines on the application of council directive 89/336/eec of 3 may 1989 on the approximation of the laws of the member states relating to electromagnetic compatibility, 1997.
- [6] Tim Williams. *EMC for Systems and Installations*. Newnes, 225 Wildwood Avenue, Woburn, MA 01801-2041, 1st edition edition, 2000. ISBN 0-7506-4167-3.
- [7] European Commission. Directive 2004/108/EC of the European Parliament and of the Council of 15 december 2004 on the approximation of the laws of the member states relating to electromagnetic compatibility and repealing directive 89/336/EEC, Dec 2004.
- [8] IEC 61000-5-2. Installation and mitigation guidelines, section 2: Earthing and cabling, 1997.
- [9] M. J. A. M. van Helvoort. *Grounding structures for the EMC-protection of cabling and wiring*. PhD thesis, Eindhoven University of Technology, Nov 1995. ISBN 90-386-0037-2.

- 
- [10] S. Kapora. *Protection by open systems: An EMC study*. PhD thesis, Eindhoven University of Technology, Sep 2005. ISBN 90-386-1743-7.
- [11] B. Demoulin, I. Bacancios, L. Kone, and C. Munteanu. Study of the transfer impedance and shielding effectiveness of cable trays for industrial wires. In *EMC Europe 2006 conference proceedings*, volume 1, pages 274–279, Sep 2006.
- [12] I. P. MacFarlane. A probe for the measurement of electrical unbalance of networks and devices. In *IEEE Transactions on Electromagnetic Compatibility*, volume 41, pages 3–14, Feb 1999.
- [13] Y. Kami and F. Xiao. Equivalent two-port network for indoor outlet and its application. In *EMC Europe 2006 conference proceedings*, volume 1, pages 420–425, Sep 2006.
- [14] U. Kappel and M. Hillgärtner. Radiating impedance of mains cabling during emissions testing. In *EMC Europe 2006 conference proceedings*, volume 1, pages 17–22, Sep 2006.
- [15] C. Gao, L. Li, X. Cui, Z. Zhao, and X. Gu. Calculation of the shielding effectiveness of reinforcing wire mesh using NEC. In *EMC Europe 2004 conference proceedings*, volume 1, pages 285–288, Sep 2004.
- [16] L. Sandrolini, U. Reggiani, and A. Ogunsola. Prediction of the electrical properties and shielding effectiveness of conductive concrete. In *EMC Europe 2006 conference proceedings*, volume 1, pages 1009–1013, Sep 2006.
- [17] X. Liu, D. W. P. Thomas, and C. Christopoulos. Prediction and experimental verification of radiated fields from interconnect cables due to common-mode currents. In *EMC Europe 2004 conference proceedings*, volume 2, pages 590–594, Sep 2004.
- [18] A. Nanni, D. W. P. Thomas, C. Christopoulos, T. Konefal, J. Paul L. Sandrolini, U. Reggiani, and A. Massarini. Electromagnetic coupling between wires and loops inside a rectangular cavity using multiple-mode transmission line theory. In *EMC Europe 2004 conference proceedings*, volume 2, pages 609–614, Sep 2004.
- [19] [www.senternovem.nl/iopemvt/algemeen/index.asp](http://www.senternovem.nl/iopemvt/algemeen/index.asp).
- [20] Peter A. Rizzi. *Microwave Engineering, Passive Circuits*. Prentice-Hall, New Jersey, 1988. ISBN 0-13-586702-9.
- [21] Clayton R. Paul. *Analysis of Multiconductor Transmission Lines*. John Wiley & Sons, INC, 1994. ISBN 0-471-02080-X.

- [22] H. H. Skilling. *Electric Transmission Lines*. McGraw-Hill book company, inc., New York, Toronto, London, 1st edition, 1951.
- [23] Philip C. Magnusson, Gerald C. Alexander, Vijai K. Tripathi, and Andreas Weisshaar. *Transmission Lines and Wave Propagation*. CRC Press, 2000 N.W. Corporate Blvd., Boca Raton, Florida, 4th edition, 2001. ISBN 0-8493-0269-2.
- [24] Heinrich Kaden. *Wirbelströme und Schirmung in der Nachrichtentechnik*. Springer-Verlag, Berlin · Göttingen · Heidelberg, 1959.
- [25] G.A. Campbell and R.M. Foster. Maximum output networks for telephone substation and repeater circuits. In *Transactions of the AIEE*, volume 39, pages 231–280, 1920.
- [26] Herbert J. Carlin. The scattering matrix in network theory. In *IRE Transactions on circuit theory*, volume CT-3, pages 88–97, June 1956.
- [27] Herbert J. Carlin. Correction. In *IRE Transactions on circuit theory*, volume CT-1, page 21, Mar 1957.
- [28] Operating manual, vector network analysers, Rohde&Schwarz ZVA/ZVB/ZVT documentation map.
- [29] NEN 3207. Insulated power cables and flexible cords. systems for the designation of types of cables., 1990.
- [30] Shen Wang, Michael Andrew de Rooij, Willem Gerhardus Odendaal, Jacobus Daniel van Wyk, and Dushan Boroyevich. Reduction of high-frequency conduction losses using a planar litz structure. In *IEEE Transactions on Power Electronics*, volume 20, pages 261–267, Mar 2005.
- [31] L. Jung and J. Luiken ter Haseborg. Improved triaxial set-ups for the measurement of complex transfer impedances and admittances of shielded multi-conductor cables inside cable bundles. In *IEEE International Symposium on Electromagnetic Compatibility*, volume 1, pages 41–44, Hamburg University of Technology, Germany, Aug 2000.
- [32] H. T. Steenstra, S. Meijer, and J. J. Smit. Transfer impedance measurement of electricity cables. In *IEEE International Electromagnetic Compatibility symposium*, volume 1, pages 262–266, Chicago, Illinois USA, Aug 2005. ISBN 0-7803-9381-3.
- [33] K. Kurokawa. Power waves and the scattering matrix. In *IEEE Transactions on Microwave Theory and Techniques*, volume 13, pages 194–202, March 1965.

- 
- [34] D. C. Smith. Current probes, more useful than you think. In *IEEE international symposium on Electromagnetic Compatibility*, volume 1, pages 284–289, Aug 1998.
- [35] IEC 61000-4-5. Surge immunity test, 1995.
- [36] IEC TR 61000-1-3. The effects of high-altitude EMP (HEMP) on civil equipment and systems, 2002.
- [37] D. V. Giri and F. M. Tesche. High-power electromagnetic (HPEM) source considerations. In *IEEE International Symposium on Electromagnetic Compatibility*, volume 2, pages 1028–1031, May 2003.
- [38] IEC 61000-1-5. High power electromagnetic (HPEM) effects on civil systems, 2004.
- [39] IEC 61000-4-2. Electrostatic discharge immunity test, 2000.
- [40] IEC 61000-4-4. Electrical fast transient / bursts immunity test, 1995.
- [41] IEC 61000-2-2. Compatibility levels for low-frequency conducted disturbances and signaling in public low-voltage power supply systems, 2002.
- [42] IEC 61000-4-3. Radiated radio frequency electromagnetic field immunity test, 2002.
- [43] IEC 61000-4-8. Power frequency magnetic field immunity test, 1993.
- [44] IEC 61000-3-3. Limitation of voltage fluctuations and flicker in low-voltage supply systems for equipment with rated current  $\leq 16\text{a}$ , 2002.
- [45] Meiden AC speed control equipment THYFREC-VT230SE.
- [46] Paul Kimuli. Introduction to GSM and GSM mobile RF transceiver derivation. In *RF Design*, pages 12, 16, 18, 20, 21, June 2003.
- [47] LINK Collaborative Research. Electro magnetic compatibility aspects of radio-based mobile telecommunications systems, final report, 1999.
- [48] Timo Halonen, Javier Romero, and Juan Melero. *GSM, GPRS and EDGE performance*. John Willey & Sons, Ltd, Chichester, UK, 2nd edition, 2003. ISBN 0-470-86694-2.
- [49] Jörg Eberspächer, Hans-Jörg Vögel, and Christian Bettstetter. *GSM Switching, Services and Protocols*. John Willey & Sons, Ltd, Chichester, UK, 2nd edition, 2001. ISBN 0471-49903-X.

- [50] IEC 61000-4-7. General guide on harmonics and interharmonics measurements and instrumentation, for power supply systems and equipment connected thereto, 2002.
- [51] Antonije R. Djordjević and Tapan K. Sarkar. Analysis of Time Response of Lossy Multiconductor Transmission Line Networks. In *IEEE Transactions on Microwave Theory and Techniques*, volume MTT-35, pages 898–908, Oct 1987.
- [52] Gilbert Strang. *Linear Algebra and its applications*. Harcourt Brace Jovanovich, Inc., Orlando, Florida 32887, 1988. ISBN 0-15-551005-3.
- [53] C. D. Taylor, R. S. Satterwhite, and C. W. Harrison, Jr. The response of a terminated two-wire transmission line excited by a nonuniform electromagnetic field. In *IEEE Transactions on Antennas and Propagation*, volume AP-13, pages 987–989, Nov 1965.
- [54] Ashok K. Agrawal, Harold J. Price, and Shyam H. Gurbaxani. Transient response of multiconductor transmission lines excited by a nonuniform electromagnetic field. In *IEEE Transactions on Electromagnetic Compatibility*, volume EMC-22, pages 119–129, May 1980.
- [55] Farhad Rachidi. Formulation of the field-to-transmission line coupling equations in terms of magnetic excitation fields. In *IEEE Transactions on Electromagnetic Compatibility*, volume 35, pages 404–407, Aug 1993.
- [56] H. T. Steenstra, A. P. J. Van Deursen, and S. Meijer. Common mode interference coupled via a buried armored cable. In *EMC Europe 2006*, pages 556–561, Barcelona, Spain, Sep 2006. ISBN 84-689-9438-3.
- [57] H. T. Steenstra and A. P. J. Van Deursen. Reduction of conducted interference by steel armor in buried cables: Measurements and modeling. In *IEEE Transactions on Electromagnetic Compatibility*, Boulder, CO 80305, USA, 2008.
- [58] D. Zhao, J.A. Ferreira, H. Polinder, A. Roch, and F.B.J. Leferink. Noise propagation path identification of variable speed drive in time domain via common mode test mode. In *Conference on Power Electronics and Applications*, pages 1–8, Denmark, Sep 2007.
- [59] Simon Ramo, John R. Whinnery, and Theodore van Duzer. *Fields and Waves in Communication Electronics*. John Willey & Sons, Ltd, Chichester, UK, 2nd edition, 1984. ISBN 0-471-87130-3.

- 
- [60] Edward F. Vance. *Coupling to shielded cables*. John Wiley & Sons, New York, London, Sydney, Toronto, 1978. ISBN 0-471-04107-6.
- [61] Robert V. Langmuir. *Electromagnetic fields and waves*. McGraw-Hill Book Company Ltd., New York, Toronto, London, 1st edition, 1961.
- [62] Emanuel Petrache, Farhad Rachidi, Mario Paolone, Carlo Alberto Nucci, Vladimir A. Rakov, and Martin A. Uman. Lightning induced disturbances in buried cables – part I: Theory. In *IEEE Transactions on Electromagnetic Compatibility*, volume 57, pages 498–508, Aug 2005.
- [63] Erling D. Sunde. *Earth conduction effects in transmission systems*. Dover Publications, New York, Dover edition, 1968.
- [64] D. Bellan and Sergio A. Pignari. Estimation of crosstalk in nonuniform cable bundles. In *IEEE international symposium on Electromagnetic Compatibility*, volume 2, pages 336–341, Chicago, Illinois USA, Aug 2005.
- [65] M.J. Coenen, Philips Applied Technologies, private communication, intended for publication.
- [66] CST studio suite 2006, CST design environment, CST microwave studio, CST EM studio, CST particle studio, CST design studio, advanced topics.
- [67] T. Weiland. A discretization method for the solution of maxwell’s equations for six component fields. In *Electronics and communication (AEÜ)*, pages 116–120, 1977.
- [68] David R. Lide, editor. *CRC Handbook of Chemistry and Physics*. CRC Press, Boca Raton, USA, 87th edition edition, 2006. ISBN 9780849304873.
- [69] Grant Bingeman. Transmission lines as antennas. In *RF Design (online at [www.rfdesign.com](http://www.rfdesign.com))*, pages 74–82, Jan 2001.
- [70] NEN-EN-IEC 60228. Conductors of insulated cables, 2005.
- [71] Draka handboek.
- [72] Draka catalogus 1, draad en kabel.
- [73] A.P.C. Fourie, O. Givati, and A.R. Clark. Simple technique for the measurement of the transfer impedance of variable length coaxial interconnecting leads. In *IEEE Transactions on Electromagnetic Compatibility*, volume 40, pages 163–166, May 1998.



- [74] Sergio A. Pignari and Antonio Orlandi. Long-cable effects on conducted emissions levels. In *IEEE Transactions on Electromagnetic Compatibility*, volume 45, pages 43–54, Feb 2003.
- [75] H. T. Steenstra, S. Meijer, and J. J. Smit. Transfer impedance of different cable types and single wire current distribution. In *EMC Europe 2006*, pages 580–585, Barcelona, Spain, Sep 2006. ISBN 84-689-9438-3.
- [76] Agilent esa series spectrum analysers data sheet.
- [77] Personal communication with J. Burggraaf, Building construction specialist.
- [78] Personal communication with Dr. Ir. C. Van der Veen, faculty of Civil Engineering, Delft University of Technology.
- [79] J. M. Illston and P. L. J. Domone. *Construction materials, their nature and behaviour*. Taylor & Francis e-Library, London, New York, 3rd edition edition, 2002. ISBN 0-203-47898-3.
- [80] Personal communication with Dr. Ir. M. De Rooij, faculty of Civil Engineering, Delft University of Technology.
- [81] [www.staff.city.ac.uk/earthquakes/masonrybrick/reinforcedbrickmasonry.htm](http://www.staff.city.ac.uk/earthquakes/masonrybrick/reinforcedbrickmasonry.htm).
- [82] S. Laurens, J.P. Balayssac, J. Rhazi, G. Klysz, and G. Arlignie. Non-destructive evaluation of concrete moisture by GPR: experimental study and direct modeling. In *Materials and Structures*, pages 827–832, November 2005.
- [83] M. Adous, P. Qu  ff  lec, and L. Laguerre. Coaxial/cylindrical transition line for broadband permittivity measurement of civil engineering materials. In *Measurement Science and Technology*, pages 2241–2246, July 2006.
- [84] J. Davis and Y. Huang. Determination of dielectric properties of insitu concrete at radar frequencies. In *Non-destructive testing in civil engineering (Symposium proceedings)*, September 2003. ISBN 3-931381-49-8.
- [85] NEN-EN-IEC 60812. Analysis techniques for system reliability – procedure for failure mode effects analysis (FMEA)(IEC 60812:2006,IDT), 2006.
- [86] John R. Carson. Wave propagation in overhead wires with ground return. In *Bell System Technical Journal*, volume 5, pages 539–554, Oct 1926.
- [87] W. H. Wise. Effect of ground permeability on ground return conductors. In *Bell System Technical Journal*, volume 10, pages 472–484, 1931.

- [88] European Commission. Council directive of 3rd may 1989 on the approximation of the laws of the member states relating to electromagnetic compatibility (89/336/EEC), May 1989.
- [89] European Commission. Cutting red tape for industry: New directive makes life of manufacturers of electronic devices easier (press release IP/05/8), Jan 2005.
- [90] European Commission. Guide to the implementation of directives based on the new approach and the global approach, 2000. ISBN 92-828-7500-8.

# Acknowledgements

The following people I would like to thank for making this thesis possible:

First of all, my promotor, prof. dr. J.J. Smit, who gave me the opportunity to perform a PhD research in his group. The regular meetings in the past years and especially in the last year, were always constructive. I always felt that the work I did was supported, despite the fact that my research was unique in the group.

Sander Meijer, my coach, who always motivated me in an enthusiastic way to perform experiments and to continue the research. He supported me very well although I often wanted to go in a somewhat different way.

Lex van Deursen, who gave me invaluable tips and hints during the discussions we have had over the years, as well as the good and pleasant co-operation. Besides, he also gave me the opportunity to do some additional research during the three months time I was employed at the Technical University of Eindhoven.

The personnel of the High Voltage Laboratory, Paul van Nes, Bertus Naagen and Aad van der Graaf, who gave me several practical tips and who were always ready to help building up measurement setups and constructing many things I needed.

The promovendi of the group, Rogier, Dhiradj, Robert, Belma, Pantelis, Riccardo, Piotr, Ben, Thomas, Tomasz and Gautam. I had a very nice time with you all!

Jan Burggraaf, who made all the photographs found in chapter 7 and who gave a lot of background information related to buildings.

Everybody who showed interest in my work and who is not mentioned in this list.

Many thanks I owe to my wife, Angélique, who gave me all possible support during these years and has been very patiently waiting for the finish. Angélique, from now we can spend time together again.

Finally, I wish to thank God, Who gave me all I needed to finish this work.



# Curriculum Vitae

Herre Tjerk Steenstra was born the 13<sup>th</sup> of February, 1972 in Kampen.

After receiving his secondary school diploma in 1991, he studied electrical engineering at the Delft University of Technology in The Netherlands. The specialization during his study was in the field of microwave engineering. He received his MSc degree in 1998.

From 1998 until 2003 he was employed at the International Research Centre on Telecommunications transmission and Radar to work on the development of a collision avoidance radar system.

In 2003 he started a PhD study to the optimization of cabling and wiring in buildings and installations at the High voltage Technology and Management group of the faculty of Electrical Engineering, Mathematics and Computer Science of the Delft University of Technology.

Currently, he is working as EMC specialist at Mapper Lithography BV in Delft, The Netherlands.

Tjerk is married to Angélique since the 24<sup>th</sup> of May, 2002 and they have a daughter, Anna, born the 8<sup>th</sup> of August, 2007.